



BERNHARD LEHOFER

Investigation of liposomal formulations suitable for pulmonary application of iloprost with different nebulizer devices

Master Arbeit

Zur Erlangung des akademischen Grades

Master of Science

an der Fakultät für Technische Chemie, Verfahrenstechnik und Biotechnologie der
Technischen Universität Graz

Begutachtet von:

Ruth Prassl, Assoz. Prof.ⁱⁿ Univ.-Doz.ⁱⁿ Dr.ⁱⁿ phil.

Institut für Molekulare Biowissenschaften (Strukturbiologie)

Karl-Franzens-Universität Graz

Institut für Biophysik, Medizinische Universität Graz

Ludwig Boltzmann Institut für Lungengefäßforschung



Ludwig Boltzmann Institute
Lung Vascular Research

Graz, Februar 2013



BERNHARD LEHOFER

Investigation of liposomal formulations suitable for pulmonary application of iloprost with different nebulizer devices

Master's Thesis

To be awarded the degree of
Master of Science
at the Faculty of Technical Chemistry, Chemical & Process Engineering
and Biotechnology
at Graz University of Technology

Supervised by:

Ruth Prassl, Assoc. Prof. Dr.
Institute of Molecular Biosciences (Structural Biology)
Karl-Franzens-University of Graz
Institute of Biophysics, Medical University of Graz

Ludwig Boltzmann Institute for Lung Vascular Research



Graz, February 2013

Zusammenfassung

Pulmonale arterielle Hypertonie (PAH) ist eine schwerwiegende seltene Erkrankung der kleinen Lungenarterien, die mit einem erhöhten Blutdruck im rechten Herzen einhergeht. Patienten die an dieser Erkrankung leiden, haben eine stark eingeschränkte körperliche Leistungsfähigkeit. Dies wiederum schränkt die Lebensqualität dieser Patienten stark ein. Unbehandelt kann die Erkrankung innerhalb weniger Jahre zum Tod führen.

Es gibt einige Behandlungsmöglichkeiten, die sowohl die Lebenserwartung dieser Patienten erhöhen als auch einen positiven Einfluss auf ihre Lebensqualität haben. Eine dieser Behandlungsmöglichkeiten ist die Inhalation von Iloprost. Bei dieser Verbindung handelt es sich um ein synthetisch hergestelltes Analogon des Prostacyclin, das wiederum eine starke natürliche gefäßerweiternde Wirkung besitzt. Iloprost hat dieselbe Wirkung und wird derzeit als wässrige Lösung zur Behandlung von Patienten eingesetzt. Einen der größten Nachteile dieser Behandlungsmethode stellt die sehr schnell abklingende gefäßerweiternde Wirkung nach der Inhalation dar. Noch dazu muss die Inhalation zwischen 6 – 9 Mal täglich erfolgen und dauert jeweils sehr lange (10 – 15 min). Ein weiteres großes Problem stellen die häufig auftretenden Nebenwirkungen dar.

Um all diesen Nachteilen entgegenzuwirken, entwickelten wir ein raffinierteres Wirkstoff - Verabreichungssystem. Um genauer zu sein, bedient sich dieses System der Verwendung von Liposomen. Bei Liposomen handelt es sich um künstlich hergestellte Vesikel, die aus verschiedensten Lipidbestandteilen aufgebaut werden können. Da diese Vesikel künstlich hergestellt werden, kann man frei entscheiden welche Lipidkomponenten man verwenden möchte und welche Zusammensetzung diese haben sollen. Aufgrund dieses Vorteils kann man Liposomen mit völlig verschiedenen Charakteristika erzeugen und diese für ganz bestimmte Applikationen maßschneidern.

Liposomen werden schon seit Jahrzehnten untersucht und sind im Feld der Wirkstoff - Verabreichungssysteme schon seit einigen Jahren vor allem für kleine organische Moleküle im Einsatz. Iloprost ist ein solches Molekül und muss vor schnellem Abbau durch β -Oxidation geschützt werden. Außerdem soll der nach der Verabreichung eintretende gefäßerweiternde Effekt von Iloprost verzögert werden.

Diese langgezogene Freisetzung soll durch die Einkapselung von Iloprost in Liposomen erreicht werden. Nach dem Einschluss des aktiven Wirkstoffs in die Liposomen, muss diese Emulsion für die Inhalation durch den Patienten vernebelt werden. Für die Erzeugung eines Aerosols für medizinische Anwendungen sind derzeit drei Typen von Verneblern mit ganz verschiedenen Arbeitsprinzipien erhältlich.

Im Rahmen dieser Arbeit wurden liposomale Emulsionen mit Verneblern von allen drei Prinzipien getestet. Die drei derzeit erhältlichen Arbeitsprinzipien sind Air-Jet, Ultraschall und Vibrating Mesh Vernebler. Jeder Vernebler wurde mit verschiedenen liposomalen Formulierungen und Konzentrationen getestet und diese anschließend biochemisch und biophysikalisch charakterisiert.

Das Hauptziel der Arbeit war es herauszufinden, wie sich verschiedener mechanischer Stress, der durch die Vernebelung erzeugt wird, auf die Liposomen auswirkt.

Die Experimente zeigten, dass grundsätzlich alle getesteten liposomalen Formulierungen im Bezug auf Widerstandsvermögen und Größe sehr stabil sind. Es zeigten sich allerdings Unterschiede bei der Fähigkeit, Iloprost während der Vernebelung eingekapselt zu behalten. Ein weiteres sehr wichtiges Ergebnis war, dass sich die Vernebler sehr stark in ihrer Fähigkeit unterschieden, ein Aerosol mit darin enthaltenen Liposomen zu erzeugen. Genauer gesagt transportierte der Ultraschall – Vernebler nur in sehr geringem Maße Liposomen ins Aerosol. Der Vibrating Mesh Vernebler war klar der effektivste; der Air-Jet lag dazwischen.

Von einem technischen Standpunkt aus gesehen, ist die Verwendung von Liposomen als Wirkstoffträger in einer aerosolischen Verabreichung möglich. Die Liposomen sind stabil genug um vernebelt zu werden, obwohl auch einige Faktoren wie die Größe, die Stabilität der Wirkstoffverkapselung und das Widerstandsvermögen stark von den eingesetzten Lipidkomponenten abhängen. Das bedeutet, dass eine Optimierung von vernebelten Liposomen durch die Änderung der Komponenten selbst oder deren Anteil im Gesamtgemisch erreicht werden könnte. Aber dennoch hat der angewandte Vernebler den größten Einfluss auf die Transporteffizienz.

Summary

Pulmonary arterial hypertension (PAH) is a severe rare disease of the small pulmonary arteries which causes a progressive rise in pulmonary vascular resistance and right ventricular pressure. Patients suffering from this dysfunction have a strongly limited physical fitness. This in turn decreases significantly the patient's quality of life. If the disease is untreated it can lead to death within a couple of years.

There are a few treatment possibilities which increase the patient's life expectancy and can have a positive effect on patient's quality of life. One of these treatment options is the inhalation of iloprost. This compound is a synthetic analogue of prostacyclin, which is a very potent natural vasodilator. Iloprost has the same vasodilating effect and has been used for patient's treatment as aqueous buffer solution so far. One big disadvantage of this treatment method is that the vasodilating effect decreases quite fast after inhalation. Moreover the inhalation procedure has to be done 6 – 9 times a day and its duration each time is quite long (10 – 15 min). Another big problem comes from frequently occurring side effects.

To counteract all these drawbacks we developed a more sophisticated drug delivery system. To be more specific this drug delivery system uses liposomes. Liposomes are artificially produced vesicles, which can be composed of many different kinds of lipids. As these vesicles are produced artificially one can decide on the types and the composition of lipids used. Because of this one can create liposomes with completely different characteristics and tailored for very specific applications.

Liposomes in general have been investigated for decades and have been used as drug delivery systems for small organic compounds for years now. Iloprost is such a small organic molecule that is chemically unstable and should be protected from degradation through β -oxidation within liposomes. Moreover the immediate vasodilating effect after administration should be sustained. To achieve a prolonged effect of iloprost it shall be encapsulated into liposomes for sustained release in the lungs. After encapsulation of the active compound into liposomes these emulsions have to be nebulized for patient's inhalation. For the production of an aerosol for medical applications there are various nebulizers with completely different working principles available on the market.

Within the scope of this thesis, nebulizers of three principles were tested for the nebulization of liposomal emulsions. The three currently available working principles are air-jet, ultrasound and vibrating mesh nebulizers. For each nebulizer different liposomal formulations and concentrations were tested and then biochemically and biophysically characterized.

The main aim of this thesis was to investigate the effects of different mechanical stress produced by the nebulization process on liposomes.

The experiments showed that basically all tested liposomal formulations are quite stable in terms of integrity and size. There were differences in the ability of keeping iloprost encapsulated during nebulization. Another very important result was that the nebulizers strongly differed in their ability of producing an aerosol containing liposomes. More precisely the ultrasound nebulizer only poorly transported liposomes into the aerosol. The vibrating mesh technology is clearly the most effective; the air-jet nebulizer is in between.

From a technical point of view, the use of liposomes as drug carriers for aerosol administration via nebulization is possible. The liposomes are stable enough to be nebulized, although some factors like liposome size, drug encapsulation, stability and liposome integrity strongly depend on the applied lipid components. This means that an optimization of aerosolized liposomes can be done by altering the components themselves or the ratio of the applied compounds. But nevertheless our data clearly indicate that the applied nebulizer has the strongest impact on the transport efficiency.

Acknowledgements

Your time is limited, so don't waste it living someone else's life. Don't be trapped by dogma, which is living with the results of other people's thinking. Don't let the noise of other's opinions drown out your inner voice. And most important, have the courage to follow your heart and intuition. They somehow already know what you truly want to become. Everything else is secondary.

Steve Jobs (1955 - 2011), Stanford Commencement Address, 2005

Somehow I really cannot believe that I am now writing the lines for the acknowledgements of my master's thesis. It feels as if I have just started with my studies a few months ago. I can exactly remember how I felt on the first day when I was sitting on the train riding to Graz and looking forward to my first lecture at university. I was so excited and also quite nervous about what would happen that day, how many people there would be and most important for me, I didn't want to be late. But then the train stopped abruptly and the train conductor announced that we could not go on with this train as the engine broke down. This was the moment when I started to panic...

Looking back I have to laugh about this situation and I can now thankfully say that everything went fine for me, although I was late on the first day.

First of all I would like to thank all of my **friends and colleagues** from the chemistry studies, who supported me for years in every possible way. Without you I wouldn't have got so far.

Then I would like to express my gratitude to my supervisor **Ruth Prassl**. I am so thankful to her because she gave me the possibility to work in her group and to be a member of the Institute of Biophysics and Nanosystems Research (IBN). Moreover she coordinated this project as cooperation with the Ludwig Boltzmann Institute (LBI) for Lung Vascular Research at the Medical University of Graz. So I had the great possibility to work, participate and learn at two completely different scientific

institutions. I really enjoyed the time working for this project and being a part of such a great scientific research team.

My special thanks go to two people that supported me every day with their knowledge and patiently introduced me to all the new techniques from the first day on. Thank you so much **Caroline Vonach** and **Gebhard Schratte**.

Moreover I would really like to thank **Regina Leber** for her special methodical support, her ongoing scientific input and her persistent motivation.

I also like to thank **Pritesh Jain**, who gave me an insight into a different scientific field. I had a lot of interesting discussions and the opportunity to give feedback from a different point of view.

Another important person for me was our group leader at the LBI **Leigh Marsh**, who I would also like to thank for his competent coordination of our group members and working plans.

At this point I would like to especially say “thank you” to **Andrea Olschewski**, who gave me the opportunity to be a member of the LBI and more precisely of program line B. I was able to actively participate in meetings and seminars and could get a great insight into the structure and organization of a modern applied research center. Furthermore I would like to thank **all members of the LBI** who welcomed me warmly and immediately accepted me as their new group member. Thank you for that!

Then I would also like to give my thanks to **all members of the IBN**, who made me part of their family. I really enjoyed working with you. Thanks to you all!

My most outstanding thanks go to **my parents**. Without them I would have never been able to reach what I have reached now. They have truly supported me whenever I needed them. You both know what important contributions you made throughout my life. Thanks so much for your support and your love!

Index

Zusammenfassung	I
Summary	III
Acknowledgements	V
Abbreviations	X
1. Introduction	1
1.1 The human heart.....	1
1.2 Pulmonary arterial hypertension (PAH)	3
1.3 Treating PAH.....	6
1.4 Iloprost	10
1.5 The human lungs	11
1.6 The human lungs as organs of absorption.....	12
1.7 Liposomes.....	13
1.8 Liposomes as drug delivery system.....	14
1.9 Liposomes for drug delivery to the lungs	16
1.10 Nebulizers	19
1.11 Working principles of nebulizers	20
1.12 Objective	23
2. Materials & Methods	24
2.1 Materials	24
2.2 Nebulizer devices and condensation equipment.....	24
2.3 Preparation of iloprost containing liposomes	25
2.4 Drug loading efficiency	27
2.5 Preparation of ANTS/DPX containing liposomes	29
2.6 Purification of liposomes from non-encapsulated ANTS/DPX.....	30
2.7 Fluorescence spectroscopy	31
2.8 Size analysis of liposomes	32
2.9 Determination of liposome concentration.....	33

2.9.1	Phospholipid assay	33
2.9.2	Phosphorus determination.....	34
2.10	Preparation of samples for mass spectrometry.....	35
2.11	Size analysis of aerosol droplets	35
2.12	Zeta potential	36
3.	Results & Discussion.....	37
3.1	Adaption of condensation equipment for nebulizers	37
3.1.1	Optineb®-ir.....	37
3.1.2	MicroDrop® <i>Pro</i>	40
3.1.3	eFlow® rapid.....	42
3.2	Adaption of breathing air condenser for nebulizers.....	43
3.2.1	Optineb®-ir.....	43
3.2.2	MicroDrop® <i>Pro</i>	45
3.2.3	eFlow® rapid.....	46
3.3	Nebulization trials with empty liposomes L-1 and L-2	46
3.3.1	MicroDrop® <i>Pro</i>	46
3.3.2	Optineb®-ir.....	51
3.3.3	eFlow® rapid.....	53
3.4	Nebulization trials with iloprost loaded liposomes LI-1 and LI-2.....	55
3.4.1	MicroDrop® <i>Pro</i>	55
3.4.2	Optineb®-ir.....	59
3.4.3	eFlow® rapid.....	62
3.5	Iloprost encapsulation after nebulization – TLC results.....	65
3.5.1	MicroDrop® <i>Pro</i>	66
3.5.2	Optineb®-ir.....	67
3.5.3	eFlow® rapid.....	68
3.6	Iloprost encapsulation after nebulization – MS results	69
3.6.1	MicroDrop® <i>Pro</i>	69
3.6.2	Optineb®-ir.....	70
3.6.3	eFlow® rapid.....	71

3.7	Zeta potential of liposomes.....	73
3.8	Droplet size measurements with nebulizers	74
3.8.1	MicroDrop® <i>Pro</i>	74
3.8.2	Optineb®-ir.....	74
3.8.3	eFlow® rapid.....	75
3.8.4	Comparison.....	76
3.9	Nebulization trials with mouse inhaler M-neb.....	76
3.10	Droplet size measurements with mouse inhaler M-neb	78
3.11	Iloprost encapsulation after nebulization – MS results – M-neb	80
3.12	Nebulization of L-1 and L-2 containing ANTS/DPX with eFlow® rapid.....	81
4.	Conclusion & Outlook.....	83
4.1	Liposomes for inhalation therapy.....	83
4.2	Iloprost containing liposomes for human inhalers	84
4.3	Iloprost containing liposomes for mouse inhaler	87
4.4	Outlook.....	87
5.	References.....	89
6.	Appendix.....	93
6.1	List of Figures.....	93
6.2	List of Tables.....	96
6.3	Nebulized and collected sample volumes.....	98
6.4	Droplet size measurements.....	100
6.5	MS results	103

Abbreviations

5-LO	5-Lipoxygenase
ALK1	Activin receptor-like kinase type 1
ANTS	8-Aminonaphthalene-1,3,6-trisulfonic acid disodium salt
BMPR2	Bone morphogenetic protein receptor type 2
CH	Cholesterol
cps	counts per second
CV	column volume
DLPC	1,2-dilauroyl- <i>sn</i> -glycero-3-phosphocholine
DLS	Dynamic light scattering
DOTAP	1,2-dioleoyl-3-trimethylammonium-propane
DPPC	1,2-dipalmitoyl- <i>sn</i> -glycero-3-phosphocholine
DPPE	1,2-dipalmitoyl- <i>sn</i> -glycero-3-phosphoethanolamine
DPX	p-Xylene-bis(N-pyridinium bromide)
EE	Encapsulation efficiency
ERA	Endothelin receptor antagonist
ET-1	Endothelin-1
FDA	U.S. Food and Drug Administration
HIV	Human immunodeficiency virus
IPL	Isolated perfused lung
LMV	Large multilamellar vesicles
LUV	Large unilamellar vesicles
MMAD	Mass Median Aerodynamic Diameter
mPAP	Mean pulmonary arterial pressure
MS	Mass spectrometry
PAH	Pulmonary arterial hypertension
PAP	Pulmonary arterial pressure
PDE-5	Phosphodiesterase-5
PDI	Polydispersity index
PEG	Polyethylene glycol
PGI₂	Prostacyclin
PH	Pulmonary hypertension

POPC	1-palmitoyl-2-oleoyl- <i>sn</i> -glycero-3-phosphocholine
PPH	Primary pulmonary hypertension
PVP	Polyvinylpyrrolidone
SA	n-Stearylamine
SOP	Standard Operating Procedure
SUV	Small unilamellar vesicles
T_c	Transition temperature
TLC	Thin layer chromatography
VEGF	Vascular endothelial growth factor
VIP	Vasoactive intestinal peptide

1. Introduction

1.1 The human heart

“Within the *pericardium* lies the heart – a hollow, muscular, four-chambered organ. It is suspended, at its base, by the great vessels. In situ, it occupies an asymmetrical position, with its *apex* pointing anteriorly, inferiorly, and about 60 degrees toward the left. Its four chambers are arranged in two functionally similar pairs, separated from each other by the cardiac *septum*. Each pair consists of a thin-walled atrium and a thicker-walled ventricle.” [1]

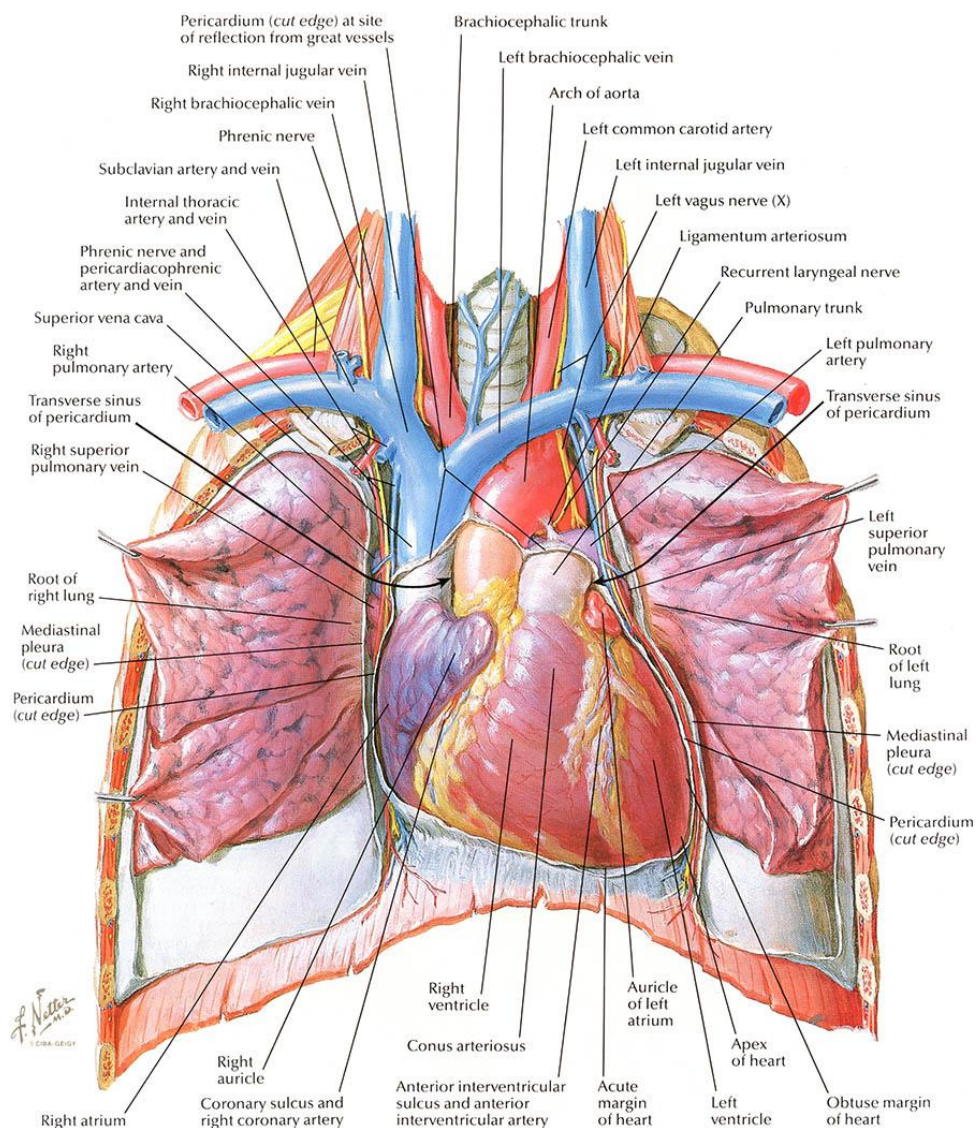


Figure 1.1: Drawing of the exposure of the human heart surrounded by vessels, lobes of the lung and musculature. Drawn by Frank H. Netter, M.D. [1]

“The *superior* and *inferior venae cavae* enter the *right atrium*, the long axis of both being inclined slightly forward.” “The right *pulmonary veins*, coming from the right lung, cross the right atrium posteriorly, to enter the right side of the *left atrium*. The two *left pulmonary veins* enter the left side of the left atrium, sometimes by a large common stem.” “The bifurcation of the pulmonary trunk lies on the roof of the left atrium, the *left pulmonary artery* coursing immediately toward the left lung, and the *right pulmonary artery* running behind the proximal superior vena cava and above the right pulmonary veins to the right lung. The aortic arch crosses the pulmonary-artery bifurcation” and leads into three main branches. [1]

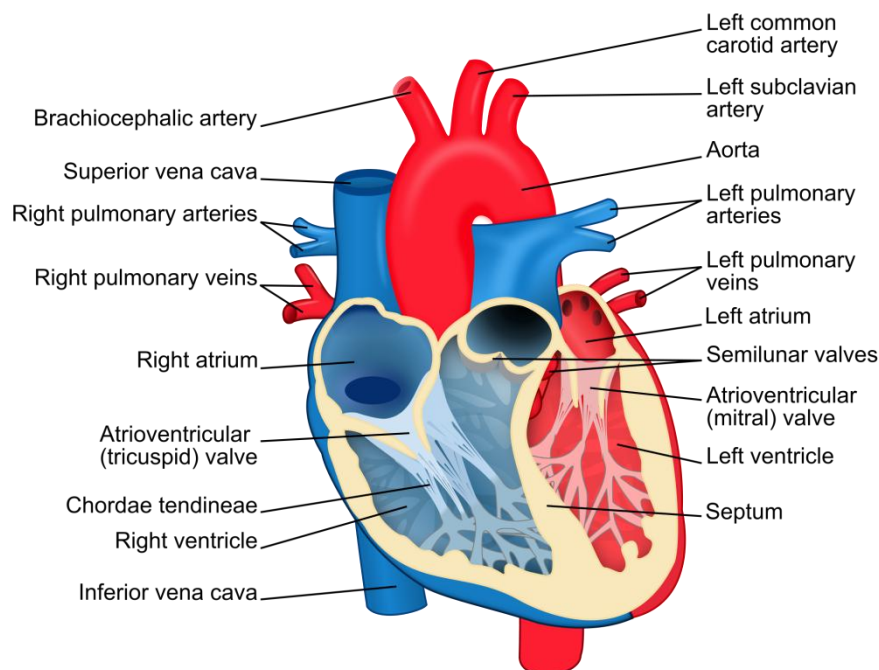


Figure 1.2: Structure diagram of the human heart from an anterior view. Blue components indicate de-oxygenated blood pathways and red components indicate oxygenated pathways. [4]

The heart’s function is to maintain a continuous blood stream throughout the body. Oxygenated blood is delivered to the organs via arteries and deoxygenated blood is returned to the heart from where it is directly pumped into the lungs for oxygenation. This circulatory system is essential for life. Without the transport of oxygen and nutrients with the blood stream, cells would be forced to die. But also the removal of carbon dioxide and waste products is very important. Moreover is the bloodstream responsible for the maintenance of the pH value and an important factor in transport of elements, proteins and cells of the immune system. [2]

The circulatory system can be subdivided into two smaller systems called the pulmonary circulation and the systemic circulation. The systemic circulation is in charge of transporting nutrients and oxygen to the organs, as described before. It starts in the left ventricle and ends in the right atrium. The pulmonary circulation is responsible for the substitution of CO₂ to O₂ in the lungs. It begins in the right ventricle and ends in the left atrium. [2] [3]

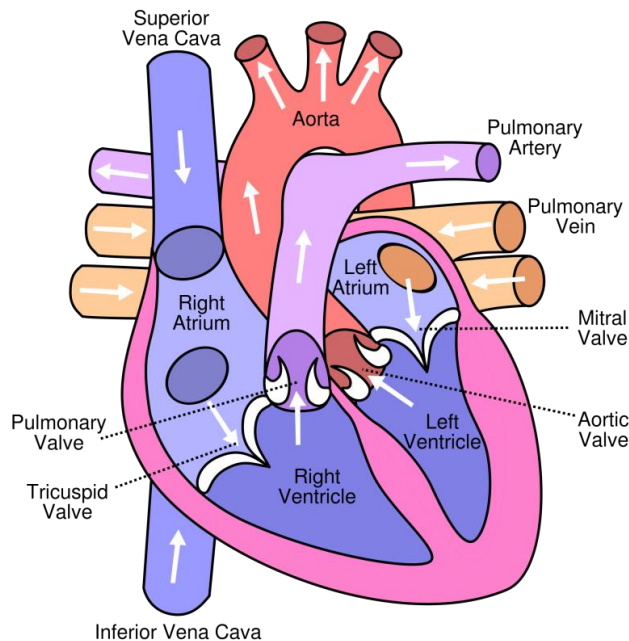


Figure 1.3: Circulation of blood through the human heart. The arrows indicate the direction of the blood flow. De-oxygenated blood from the organs flows first into the right ventricle and is then transported through the pulmonary arteries to the lungs. There it gets oxygenated and flows back through the pulmonary veins into the left ventricle. Afterwards the oxygenated blood is transported back to the organs. [4] [5]

Both left atrium – ventricle and right atrium – ventricle are synchronized with each other and are separated just by the cardiac septum. The right heart (first the right atrium then the right ventricle) takes the deoxygenated

venous blood from the organs and forwards it to the lungs. This transport is done via the pulmonary arteries (Figure 1. 3). The left heart (first the left atrium then the left ventricle) obtains oxygenated blood from the lung circulation and forwards it again to the body circulation. [2] [3]

1.2 Pulmonary arterial hypertension (PAH)

PAH is a severe rare dysfunction. Pulmonary hypertension (PH) is generally characterized by an increase of blood pressure in the pulmonary artery, pulmonary vein or pulmonary capillaries. PH does exist if the mean pulmonary arterial pressure (mPAP) exceeds 25 mmHg at rest or 30 mmHg under physical stress. An increased mPAP leads to a larger work load for the right ventricle. Generally the right ventricle is able to build up pressures of about 40 mmHg for a short period of time without decompensation. In case of a chronic dysfunction the right ventricle can tolerate even higher pressures, because of its possibility to adopt the condition. [6] [7]

The reasons for PH are very diverse. A reason can be an increase of resistance to the bloodstream because of vascular changes of the pulmonary vessels (pulmonary arterial hypertension, pulmonary venous hypertension). Other reasons can be hypoxic vasoconstriction, occlusion via emboli or left heart insufficiency coupled with an increase of pressure in the pulmonary circulation. [6] [7]

Patients suffering from this dysfunction have a strongly limited physical fitness. The disease leads to shortness of breath, dizziness, fainting and several other symptoms which mainly occur during exertion. Patients who are not administered an adequate therapy have a life expectancy of less than three more years after diagnosis. The main cause of death from PH is right ventricular failure. [6] [7] [8] [9]

The first international conference on PH, more precisely on PPH (primary pulmonary hypertension), was organized by the World Health Organization in 1973. At this conference the first clinical classification was proposed, which at this point had only two categories, PPH and secondary PH. From then on the classification has undergone a lot of changes and improvements. [10]

But it was only after twenty-five years in 1998 that a Second World Symposium on PH was organized and held in Evian, France. At this symposium the participants tried to reach a consensus on a new classification of PH. The attempt was successful and the new categorization had now five subgroups, with each of them showing similarities in pathologic and clinical features as well as therapeutic options. Such a clinical classification is very important in communicating about individual patients, in standardizing diagnosis and treatment and in conducting trials with homogeneous groups of patients, which could then give evidence about novel pathobiological abnormalities. This new and much broader classification allowed the initiation of clinical trials with much better defined groups of patients. [10] [11] Until now this fact has led to several approved medications for PAH. [10] [12]

Five years later in 2003, the 3rd World Symposium on PH was held in Venice, Italy. The main aim of this conference was to evaluate the 'Evian classification'. The architecture of the categorization stayed almost the same, although some changes were done, primarily in terms of nomenclature. [10] [11]

Another five years later in February 2008, the 4th World Symposium on PH held in Dana Point, California led to slight changes again, but the general philosophy and organization of the Evian-Venice classification (Evian classification, 1998 and Venice

classification, 2003) were maintained. Some slight modifications were done on Group 1 (PAH), which were mainly due to new scientific findings from the years before. [10]

In total there have been four world symposia on PH so far, where clinical classifications for the disease similarities in pathophysiologic mechanisms were defined. [10]

A complete list of Dana Point clinical classifications of PH and the particular causes can be found in Table 1. 1.

Table 1. 1: Updated Clinical Classification of Pulmonary Hypertension (Dana Point, 2008), ALK1 = activin receptor-like kinase type 1; BMPR2 = bone morphogenetic protein receptor type 2; HIV = human immunodeficiency virus. [10]

Updated Clinical Classification of Pulmonary Hypertension (Dana Point, 2008)

1. Pulmonary arterial hypertension (PAH)

- 1.1. Idiopathic PAH
- 1.2. Heritable
 - 1.2.1. BMPR2
 - 1.2.2. ALK1, endoglin (with or without hereditary hemorrhagic telangiectasia)
 - 1.2.3. Unknown
- 1.3. Drug- and toxin-induced
- 1.4. Associated with
 - 1.4.1. Connective tissue diseases
 - 1.4.2. HIV infection
 - 1.4.3. Portal hypertension
 - 1.4.4. Congenital heart diseases
 - 1.4.5. Schistosomiasis
 - 1.4.6. Chronic hemolytic anemia
- 1.5 Persistent pulmonary hypertension of the newborn
- 1'. Pulmonary veno-occlusive disease (PVOD) and/or pulmonary capillary hemangiomatosis (PCH)

2. Pulmonary hypertension owing to left heart disease

- 2.1. Systolic dysfunction
- 2.2. Diastolic dysfunction
- 2.3. Valvular disease

3. Pulmonary hypertension owing to lung diseases and/or hypoxia

- 3.1. Chronic obstructive pulmonary disease
- 3.2. Interstitial lung disease
- 3.3. Other pulmonary diseases with mixed restrictive and obstructive pattern
- 3.4. Sleep-disordered breathing
- 3.5. Alveolar hypoventilation disorders
- 3.6. Chronic exposure to high altitude
- 3.7. Developmental abnormalities

4. Chronic thromboembolic pulmonary hypertension (CTEPH)

5. Pulmonary hypertension with unclear multifactorial mechanisms

- 5.1. Hematologic disorders: myeloproliferative disorders, splenectomy
 - 5.2. Systemic disorders: sarcoidosis, pulmonary Langerhans cell histiocytosis: lymphangioleiomyomatosis, neurofibromatosis, vasculitis
 - 5.3. Metabolic disorders: glycogen storage disease, Gaucher disease, thyroid disorders
 - 5.4. Others: tumoral obstruction, fibrosing mediastinitis, chronic renal failure on dialysis
-

1.3 Treating PAH

Most progress for the medical treatment of PAH was made during the four World Symposia on PH, as these events served as a forum for mutual scientific exchange. On the one hand these symposia give an opportunity to present state-of-the art research about the pathobiological and clinical aspects of PAH and on the other hand they are a place for the international scientific community to explore future directions of research and collaboration. [13]

The common definition of PH has been simplified recently and is now based on currently available evidence. PH is defined as “a resting mean pulmonary arterial pressure (mPAP) >25 mmHg, or an mPAP with exercise >30 mmHg.” [14]

Nevertheless this updated definition has weaknesses again, because the level, type and posture of the mentioned exercises were not specified in more detail. Moreover the PAP varies with age. [14]

Less than twenty years ago, the treatment of PAH was mainly done through empiric studies and usually ineffective. The molecular mechanisms and pathogenesis of the disease were hardly understood. But the treatment of PAH has dramatically advanced over the last two decades. There were a lot of clinical studies demonstrating efficacy of several therapies. Moreover the treatment has evolved from a continuous intravenous (IV) delivery to oral or inhaled drug delivery systems. As it is also for other complex diseases, targeting a single pathway is unlikely to be uniformly successful. [12] [13]

The knowledge about the pathomechanisms that participate in PAH has significantly increased over the last decade. At the Dana Point Meeting experts presented their most novel findings on vascular remodeling characteristics. Vascular remodeling may have its origin in disruptions or alterations in lung circulation. Moreover experts stated that inflammation is involved in all of the mechanisms of vascular remodeling. Generally “PAH is characterized by cellular changes in the walls of pulmonary arteries.” [8] “PAH consists of a group of heterogeneous but distinct disorders characterized by complex proliferation of the pulmonary vascular endothelium and progressive pulmonary vascular remodeling that leads to right ventricular failure and death.” The “development of PAH entails a complex, multifactorial pathophysiology”. The “increasing insight into the pathobiology has led to a ‘multiple hit’ hypothesis to

explain the development and progression of clinical PAH. A complex interplay of genetic mutations, exogenous exposures, and acquired disease states can predispose to PAH.” Processes involved in later stage of the disease are vasoconstriction, cellular proliferation and thrombosis. [9] [12] “These processes are influenced by a complex and dysregulated balance of vascular effectors controlling vasodilatation and vasoconstriction, growth suppressors and growth factors, and prothrombotic *versus* antithrombotic mediators [12].” Details are listed in Figure 1. 4.

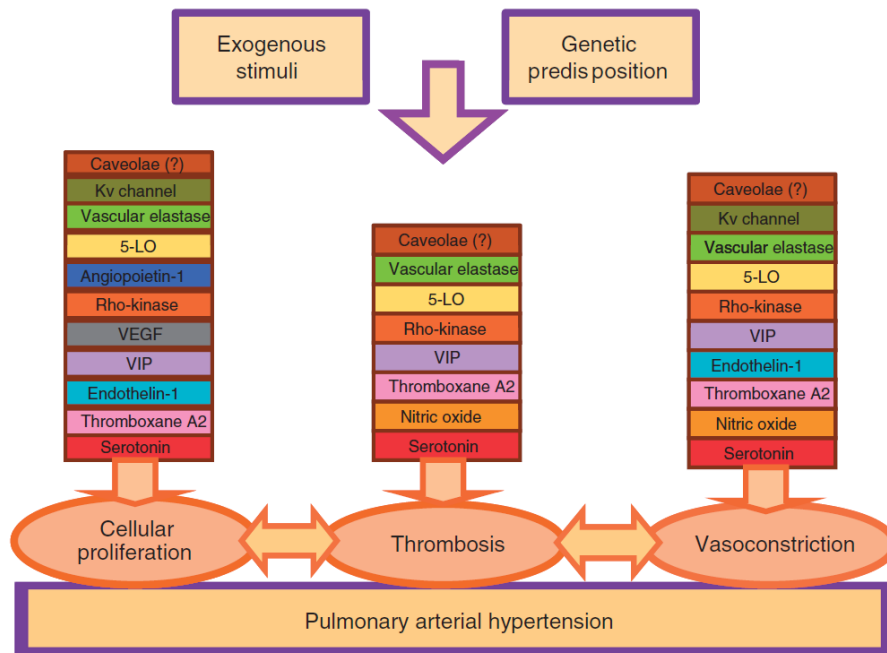


Figure 1. 4: Pathogenesis and pathobiology of pulmonary arterial hypertension. 5-LO, 5-lipoxygenase; VEGF, vascular endothelial growth factor; VIP, vasoactive intestinal peptide. [12]

There is presently no cure for PAH. Target of currently applied therapeutics are the “mediators of the three main biologic pathways that are critical for its pathogenesis and progression”. [12]

These three major classes are endothelin receptor antagonists, phosphodiesterase-5 inhibitors and prostacyclin derivatives. All three classes have shown to have positive effects on hemodynamic parameters and to improve functional capacity and exercise tolerance. [8] [12] With this currently available therapeutics clinicians can improve life expectancy and quality of life for many patients with PAH. [8]

The first group of drugs is the endothelin receptor antagonists (ERAs). ET-1 is a very potent vasoconstrictor and has also effects on the proliferation of vascular smooth muscle cells. So blockage of the endothelin receptor is one option. There are several

ERAs approved and available at the moment, which greatly differ in their selectivity towards the receptors. FDA approved examples are bosentan, ambrisentan and sitaxsentan. [12]

The second group are phosphodiesterase-5 inhibitors which support locally produced nitric oxide (NO). By inhibiting the breakdown of NO's second messenger, cyclic guanosine monophosphate (cGMP) it promotes pulmonary vasodilation and inhibits smooth muscle cell growth. [12] [15] Two by the FDA approved drugs are sildenafil and tadalafil. Interestingly PDE-5 inhibitors like ERAs have no observed effect on mortality. [12] [16]

The third group and for our work the most interesting one are the prostanoids. The level of prostacyclin synthase is reduced in patients with PAH, which in turn leads to a diminished level of available prostacyclin. As a consequence there is no "adequate vasodilation and loss of the antiproliferative effects on the smooth muscle cells in the vascular wall." [12] [9] Because of their capability of acting "as potent pulmonary artery vasodilators, prostanoid medications have been used in the treatment of PAH for over 15 years." The first of the FDA approved drug for PAH was epoprostenol, a prostanoid. [12]

Currently there are a few other longer-acting FDA approved prostacyclin analogs available for different types of application. There is for example "treprostinil, approved for subcutaneous and intravenous use in the USA; iloprost, approved for inhaled use in the USA and for intravenous and inhaled use in Europe; and Beraprost®, an oral medication approved in Japan" [12].

Prostacyclin, as a drug also known as 'epoprostenol', is one of the best studied medications. It is capable of lowering the mPAP and the pulmonary arterial resistance. A major disadvantage of this drug is the permanent need for administration via intravenous access. [12] This may lead to infections of the intravenous catheter. As the drug is administered directly into the bloodstream, there is a lack of pulmonary selectivity and this can lead to severe side effects like flushing, cough, headache, flu syndrome, nausea, hypotension and some others. Moreover this implicates a bad drug targeting and rising tolerance leads to progressive increases in the dose. [17] In addition prostacyclin itself is chemically unstable at physiological temperatures and pH and is degraded rapidly to an inactive breakdown product. [18]

Treprostinil is a prostacyclin analog and stable at room temperature, but has the same pharmacologic profile as epoprostenol. Because of its much longer half-life it can be administered subcutaneously, which is a great advantage. Beraprost is absorbed quite fast after administration via tablets and has an elimination half-life of 35-40 min. [12]

Iloprost is an inhalable prostanoid drug. It causes selective pulmonary vasodilation and improves hemodynamics and exercise capacity [17]. The administration route with a nebulizer and the “low incidence of adverse events” are definitely immense advantages of this medication. The aim was to combine the beneficial effects of a prostanoid drug with an inhalative application [17]. A quite big drawback is the high required frequency of administration for the inhaled iloprost. [12] Another major advantage of prostanoid treatment is that a significant mortality benefit could be observed. [16]

Generally it is necessary to state that more and more therapeutic options are available for the treatment of PAH, but a quick and reliable diagnosis method has to be developed to ensure early and accurate diagnosis. [8] Without this as a prerequisite all the investigated therapeutics are useless. Fortunately there have also been great advances in the imaging techniques and biomarkers, which can be used to screen patients for the disease. [14]

A future challenge will be to develop methods to measure and compare the relative effects of different treatment options. This is especially necessary as a randomized, placebo-controlled patient group using survival as an end point would be unethical to perform in PAH. The best alternative would be a noninvasive marker of disease severity like a biomarker or a physiological test. [13]

To sum up the “treatment of PAH with prostanoids reduces mortality and improves multiple other clinical and hemodynamic outcomes. ERAs and PDE5 inhibitors improve clinical and hemodynamic outcomes, but have no proven effect on mortality. The long-term effects of all PAH treatment requires further study.” [16]

1.4 Iloprost

The therapy of PAH patients with continuously intravenously administered PGI₂ and analogues has been successfully applied for decades, but serious side effects increased the need for an alternative route of application, namely inhalation. [9]

Iloprost is a synthetic and more stable analogue of the naturally occurring prostacyclin (PGI₂). [17] [9] (see Figure 1. 5) It is “stable at room temperature and in ambient light at pH 7.4 and offers a longer half-life (20-25 min) compared to aerosolized PGI₂ or epoprostenol” [9]. Iloprost is associated with a longer duration of vasodilation. When administered inhalative to patients with PH, the potency of the drug is comparable to that of PGI₂, but the effects last much longer. With iloprost the vasodilation lasts for 30 to 90 minutes, with PGI₂ only for 15 minutes. [17] Because of severe side effects with intravenous application, the use of inhaled iloprost has become a mainstay in PAH therapy. It is currently used extensively in Europe and the US for the treatment of PAH. [9] [18] Still there is the necessity for 6 to 9 inhalations per day, which can be seen as one of the largest drawbacks. [9]

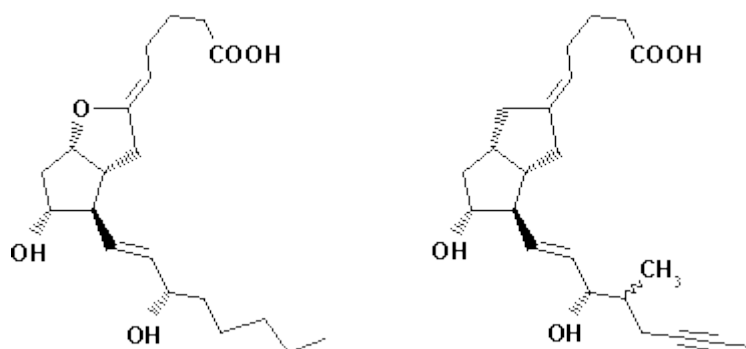


Figure 1. 5: Chemical structure of prostacyclin (left) and iloprost (right). [19]

When iloprost is inhaled it is deposited in the lung parenchyma during normal breathing. The effect of inhaled iloprost is afterwards terminated by β -oxidation and the production of an inactive degradation compound. [9]

Prostacyclin and its analogues like iloprost, elicit their pharmacological and biochemical effect when binding and activating specific receptors. There are many identified naturally occurring prostanoid receptors e.g. IP, EP₁, EP₂, EP₃, EP₄, DP₁, FP and TP receptor. The IP, EP₂, EP₄, DP₁ receptors are classically known to be G-protein coupled receptors. [18] Iloprost has a very high binding affinity to the membrane-associated IP receptor and shows a very high activity in elevating

cyclic AMP (cAMP) levels. The cyclase activity is increased 10- to 15-fold. [18] [20] [21] This leads to relaxation of the smooth muscle cells and in turn to relaxation of vessels. [22] Progress was made in terms of inhalation devices. The inhalation time could be reduced from 15 minutes per inhalation with the air-jet nebulizer to 4 minutes with the use of an ultrasonic nebulizer. [9] “Inhaled iloprost is an effective therapy for patients with severe pulmonary hypertension [17].”

1.5 The human lungs

The human lungs are built up by a system of airways, which diminish in diameter from the trachea, to the bronchi and bronchioles and finally to the alveolar ducts and sacs, the actual sites of gas exchange. There is a big difference between cells in the airways (trachea to bronchioles) and the cells of the alveolar epithelium. The airways are composed of mucus secreting and ciliated cells which are responsible for the mucociliary clearance mechanism of the lungs. On the contrary the alveoli are built up by Type I cells, which are responsible for stability of the alveolar wall and Type II cells, which mainly produce lung surfactant to lower the surface tension and promote gas exchange. [1] [23] [24]

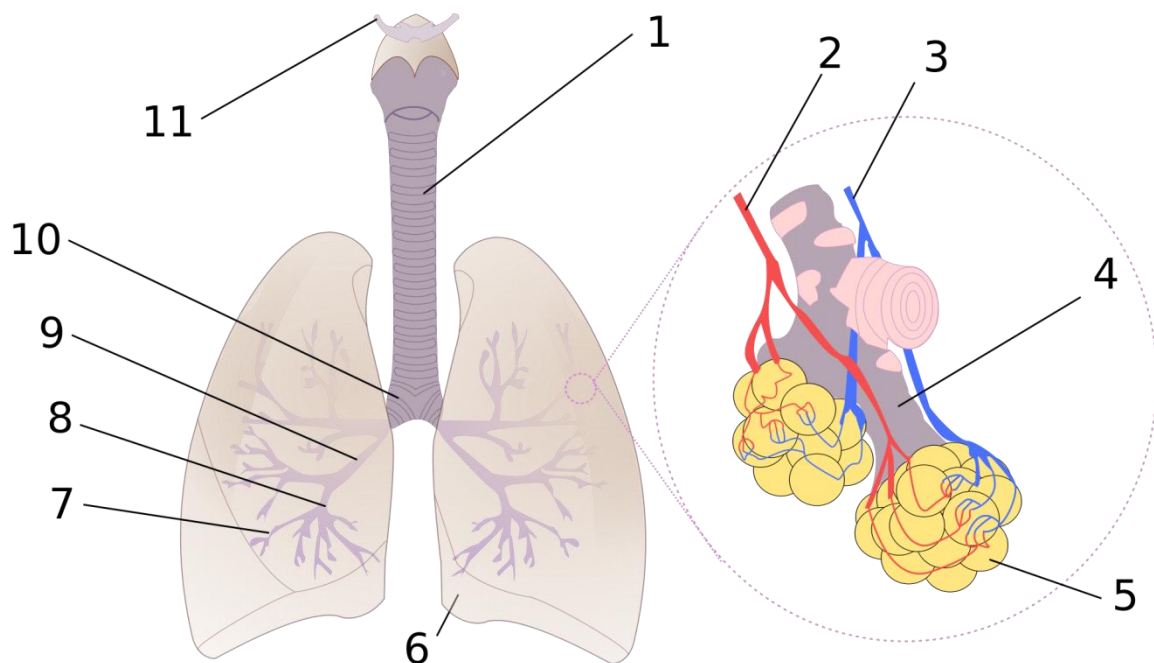
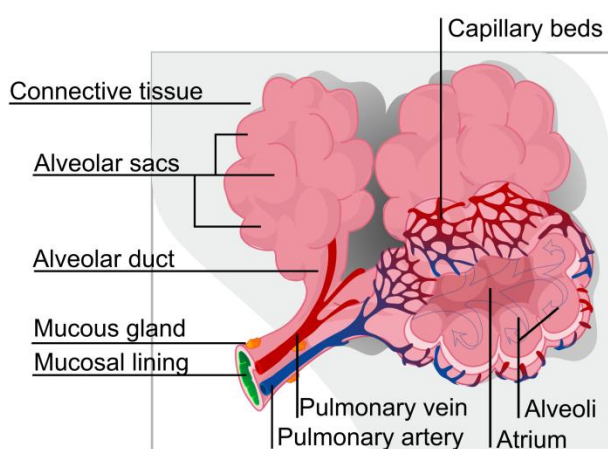


Figure 1. 6: Graphical representation of the human lung (left) and detailed depiction of the alveoli (right). Indicated numbers stand for: 1: Trachea 2: Pulmonary vein 3: Pulmonary artery 4: Alveolar duct 5: Alveoli 6: Cardiac notch 7: Bronchioles 8: Tertiary bronchi 9: Secondary bronchi 10: Primary bronchi 11: Larynx. [25]

There are big differences between the structures of the airways and the alveolar regions. First the thickness of the epithelium layer decreases from 50-60 μm in the airways to 0.2 μm in the alveolar region. Second the volume that is comprised by the conducting airways is approximately 150 mL that of the respiratory zone between 2.5-3.0 L. Third the surface area is completely different. The alveolar region makes up the vast majority of lungs surface area with approximately 100 m^2 . The upper airways comprise only a few m^2 . [3] [23]

1.6 The human lungs as organs of absorption

Over the last decades the understanding of the absorption properties of the lungs has increased steadily. This is one of the reasons why the lungs as site of drug deposition are getting more and more into the focus of research. A very large surface area, decreased metabolic activity (relative to the gastrointestinal tract), a very thin alveolar epithelium in the lower airways and a rich blood supply are ideal prerequisites for the delivery of active compounds to the human body. Drugs are absorbed rapidly and show high bioavailability. Another important advantage is that



the administration to the lungs is a non-invasive method. The alveolar regions appear to be the optimum site for absorption of many drugs, especially macromolecules like peptides or proteins. Smaller hydrophobic compounds are absorbed throughout the lungs. [23] [26]

Figure 1. 7: Graphical representation of a pulmonary alveolus. "An alveolus is an anatomical structure that has the form of a hollow cavity. The pulmonary alveoli are spherical outcroppings of the respiratory bronchioles and are the primary sites of gas exchange with the blood. [24]

Despite all these great advantages, the lungs present some barriers against systemic drug delivery. The organ has a highly branched architecture, which makes it hard to efficiently deliver aerosol to the lower lungs where most of the drugs are absorbed [3] [23]. Particles with sizes between 1-5 μm are deposited best in the lower lungs. Bigger particles remain in the throat, smaller ones are exhaled again. But a lot of

other factors play a major role in deposition “including the size, density, shape, velocity, charge, hygroscopicity and surface properties of the particles” as well as the patient’s breathing pattern, age, sex, anatomy, lung volume and disease state. [23]

Other physiological barriers are the alveolar epithelial cells, which are only permeable to water, gases and other lipophilic substances and the mucociliary clearance mechanism in the trachea-bronchial tree, which is responsible for the removal of unwanted and potentially irritable particles including insoluble drugs or insoluble drug delivery systems. Macrophages represent a further barrier, as insoluble drugs and carriers in the alveolar region will rapidly be taken up and removed. [23]

Nevertheless, the advantages of pulmonary delivery over other routes are predominant. “Drug metabolizing enzymes are present in much lower concentrations in the lungs than in the gastrointestinal tract [23]”. [26] The bioavailability is higher than through oral delivery, mainly due to lower levels of drug efflux in the lung epithelium than in gastrointestinal epithelium. [23] [26]

Using the lungs as site of systemic drug delivery has great advantages compared to other routes, but also presents barriers that future research has to overcome. Considering the pros and cons of pulmonary delivery one can say that for certain drug types and diseases this route offers a great new field of enhanced possibilities.

1.7 Liposomes

Liposomes are artificially produced lipid vesicles, which are mainly composed by lipid bilayers. Liposomes should not be confused with micelles or reverse micelles which are only composed of a monolayer. They can consist of one or several concentric membranes. [27] [28] Their size ranges from 20 nm to several μm . The thickness of the membrane is

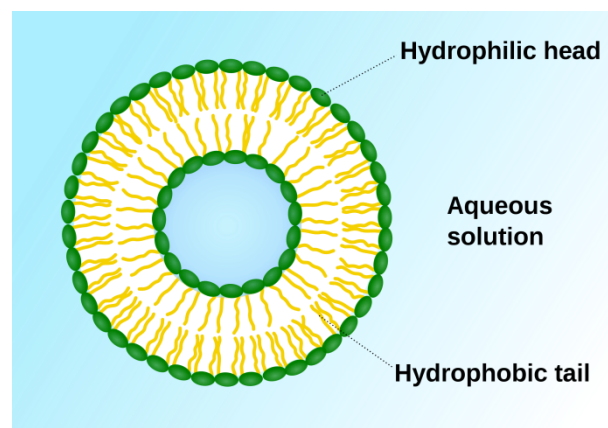


Figure 1. 8: Simple cross-section scheme of a liposome. [59]

around 4 nm. The first one who observed and recognized the important characteristics of liposomes was Alec Bangham in 1965. He realized that liposomes are able to encapsulate solvent into their interior, that they are osmotically active and that they show completely different permeability characteristics to various molecules

and ions. His early work played a major role in understanding the importance of surface charge and he already foresaw several potential applications. [27] [29] [30]

Liposomes can be prepared by the hydration of a lipid film or lipid cake, the ethanol injection method or disruption of biological membranes through sonication. The most frequently used method is the hydration of prepared lipid films. [27] [28] [29]

During the hydration process the lipid sheets become fluid, swell and detach from the surface during agitation to self-close and build large, multilamellar vesicles (LMVs). To reduce the size of the LMVs energy input is necessary either in the form of sonication or mechanical energy through filter extrusion. The results are either small unilamellar vesicles (SUVs) or large unilamellar vesicles (LUVs). The procedure of hydrating a prepared lipid film and subsequent size reduction is usually the same totally independent from the lipid composition. [27] [29]

Basically there are no limits for the choice of lipids used for the preparation of liposomes. One can use naturally occurring or synthetic phospholipids (e.g. DPPC), sterols (e.g. cholesterol), artificial compounds (e.g. DOTAP) or other long-chain hydrocarbon compounds (e.g. stearylamine). Another great advantage of artificially prepared liposomes is that one can easily influence their properties and physiological targeting, which is of special interest when it comes to medical applications. It is possible to influence the surface charge by using positively or negatively charged lipids. The rigidity of the bilayer can be altered by using different ratios of cholesterol and the transition temperature (T_c) can be easily influenced by using different lipids with higher/lower T_c . Moreover it is possible to protect liposomes from rapid degradation and the attack of macrophages by shielding them with polymers (e.g. Polyethylene glycol, PEG). These so-called stealth liposomes are not recognized by the body's immune system, are inert and have a longer circulatory life for their drug delivery (see Figure 1. 9). A further possibility is to attach ligands (e.g. antibodies or antigens) to the liposomes' surface to target very specific cell types in the body. [27]

1.8 Liposomes as drug delivery system

A major field of application is the administration of pharmaceutical drugs. Over the past few decades, there have been a lot of efforts to develop new drug delivery systems in order to improve the poor benefit/risk ratio. But this is a very complex challenge as it combines so many different scientific fields like physical, organic and

analytical chemistry, biology, pharmacology, toxicology, medicine and further disciplines. Design and optimization of liposomal formulations for medical applications requires skillful concepts and knowledge. [27] [31] [30]

Generally the administration of liposomal drugs wants to achieve the following goals:

- 1) Favorably alter the pharmacokinetics.
- 2) Protect against degradation.
- 3) Reduce distribution to sensitive tissues and hence toxicity.
- 4) Enhance distribution to target tissues and hence efficacy. [31]

Liposomes encapsulate regions of aqueous solution with a lipid bilayer and therefore are able to transport hydrophilic molecules within their aqueous core and prevent those water soluble compounds from emerging outside into the bulk fluid. But also hydrophobic molecules can be transported, as these compounds are dissolved within the membrane in the hydrophobic area. This fact offers great possibilities for drug delivery. When reached the site of action the liposomes deliver its contents through different mechanisms. [27] [30]

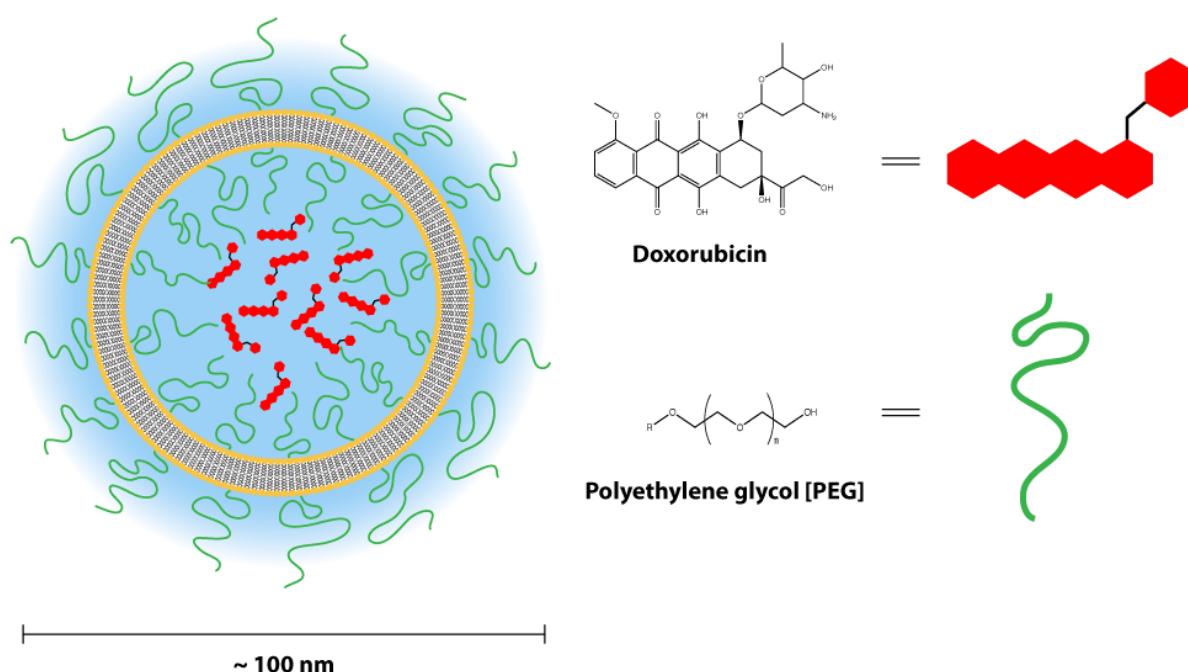


Figure 1. 9: Graphical representation of a "stealth liposome", consisting of a lipid bilayer which is coupled to the polymer PEG. The active drug, in this case doxorubicin used in cancer chemotherapy, is enclosed in the interior. The polymer binds a water cloud and hides the liposome from the immune system. [32]

As already mentioned before, there are several options to alter the characteristics of liposomes. The probably most important for medical uses is the protection from the human immune system. This is achieved by coupling a polymer to the lipids that build up the liposome. This polymer binds a lot of water creating a water cloud around the liposome, which hides it from the immune system. [27]

The general goals of altering the properties of liposomes are:

- (1) Prolonged blood circulation, to provide enough opportunities to encounter the region of disease. (mainly for intravenous delivery)
- (2) Adequate access to the pathological tissue and target cells
- (3) Ability of the liposomes to arrive at the target site with the encapsulated drug and to release it in an active form.

The most important factor is to design a “composition capable of retaining the drug in the liposomes during prolonged circulation but releasing it once the liposomes have accumulated in the site of pathology [31]”. Challenges like large-scale preparation, stability and sterility were mainly solved. But a further very critical issue is the still insufficient control of liposome biodistribution and stable entrapment of the encapsulated drug. [33]

Currently there are already a few FDA approved liposomal drug delivery systems available like liposomal amphotericin B (AmBisome®), liposomal daunorubicin (DaunoXome®), liposomal doxorubicin (Doxil®) and several others. [31] [33]

1.9 Liposomes for drug delivery to the lungs

The lung is an attractive organ for the delivery of drugs either for systemic or local therapy. As it was already mentioned before has the lung several great advantages including non-invasive access, a huge surface area and a rich blood supply. The drugs have to be applied by the inhalation of a liquid aerosol, a dry powder aerosol or a pressurized metered dose aerosol. The site of deposition depends on the particle size, with only very small particles about 1 μm being delivered to the alveoli. Material delivered to the alveoli is cleared relatively slowly. This is the main reason why a delivery to the alveolar ducts or the alveoli is desirable. [26] [27]

Generally it can be said that particles with diameters between 1 – 5 μm are likely to deposit in the airways. Larger particles will stick in the throat and trachea during inhalation. Particles smaller than 1 μm are likely to be exhaled again and therefore are inefficient and effectless. [26]

A general disadvantage of parenteral drug administration is the absorption into systemic circulation, where drugs can cause unwanted systemic toxicity and thereby having a lower concentration at the desired site of action. [27]

Liposomes can, if designed properly, reduce these unwanted systemic side effects and be a system for sustained release. The release rate can be controlled by liposome composition. “The duration of the drug action can be varied almost two orders of magnitude by preparing liposomes with appropriate compositions [27]”. [29]

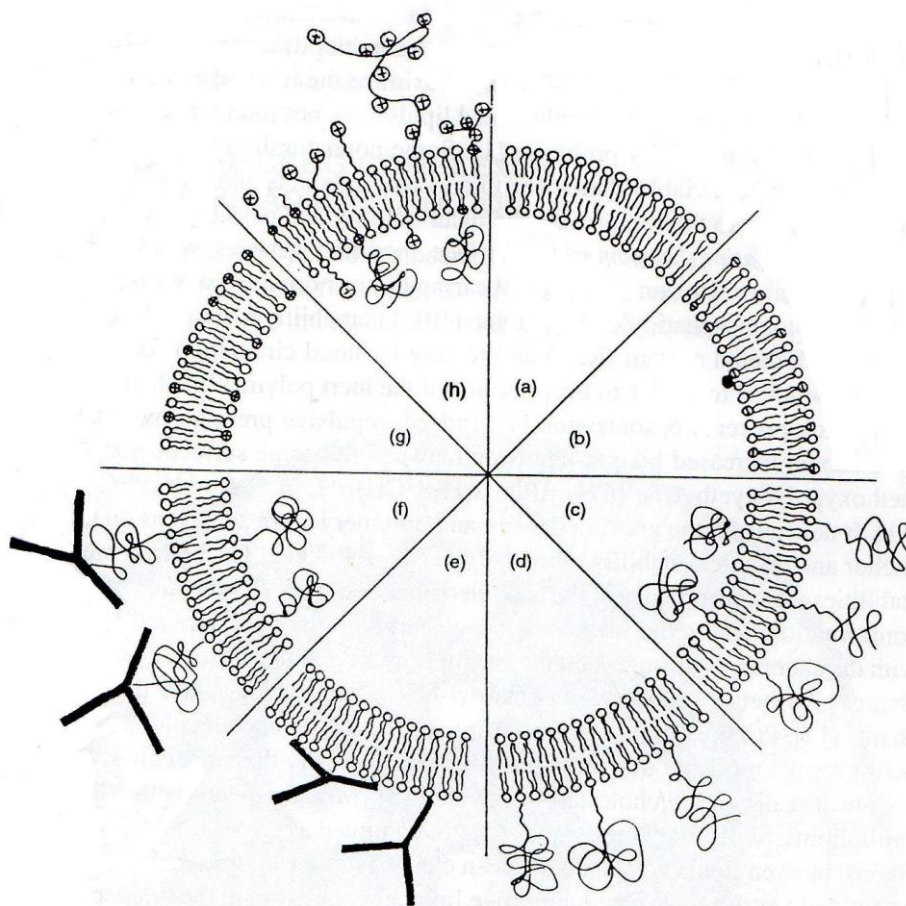


Figure 1. 10: Schematic representation of liposome classification according to their surface properties. (a) neutral, (b) negatively charged, (c) stealth liposome with polymer brush on both sides and (d) on the outside only, (e) targeted liposome with antibody, (f) targeted stealth liposome with antibody, (g) positive charge using cationic surfactants, (h) positive groups attached to spacers and polyelectrolytes. [29]

The efficacy of inhaled drugs is dependent on its absorption across the lung epithelial layer and the localization to its pharmacological site of action. The various ways that inhaled drugs can take and the barriers that these aerosols have to cope with are summarized in Figure 1. 11. Mostly these are defense mechanisms of the lung to deal with extrinsic particles. Some of these mechanisms include a highly effective mucociliary clearance or macrophages in the alveolar airspace. [26]

The advantages of liposomes as carrier systems over aerosol delivery of non-encapsulated drugs are:

- possible transport of poorly soluble drugs
- providing a sustained release drug reservoir
- prevent irritation of the lung tissue and reduce the toxicity of drugs
- targeting of specific areas or cell types via ligand/antibody binding
- absorption via the epithelium to systemic circulation [26]

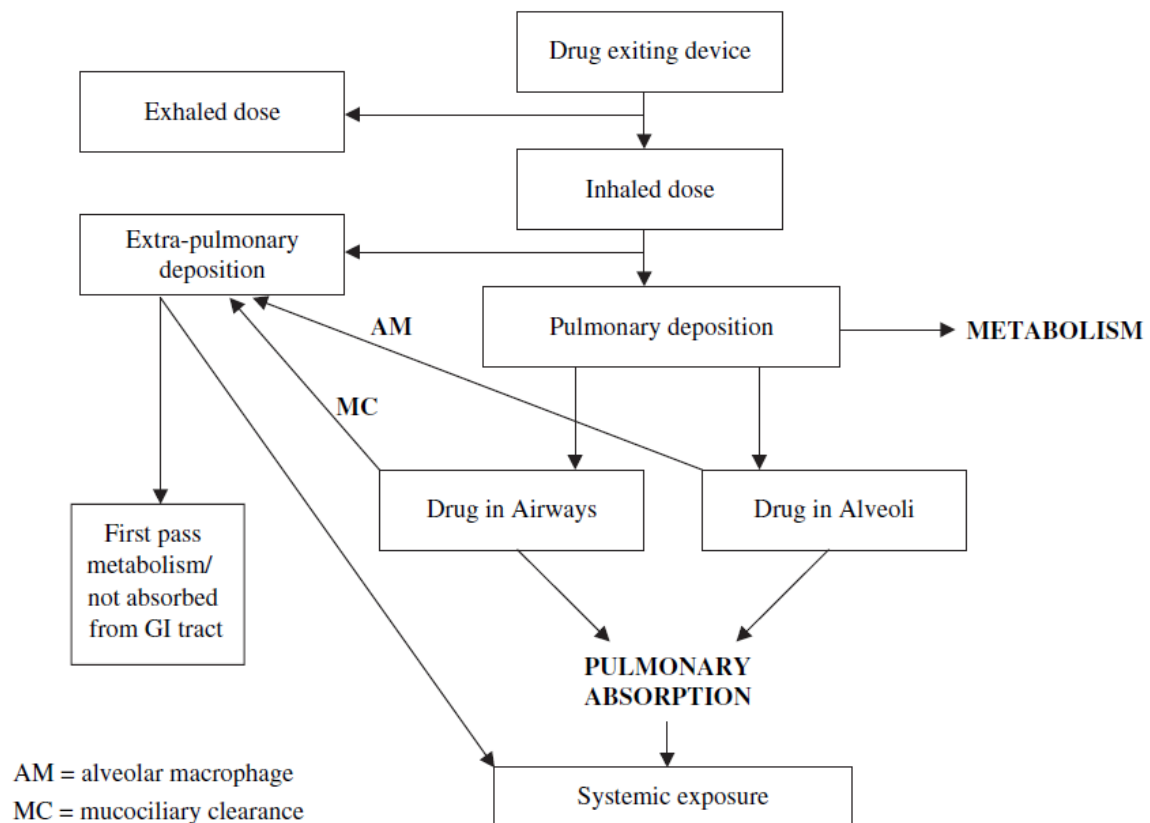


Figure 1. 11: Schematic illustration of the fate of an inhaled drug. [26]

So far, a huge number of different nebulizer devices with various liposomal formulations have been tested. The results strongly depended on the applied nebulizer device and liposomal formulation. For some formulations the stability and

mass output gave promising results. This is also the reason why various inhalative liposomal drugs are currently in pre-clinical assessments. Among them is liposomal amphotericin B (antibiotic), 9-N-Camptothecin (anticancer drug) or gene lipid complexes for the treatment of cystic fibrosis. Mainly for areas where the drug load has to be protected or the drug's release should be sustained, liposomal aerosols will be the choice in the future. [26]

1.10 Nebulizers

A nebulizer is a device that can convert a liquid into aerosol droplets suitable for patient inhalation. Nebulizers are used for the treatment of a number of pulmonary diseases e.g. cystic fibrosis, COPD or asthma.



Figure 1. 12: Drawing of the first pressurized inhaler invented by Sales-Giròns in 1858. The aerosol was produced near the patient's mouth by pumping liquid through an atomizer. [34]

The first pressurized inhaler was invented by Sales-Giròns in France in 1858. The device used pressure to nebulize the liquid, which was filled into a reservoir. The working principle of the pump was comparable to a bicycle pump. When pulling the pump up, the liquid was taken in and afterwards pressed through an atomizer to produce a mist near the patient's mouth. This first very primitive form of a nebulizer was used to treat respiratory diseases by inhaling different solutions believed to have a curative effect. [34]

A few years later, in 1864 the first steam-driven nebulizer was invented in Germany. This device used the Venturi principle for aerosol generation. The importance of droplet size was not recognized at that time, so the efficacy of this first nebulizer device was quite low. [34]

The first electrical device was invented in the 1930s. It produced an aerosol from a medical liquid driven by a compressor. But this type of inhaler was not very widespread at that time. Many people stuck to use a cheaper hand-driven device.

In 1964 another type of electrical nebulizer was introduced as alternative to the compressor-driven inhaler, the so-called ultrasonic nebulizer. [34]

The most novel type of nebulizers was introduced to the market just a few years ago. These are the so-called vibrating mesh inhalers, which use a completely different technique as the other two electrical principles.

1.11 Working principles of nebulizers

Nebulizers use different physical principles to produce inhalable aerosols. In case they use compressed air they are so-called air-jet nebulizers. But a nebulizer can also use ultrasonic power, so-called ultrasonic nebulizers or the mechanical energy of a high frequency vibration, the so-called vibrating mesh nebulizers.

All three types of nebulizers convert a medical solution or suspension into very small aerosol droplets that can be directly inhaled by the patient through a mouthpiece of the device. For an inhalation therapy the produced droplets have to have a certain size to be effectively administered into the lung. This is due to the lungs anatomy and was already discussed in more detail before.

(1) Air-jet nebulizer

As already mentioned before, jet nebulization was the first technical operation for aerosol production. The jet nebulizer uses a gas flow either from a compressor or a central air supply. The chamber of the nebulizer is filled with the drug solution. The flow of gas is driven up a tube through the center of the chamber, creating an area of low pressure, which draws the drug up to the top of the chamber itself. While passing through this very small aperture the liquid drug is atomized. The aerosol produced is then forced at very high speed against the so-called baffle, which recycles the large particles. Almost 90% of the produced droplets are impacted by the baffle and forced onto the side of the nebulizer to be recycled. The mist of appropriately sized particles of the drug flows then out of the chamber and is ready for inhalation. [26] [35] (see Figure 1. 13)

Drug loss occurs mainly due to incomplete nebulization of the applied drug solution. This part is trapped as residual mass in the nebulizer. Another reason is the loss during exhalation. [35]

The applied air-jet nebulizer for this thesis was the MicroDrop® *Pro* (MPV Truma, Putzbrunn, Germany) operated with the MicroDrop® compressor (see chapter 2). This nebulizer has a continuous output during the patient's inhalation and exhalation phase.

Jet nebulizers can work with almost all types of liquids (e.g. solutions, suspensions, oils, etc.), but have a quite big dead volume and exert high shear forces on the drug compounds. This can lead to partial destruction of active drug molecules. They are often portable and disposable, but the compressors are bulky and noisy. [35]

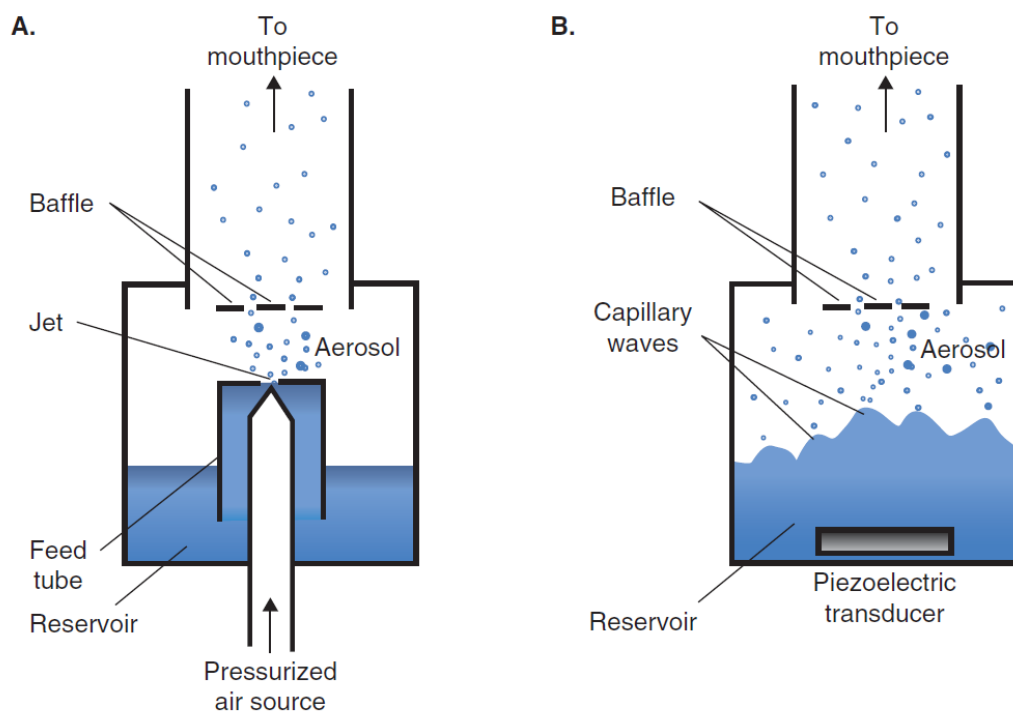


Figure 1. 13: Schematic illustration of working principles of a typical (A) air-jet nebulizer and (B) ultrasonic nebulizer.[36]

(2) Ultrasonic nebulizer

The ultrasonic nebulizer was a new technology introduced to the market in 1964 as mentioned beforehand. The ultrasonic nebulizer uses the vibration of a piezo-electric crystal to produce an aerosol. The piezo-electric element is forced to vibrate (1.2-2.4 MHz) and transmits its energy to a liquid drug. This transmission can be either directly or through a transmitter liquid, which in turn gives the energy to the liquid drug. This may be important because of heat produced during vibration. In case the

drug is very heat sensitive this could have severe effects on the drug's stability. The applied vibration then generates a liquid fountain comprising small and large droplets. Again this aerosol is first forced against a baffle to recycle large droplets. The small inhalable fraction is stored in the chamber to be inhaled by the patient. [26] [35] (see Figure 1. 13)

Drug loss also occurs for this type of nebulizer as some residual mass is trapped in the nebulizer. The applied ultrasonic nebulizer for this thesis was the Optineb®-ir (NEBU-TEC, Elsenfeld, Germany) operated with a frequency of 2.4 MHz. This nebulizer did not work continuously but with time intervals to enable the inhalation of the produced aerosol cloud out of the chamber. Moreover it had a water interface, so the drug solution was not directly in contact with the piezo-electric element and thus protected from emerging heat.

Generally ultrasonic nebulizers do not aerosolize liquids with high viscosity or high surface tension. They are silent but often bulky. [35]

(3) Vibrating mesh nebulizer

The most novel types of nebulizers are the so-called vibrating mesh nebulizers. They use the deformation and vibration of a mesh plate, which is in direct contact with the liquid drug solution, to produce droplets. The mesh plate is connected to an annular piezo element that is used to produce a vibration around the mesh. This leads to deformation of the mesh into the liquid side, therefore pumping small droplets through the holes of the mesh. Only approximately 10 mm in diameter these mesh plate contains over 4,000 precision formed tapered holes. As energy is applied the mesh plate vibrates around 120,000 times per second. This rapid vibration causes each aperture to act like a micropump drawing liquid through the holes to form consistently sized droplets. [35] (see Figure 1. 14)

The applied vibrating mesh nebulizer for this thesis was the eFlow® rapid (PARI, Starnberg, Germany) operated with a frequency of 117 kHz. Its metallic mesh was obtained by a high-speed laser drilling process. The nebulizer consists of a valved reservoir and an AC power adapter. The aerosol is produced horizontally and in very low velocity. This aerosol cloud is ready for inhalation. This nebulizer works continuously and owns an inhalation and exhalation valve. [35]

Vibrating mesh nebulizers are small enough to be carried, have a low weight and are completely silent. So they are most convenient for patients.

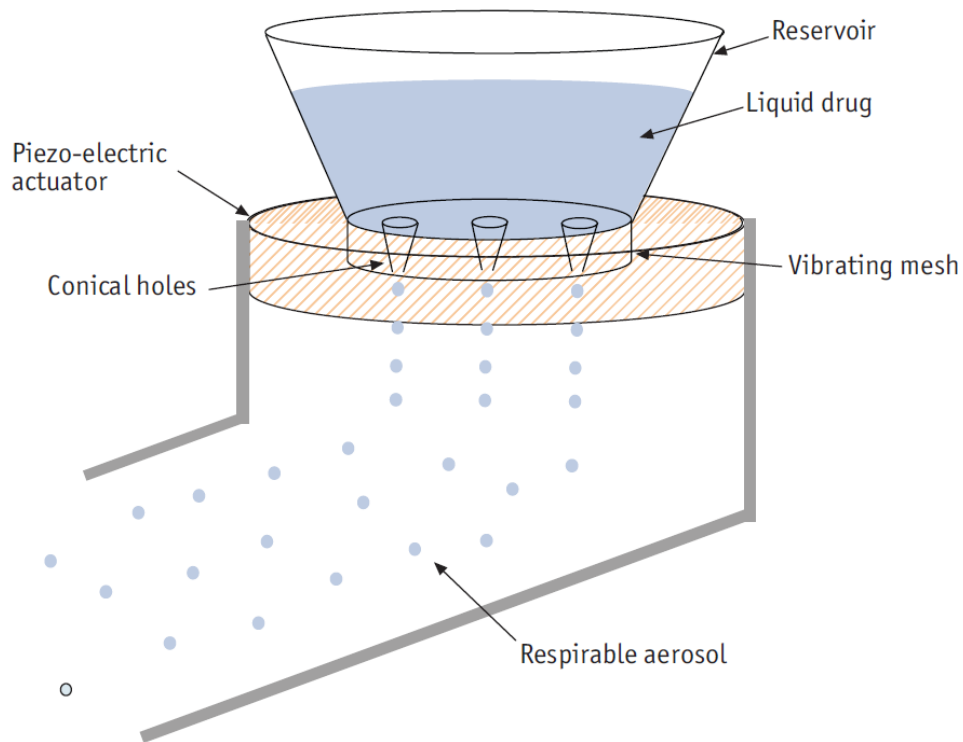


Figure 1. 14: Schematic illustration of the working principle of a vibrating mesh nebulizer.[35]

1.12 Objective

The aim of this master thesis is to compare different empty or iloprost encapsulating liposomal formulations for their suitability for nebulization. A nebulizer for each single working principle was applied and tested for liposomal stability, size changes, mass output and integrity.

The same experiments were also done with liposomal formulations encapsulating a fluorophore-quencher system, to measure the amount of occurring leakage during nebulization.

The results give information about possible future application of inhalative liposomal iloprost for sustained release.

2. Materials & Methods

2.1 Materials

The laboratory work was done at the Institute of Biophysics and Nanosystems Research (IBN, Austrian Academy of Sciences, Graz, Austria). If not stated otherwise the equipment was provided by the IBN and experiments were done in the laboratory of the IBN. Phospholipids were purchased from Avanti Polar Lipids (Alabaster, AL, USA). All other chemicals were of analytical grade and purchased from Sigma-Aldrich (Sigma-Aldrich Handels GmbH, Vienna, Austria).

2.2 Nebulizer devices and condensation equipment

The nebulization experiments with liposomal formulations were done with three different nebulizers, each one representing another working principle. Three nebulizers were employed: (A) the air-jet nebulizer MicroDrop® *Pro* (MPV Truma, Putzbrunn, Germany) operated with the MicroDrop® compressor, (B) the ultrasonic nebulizer Optineb®-ir (NEBU-TEC, Eisenfeld, Germany) operated with a frequency of 2.4 MHz, and (C) the vibrating mesh nebulizer eFlow® rapid (PARI, Starnberg, Germany) operated with a frequency of 117 kHz.



Figure 2. 1: Tested nebulizer devices, each one representing another nebulization principle. (A) MicroDrop® (MPV Truma) with air-jet principle, (B) Optineb®-ir (NEBU-TEC) with ultrasound technique, (C) eFlow® rapid (PARI) with vibrating mesh technology.

A breathing air condenser and extra equipment for the operation of the machine was provided by the Division of Pulmonology, Medical University of Graz, Austria. Further tubing equipment necessary for the assembly and the connection of the different nebulizer devices with the breathing air condenser was provided by the IBN.

Moreover the mouse nebulizer M-neb with vibrating mesh technology was also tested and provided by NEBU-TEC (Elsenfeld, Germany). This nebulizer is made for future applications with the isolated perfused lung (IPL) model and was also connected to the breathing air condenser for nebulization trials with liposomal formulations.



Figure 2. 2: M-neb mouse inhaler (NEBU-TEC) for IPL system

2.3 Preparation of iloprost containing liposomes

Empty and iloprost loaded liposomes were prepared with two slightly different formulations. The first formulation was composed of a ternary mixture of palmitoyl-oleoyl-phosphatidylcholine (POPC), stearylamine (SA) and polyethylene glycol-conjugated dipalmitoyl phosphatidyl ethanolamine (DPPE-PEG2000) with a molar ratio of 87:10:3 mol%. The second formulation was composed of POPC, SA and Kollidon® 17 PF (Polyvinylpyrrolidone PVP pharmaceutical grade, BASF) with a molar ratio of 87:10:3 mol%.

For each ingredient a stock solution was prepared freshly. Appropriate amounts of lipids were weighed in at the analytical balance AG245 (Mettler Toledo, Vienna, Austria) and dissolved in chloroform:MeOH 2:1. Appropriate amounts of the components were pipetted together and vortexed. For those liposomes with iloprost, the drug was directly added to the dissolved lipid components. 100 µL of an ethanolic solution of iloprost (Bayer© iloprost stock solution 0.5 mg/mL, Bayer AG, Leverkusen,

Germany) were added to the lipid solution and mixed carefully. The total lipid concentration was 6 mg in all cases.

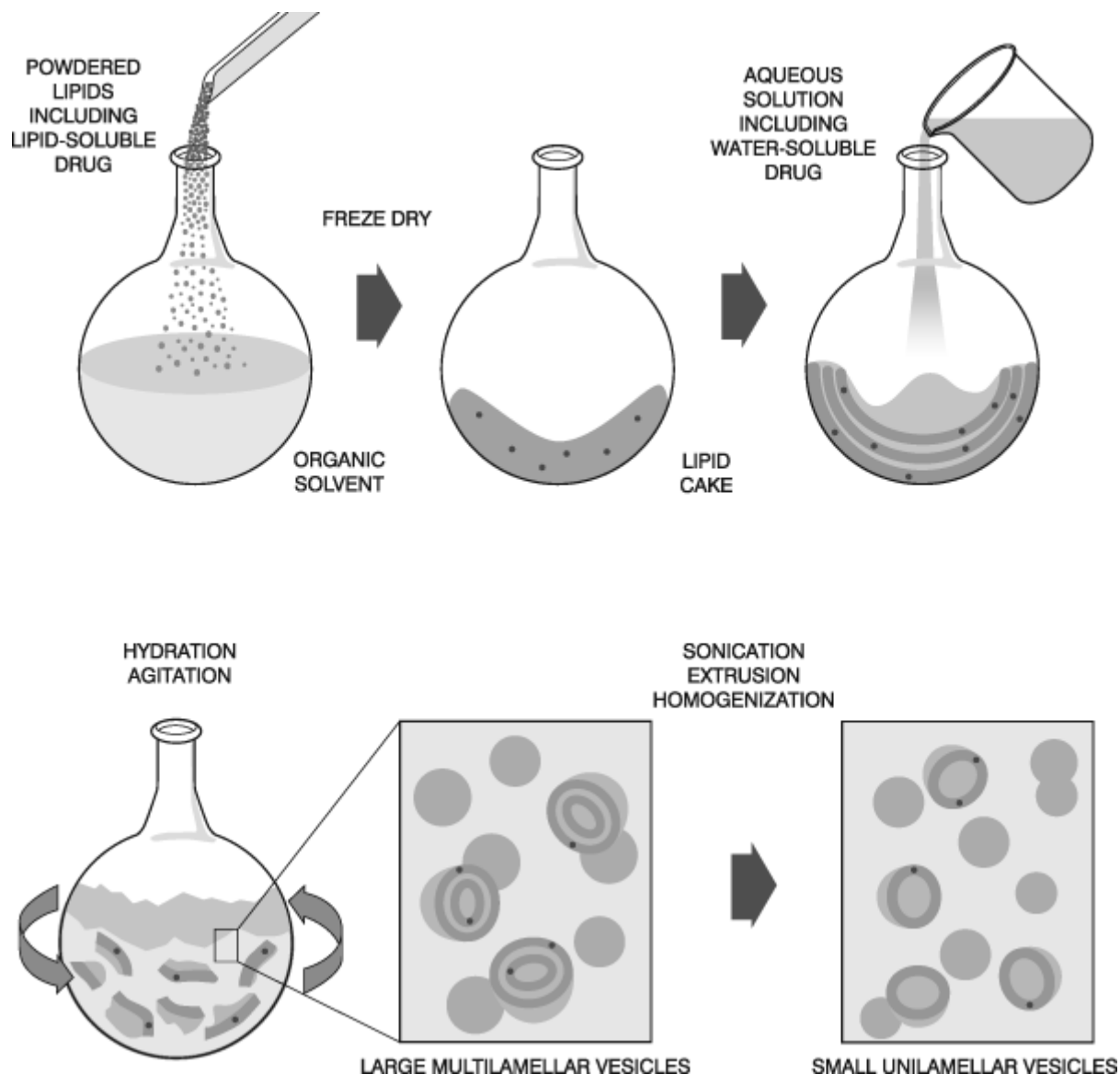


Figure 2. 3: Liposome preparation procedure as carried out for the experiments. The powdered lipids were dissolved in organic solvent and mixed. The drug was added with the organic solvent as it is an amphiphilic drug (step 1). The organic solvent was evaporated with nitrogen to gain a lipid cake (step 2). The aqueous buffer solution was added for rehydration (step 3). Periodical agitation was used to rehydrate the lipid film (step 4). The results are LUVs which were extruded with polycarbonate filters to get SUVs (step 5). [37]

The lipid as well as the lipid/iloprost mixtures were dried under a stream of nitrogen to produce lipid thin films. The thin films were stored over night in a vacuum chamber to remove any remaining solvent. These absolutely dry lipid films were then rehydrated at room temperature (T_c for POPC -2°C) with 1 mL sterile 10 mM Tris/HCl buffer pH 7.0. For this reason the films were strongly vortexed 6 times for 1 minute every 10

minutes. The rehydrated lipid emulsion was then further processed by 6 freeze and thaw cycles, where the entire emulsion was first frozen in liquid nitrogen, then thawed again at room temperature and then powerfully vortexed before frozen again.

All liposomal emulsions were extruded through polycarbonate filters (Millipore, Vienna, Austria) with 200 nm pore size, using an Avanti Mini-Extruder (Avanti Polar Lipids, Alabaster, AL, USA). 21 extrusion steps at room temperature guarantee a homogeneous preparation of unilamellar vesicles. Approximately 10% of the applied volume is lost during the extrusion procedure.

For all liposomal preparations the size was checked with Dynamic Light Scattering (DLS) and the encapsulation efficiency was determined with TLC.

2.4 Drug loading efficiency

To determine the drug encapsulation efficiency (EE) of liposomes directly after their preparation and to check drug loading efficiency after nebulization processes thin layer chromatography (TLC) method was used. The TLC leads to a single iloprost band, which can be easily identified by applying a separate iloprost standard. Moreover with the intensity of the occurring bands it is possible to do a semi quantitative concentration determination of iloprost. As a first step the iloprost encapsulated within liposomes had to be separated from the free non-encapsulated iloprost. This was done with the help of centrifugal filter devices, which absorbed the free iloprost into their membrane and separated it from the intact liposomes.

A total amount of 4 µg iloprost should be applied on the TLC. For this reason 80 µL of prepared liposome sample (6 mg/mL total lipid concentration containing 50 µg iloprost) were mixed with 10 mM Tris/HCl buffer pH 7.0 to reach at least a volume of 200 µL, which is necessary to cover enough filter membrane area. Optional the sample volumes were altered for nebulized samples according to their liposome concentration after nebulization to reach a total iloprost concentration of 4 µg on the TLC.

The appropriate sample was put into an Amicon® Ultra-4 10K device (Millipore Ireland B.V., Ireland) with a molecular cut-off of 10 kDa and centrifuged (SIGMA 3K18 centrifuge, SIGMA Laborzentrifugen GmbH, Osterode am Harz, Germany) with rotor 11133 at 4000 g and 18°C for 15 minutes. The flow through was discarded and

again the same volume of 10 mM Tris/HCl buffer pH 7.0 added to wash the liposomes. The liposomes were centrifuged again with the same conditions. The flow through was discarded and the supernatant containing the liposomes was collected into Pyrex tubes (SciLabware Limited, Staffordshire, United Kingdom). To be sure to have the entire liposomes collected from the device, the membrane was washed with buffer once more and put to the collected liposomes.

During the centrifugation steps the free iloprost was absorbed by the membrane and is now released from the filter membrane by putting at least the same volume of 70% EtOH into the filter device as at the beginning. The devices were centrifuged with the same conditions and the flow through containing the non-encapsulated iloprost collected into Pyrex tubes.

For the subsequent chromatography the TLC chamber had to be prepared at least one hour beforehand to get a satisfying saturation with the mobile phase. The eluent was composed of chloroform:MeOH:ammoniac 65:35:1.5 (v:v:v).

As a next step a Folch extraction was carried out. Twenty times the volume of chloroform:MeOH 2:1 per volume of the collected liposome sample was added. This should lead to a single phase mixture. The samples were vortexed (Heidolph Reax top, Heidolph Instruments, Switzerland) at room temperature every 5 min for 20 min and afterwards mixed with 0.2 times the volume of 0.034% MgCl₂-solution. This mixture was vortexed and centrifuged for 5 min at 2500 rpm. The upper phase was discarded carefully and the remaining organic phase was evaporated under a stream of nitrogen until the tube was completely dry.

The dry film was dissolved in 35 µL chloroform:MeOH 2:1 each, quickly vortexed and immediately put on the layer of a prepared TLC plate. The bands were applied as thin as possible to get sharp bands. As a standard reference a volume of 20 µL from 100 µg/mL Cayman iloprost was applied on the layer. The TLC plate was put into the prepared TLC chamber and ran to the desired end point. It was dried carefully from the mobile phase and put into a CuSO₄ bath for 10 seconds. After this the TLC was developed at a Camag TLC Plate Heater III (CAMAG, Berlin, Germany) at 188°C and scanned.

2.5 Preparation of ANTS/DPX containing liposomes

8-Aminonaphthalene-1,3,6-trisulfonic acid disodium salt (ANTS) and p-Xylene-bis(N-pyridinium bromide) (DPX) are a fluorophore-quencher system. As long as they are in spatial proximity the emitted light of the excited fluorophore is transferred to the quencher by Förster resonance energy transfer (FRET) and absorbed. No observable fluorescence occurs. When they are sterically away from each other, the fluorophore can emit its energy in the form of light without hindrance.

ANTS/DPX loaded liposomes were prepared with two slightly different formulations. The first formulation was composed of a ternary mixture of palmitoyl-oleoyl-phosphatidylcholine (POPC), stearylamine (SA) and polyethylene glycol-conjugated dipalmitoyl phosphatidyl ethanolamine (DPPE-PEG2000) with a molar ratio of 87:10:3 mol%. The second formulation was composed of POPC, SA and Kollidon® 17 PF (Polyvinylpyrrolidone PVP pharmaceutical grade) with a molar ratio of 87:10:3 mol%. These are the same formulations as for the iloprost loaded liposomes.

For each ingredient a stock solution was freshly prepared. Appropriate amounts of lipid were weighed in at the analytical balance AG245 (Mettler Toledo, Vienna, Austria) and dissolved in chloroform:MeOH 2:1. The appropriate amounts of the components were pipetted together and vortexed. The lipid mixtures were dried under a stream of nitrogen to produce lipid thin films. The thin film had a total lipid concentration of 12.0 mg. The thin films were stored over night in a vacuum chamber to remove any remaining solvent. These absolutely dry lipid films were then rehydrated at room temperature (T_c for POPC -2°C) with 1 mL fluorophore buffer (HEPES 10 mM pH 7.4, NaCl 68 mM, ANTS 12.5 mM, DPX 45 mM). So the fluorophore-quencher system was added via this rehydration step.

For this reason the films were strongly vortexed 6 times for 1 minute every 10 minutes. The rehydrated lipid emulsion was then further processed by 6 freeze and thaw cycles, where the entire emulsion was first frozen in liquid nitrogen, then thawed again at room temperature and then powerfully vortexed before frozen again. Furthermore the samples have to be protected from light for the entire process, as the fluorophore-quencher system is very light-sensitive.

All liposomal emulsions were extruded through polycarbonate filters (Millipore, Vienna, Austria) with 200 nm pore size, using an Avanti Mini-Extruder (Avanti Polar Lipids, Alabaster, AL, USA). 21 light-protected extrusion steps were done at room temperature. Approximately 10% of the applied volume is lost during the extrusion procedure. For all liposomal preparations the size was checked with DLS. If the extrusion was successful then the size distribution was quite homogeneous.

At this point the ANTS/DPX liposomes were successfully formed, but had to be purified from non-encapsulated fluorophore. For this reason the samples were purified via size exclusion chromatography.

2.6 Purification of liposomes from non-encapsulated ANTS/DPX

To purify the liposomes from the non-encapsulated fluorophore and quencher molecules, a size exclusion chromatography was carried out. For this reason a freshly packed column (Bio-Rad, 1.45 x 5.0 cm, 8.3 mL) with Sephadex G75 material (Sigma-Aldrich) was prepared.

First 2 g of Sephadex G75 powder are dissolved in 100 mL elution buffer (HEPES 10 mM pH 7.4, 140 mM NaCl) and mixed with a few milligrams of NaN_3 to protect it from microbial growth. Let it soak overnight at 4°C. Before filling the soaked material into the new column it was put into an ultrasonic bath for 15 minutes. Then an empty column was taken and filled step by step with the Sephadex G75 material. This has to be done very carefully with a glass rod to prevent the formation of air bubbles. From time to time the material was washed with fresh buffer. When the column material settled down to the desired level a filter membrane was applied carefully at the top.

Before the purification can be started the packed column was washed with 2 column volumes (CVs) of elution buffer (HEPES 10 mM pH 7.4, 140 mM NaCl). Before applying the sample volume of 1 mL on the column's filter membrane, the liquid level had to come down to the column's surface but the column must not get dry. Then the sample (1 mL) was carefully applied with a glass rod and when it had almost completely infiltrated more buffer was applied on it again.

Then the elution was started with elution buffer and the liposomal fractions (~ 5 fractions, dilution factor ~ 4-5) were collected in Eppendorf tubes (Eppendorf AG, Vienna, Austria). For each fraction 10 drops (equals about 550 μL) were collected in

a single tube. The turbid liposomal fractions were pooled and afterwards the fluorophore was eluted completely from the column. Again the column was washed with 2 CVs of elution buffer. Then the next purification step can be started. The encapsulation efficiency of fluorophore was determined with fluorescence spectroscopy.

2.7 Fluorescence spectroscopy

The fluorescence measurements were done with the SPEX FluoroMax-3 fluorescence spectrophotometer (HORIBA Jobin Yvon GmbH, Bensheim, Germany). For each measurement 2 mL of appropriate sample buffer were put into a 10 mm x 10 mm fluorescence quartz cuvette and mixed with a proper amount of liposome sample. The amount of liposomal sample depends on its liposome and thereby fluorophore concentration. The more concentrated the sample was the less volume was taken for the measurement. The detector of fluorescence intensity should measure values between 10^5 and 10^6 counts per second (cps). The measurements were made at an excitation wavelength of 360 nm and an emission wavelength of 530 nm.

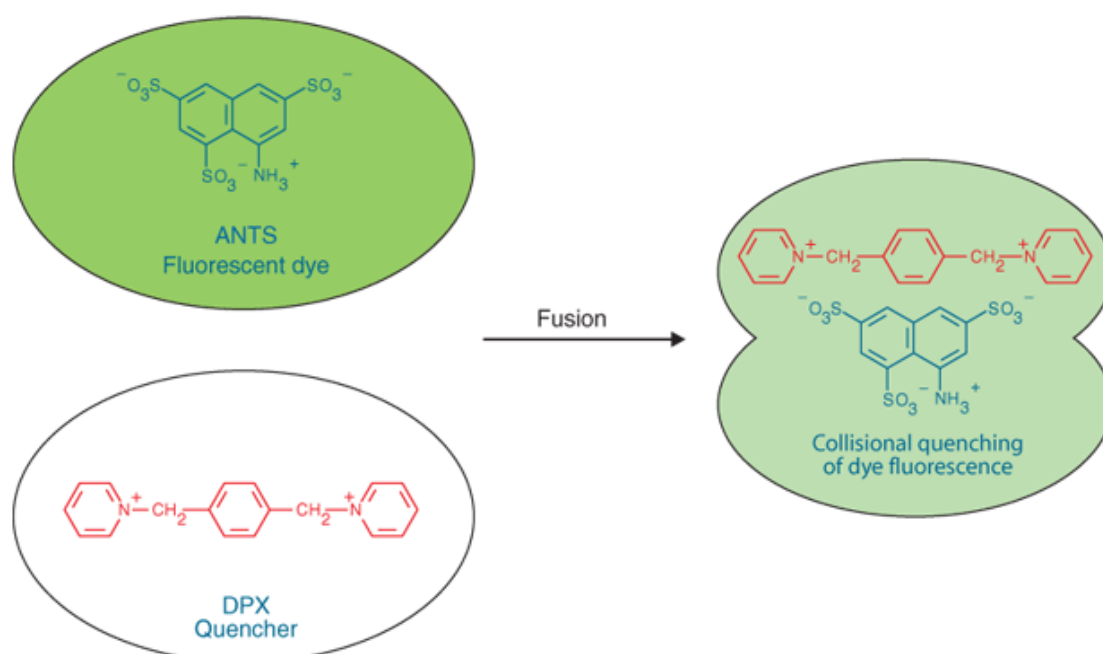


Figure 2. 4: Applied fluorophore-quencher system consisting of the fluorescent dye ANTS and the quencher DPX. Both molecules were encapsulated together in liposomes. Because of their sterical proximity the quencher can absorb the fluorophore's emitted light and no fluorescence can be observed. This process is called Förster resonance energy transfer. [38]

As a first step the fluorescence intensity of the freshly prepared and purified liposomes was measured (background radiation I_0). Each measurement was recorded for 90 seconds. Next 10 μL of TritonX-100 10% were added to the cuvette and mixed carefully. The detergent destroys the entire liposomes and releases all ANTS/DPX. Again the measurement was recorded for 90 seconds to quantify the maximum possible fluorescence intensity (I_{max}). The same approach was done for nebulized samples.

With I_0 and I_{max} the encapsulation factor f was determined with the following equation:

$$f = I_{\text{max}}/I_0$$

2.8 Size analysis of liposomes

The liposomes' size was analyzed with Dynamic Light Scattering (DLS) and measured with a Zetasizer 3000 HSA (Malvern Instruments, Worcestershire, United Kingdom).

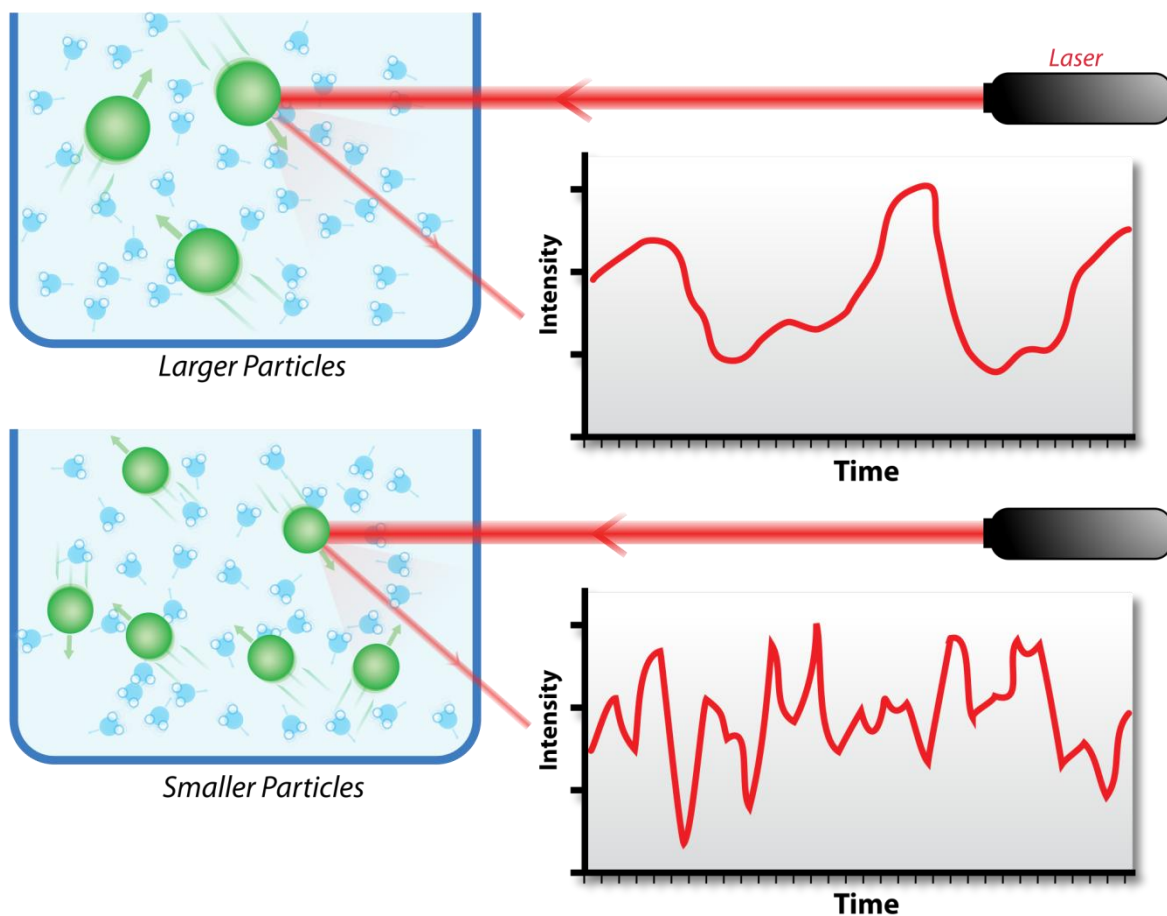


Figure 2. 5: Scheme of the working principle of Dynamic Light Scattering DLS. This hypothetical example shows larger particles on the top and smaller particles on the bottom. They produce different scattering curves because of their dissimilar characteristics in the fluctuation pattern. [39]

The liposomal size was calculated by an auto-correlation function, which is achieved from a time-dependent fluctuation in the scattering intensity of the irradiated light. This fluctuation is caused when the light hits very small particles and scatters in all directions. As a result one gets a size distribution profile.

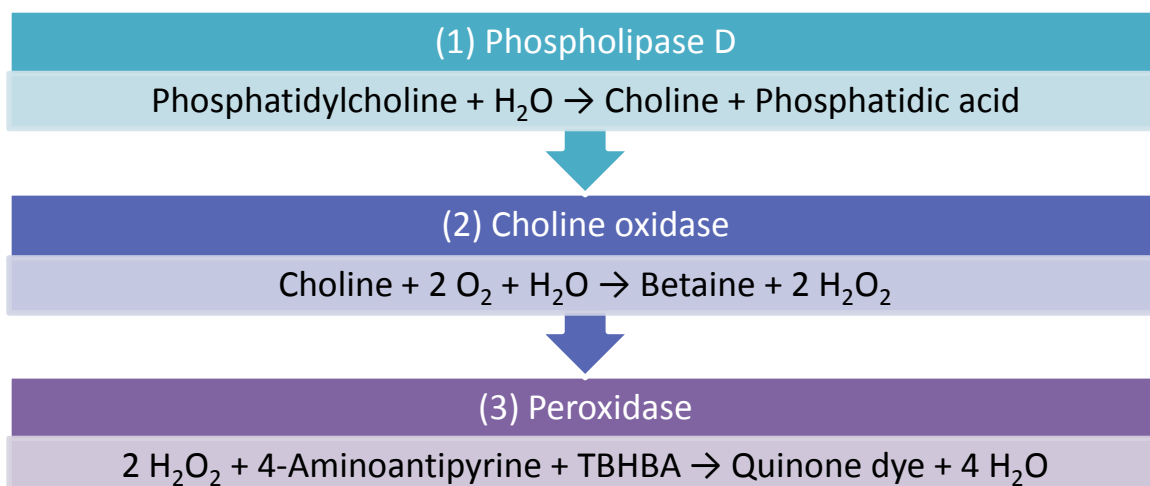
The polydispersity index (PDI) gives information about the width of the size distribution and has a value between 0 and 1. It is a quality parameter for the homogeneity of the liposomal preparation. The smaller the PDI's value is, the narrower the measured size distribution.

The DLS analysis was used both to determine size distribution of freshly prepared liposomal solutions and to check size after different nebulization steps.

2.9 Determination of liposome concentration

2.9.1 Phospholipid assay

The liposome concentration after nebulization was determined using a phospholipid assay suitable for the photometric *in vitro* determination of cholin containing phospholipids. The Phospholipids FS Assay (DiaSys Diagnostic Systems GmbH, Holzheim, Germany) is an enzymatic assay that produces a photometrically measurable dye through several enzymatic reactions.



The intensity of the generated quinone dye can be measured and compared to a phospholipid standard (DiaSys Diagnostic Systems GmbH, Holzheim, Germany). All measurements were done at a wavelength of 570 nm, 37°C and in duplicate. Each measurement sample was prepared in a separate disposable cuvette (thickness 1 cm). As a first step 10 µL of each sample (liposome samples, standards and

blanks) were pipetted into a cuvette and mixed with reagent 1 (Tris buffer pH 8.0, TBHBA, Choline oxidase, detergents and stabilizers). This mixture was incubated at 37°C for 5 min and afterwards the photometric extinction E1 was measured (Hitachi U2000 Spectrophotometer, Hitachi High-Technologies Corporation, Germany). Next 200 µL of reagent 2 (Tris buffer pH 8.0, 4-Aminoantipyrine, Peroxidase, Phospholipase D, detergents and stabilizers) were added and mixed. Again the cuvettes were incubated at 37°C for exactly 5 min and their extinction E2 measured immediately afterwards.

With a simple calculation of the extinction difference between the standard and the sample and the known concentration of the standard the amount of choline can be calculated with the following formulas:

$$\Delta E = (E2 - E1)$$

$$\text{Phospholipids [mg/mL]} = \frac{\Delta E \text{ sample}}{\Delta E \text{ standard}} \times \text{conc(standard)} 3.1 \text{ [mg/mL]}$$

2.9.2 Phosphorus determination

The determination of phosphorus content in samples is another possibility to calculate liposome concentration as each single phospholipid molecule contains exactly one atom of phosphorus. The experimental procedure has to be done under the fume hood and all chemicals and equipment have to be absolutely phosphorus free. The calibration curve was done with a KH_2PO_4 standard and resulted in the following equation: $y=0,066499x + 0,000793$ [$y=\text{Abs}$, $x=\mu\text{g P}$].

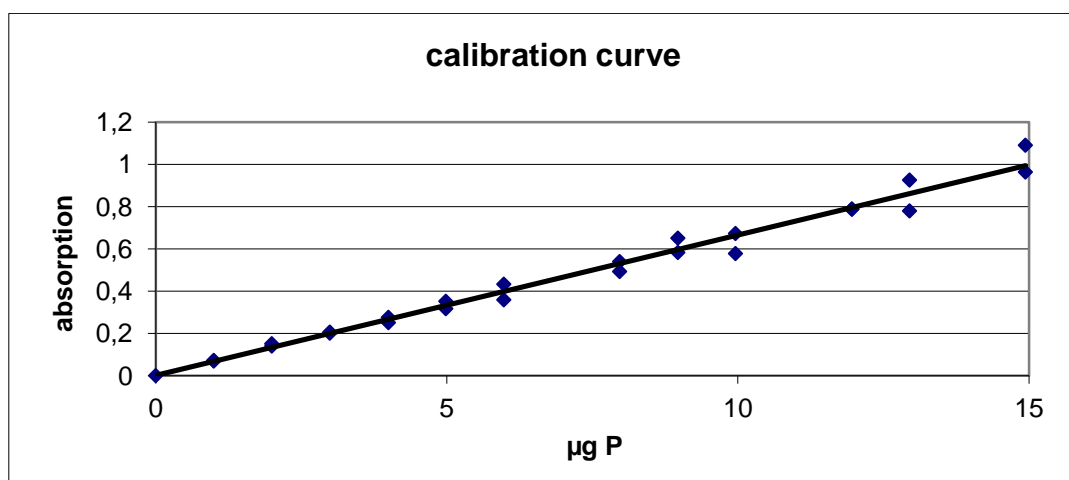


Figure 2. 6: Calibration curve for the determination of phosphorus made with a KH_2PO_4 standard. The calibration curve's equation is $y=0,066499x + 0,000793$.

30 µL of sample were put into each Pyrex test tube. The test tubes were heated to completely ash the samples. From time to time they were carefully rotated to ash the sample quantitatively. As a next step the tubes were cooled down to room temperature and 0.4 mL of the acidic mixture $\text{H}_2\text{SO}_4_{\text{conc}} : 72\% \text{HClO}_4 / 9 : 1$ (v:v) was added to each tube. The samples were vortexed intensively until all of the ash was dissolved in the acid. Again the tubes were heated for 30 minutes until fumes were emitted. Then the tubes were cooled down again to room temperature and 9.6 mL of a molybdate solution (0.26% solution of Ammonium Heptamolybdate) mixed with ANSA solution (8.42 mM 8-Anilinonaphthalene-1-sulfonic acid (ANS) + 722 mM $\text{Na}_2\text{S}_2\text{O}_5$ + 39.67 mM Na_2SO_3) at a volume ratio of 22.7:1 (v:v) were added. Once again the tubes were vortexed, closed with a lid and incubated at 90°C for 20 minutes. Afterwards they were cooled down and measured photometrically at a wavelength of 600 nm.

2.10 Preparation of samples for mass spectrometry

The preparation of samples for mass spectrometry (MS) includes the same procedure as for the TLC. The free non-encapsulated iloprost has to be separated from liposomes encapsulating iloprost (pre and post nebulization). For this aim the same procedure and filter devices are used as for the TLC preparation. The method is done identically and stops before the Folch extraction, when free and encapsulated iloprost are successfully separated. (see chapter 2.4) The prepared MS samples were analyzed at the Core Facility Mass Spectrometry (ZMF – Center for Medical Research, Medical University of Graz, Austria) for an exact quantification of iloprost.

2.11 Size analysis of aerosol droplets

The measurements for the aerosol droplet size were done with a Mastersizer 2000 (Malvern Instruments, Worcestershire, United Kingdom) at the Institute of Pharmaceutical Sciences at the Karl-Franzens University of Graz.

The particle size distributions for all three investigated nebulizers were analyzed. The nebulizers were filled with appropriate samples and adapted to the Mastersizer 2000. The intensity of the aerosol stream had to be regulated to a certain level to be suitable for laser diffraction measurement. The Mastersizer 2000 uses this technique

to calculate the size of particles by measuring the intensity of light scattered as a laser beam when passing through a dispersed particulate sample. The dispersed sample has to pass the measurement area of the so-called optical bench, where the laser beam illuminates the particles. A series of detectors over a wide range of angles measures the intensity of the scattered light and produces the information necessary for particle size calculation.

2.12 Zeta potential

The measurements for the zeta potential were done with a Zetasizer Nano ZS (Malvern Instruments, Worcestershire, United Kingdom) at the Institute of Pharmaceutical Sciences at the Karl-Franzens University of Graz.

First the samples were diluted to a lipid concentration of 0.3 mg/mL. The Zetasizer Nano was operated with a computer and the appropriate software. Special cuvettes for the measurement of the zeta potential have to be cleaned carefully with H₂O and ethanol. Then the sample (~500 µl) was put into the cuvette and filled up to the upper edge without enclosing any air bubbles. The cuvette was closed with two small plugs and put into the Zetasizer Nano for the measurement. A Standard Operating Procedure (SOP) file was created containing the following parameters:

<i>Material: liposomes</i>	<i>Equilibration time: 10 – 30 s</i>
<i>Dispersant: water</i>	<i>Cell: clear disposable zeta cell DTS1060C</i>
<i>Calculating theory: Smoluchowski</i>	<i>No. of measurements: 5</i>
<i>Temperature: 25°C</i>	<i>Measurements: 10 runs</i>

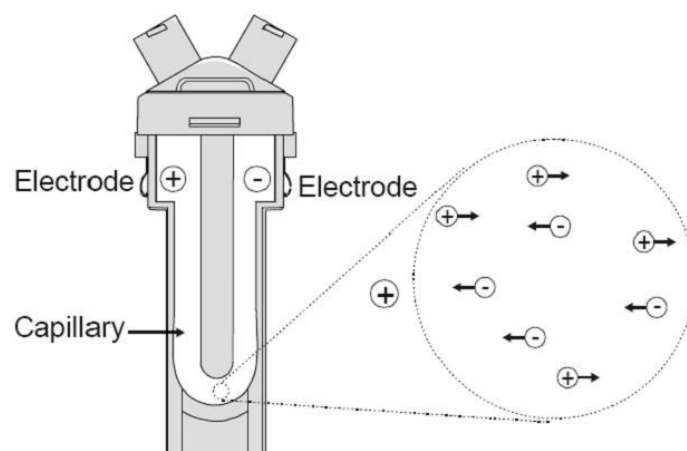


Figure 2. 7: Picture of a cuvette suitable for zeta potential measurement. The cuvette contains a capillary tube and two electrodes. An electric field is applied across the dispersion and the particles with a zeta potential will migrate to the electrode of opposite charge with a velocity proportional to its own charge. [40]

3. Results & Discussion

3.1 Adaption of condensation equipment for nebulizers

To test the suitability of liposomal formulations for respiratory applications, nebulization studies were performed. A prerequisite to do appropriate analysis steps after the sample has been nebulized is to establish a functioning method to collect the aerosolized solution.

3.1.1 Optineb®-ir

The first trials were done with the Optineb®-ir (ultrasound), as this is the nebulizer with the lowest aerosol output in terms of volume, intensity and velocity. So if the developed condensation technique would work for the Optineb®-ir, then it would also work for the other two nebulizers with a higher aerosol output. First the Optineb®-ir was connected via a mouthpiece adaptor to a tubing system (A) with its terminus attached to an Eppendorf tube (B). This Eppendorf tube had a number of prepared holes in it to enable the aerosol to flow outside. The tubing with the Eppendorf at the final point was in turn put into a Pyrex tube (C) to collect the condensed aerosol. Then the whole assembly was put into an ice bath to cool the surfaces and enable condensation. (see Figure 3. 1)

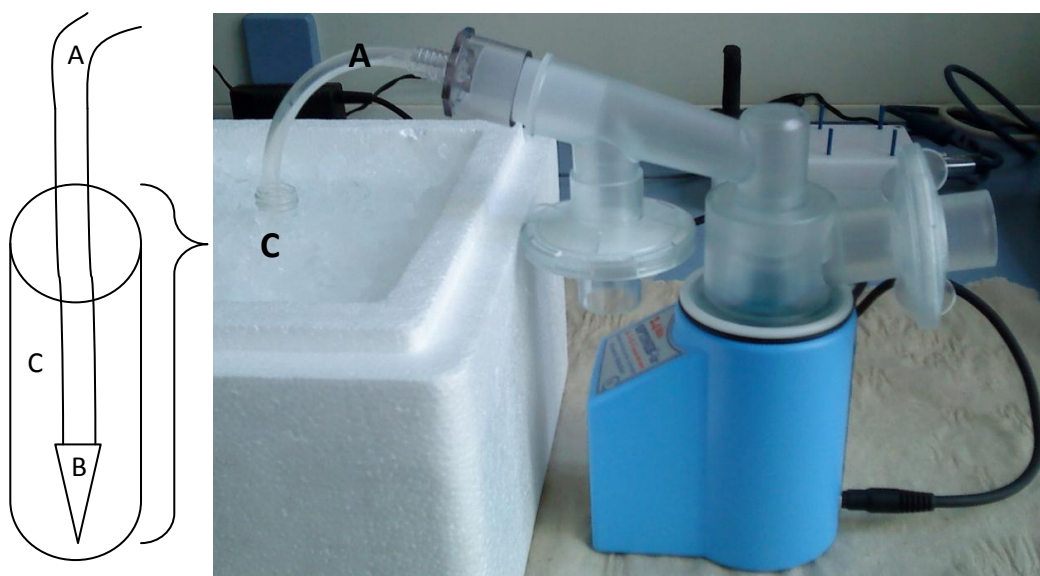


Figure 3. 1: First prototype of aerosol condensation equipment arranged with the Optineb®-ir. The scheme shows the Pyrex tube in the ice bath in more detail. The tubing system (A) connected to the mouthpiece, the Eppendorf tube (B) at the end of the tubing system and the Pyrex glass tube (C).

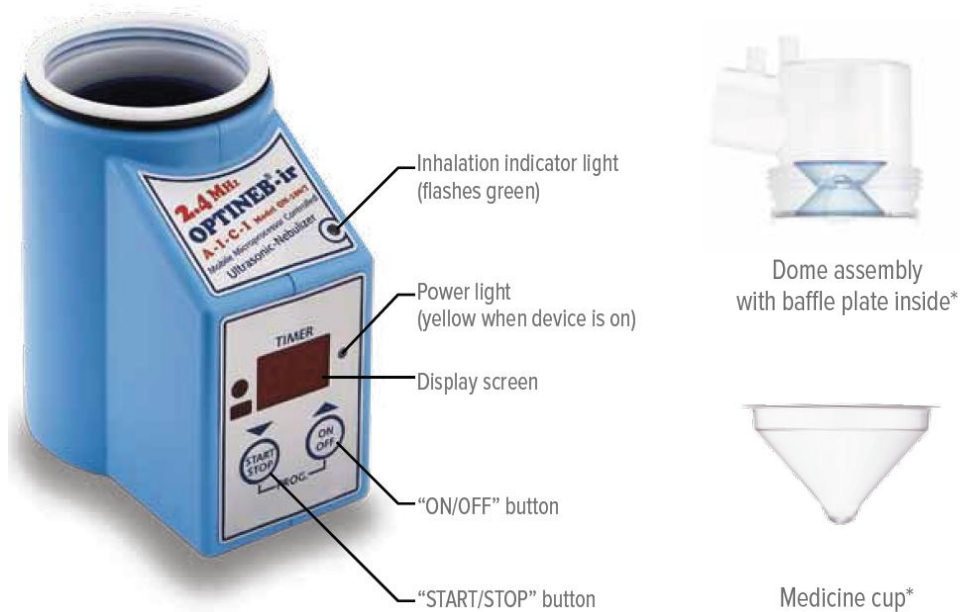


Figure 3. 2: Description of the main user items of the Optineb®-ir (left) and pictures of the dome assembly with baffle and the medicine cup. [41]

The experiments testing prototype condensation equipment were done with H_2O_{bidest} . The Optineb®-ir has to be filled with 45 mL of water (recommended to use H_2O_{deion} to avoid the deposition of calcium carbonate in the nebulizer and to guarantee proper functioning) to build up the water interface responsible for the ultrasonic energy transfer between the piezo-electric transducer and the drug solution. The drug solution (or H_2O_{deion} for trials) was pipetted into special available medicine cups made of plastic. The medicine cup was deposited in the water interface, so that the transducer liquid covered the bottom tip of the cup. (see Figure 3. 3)

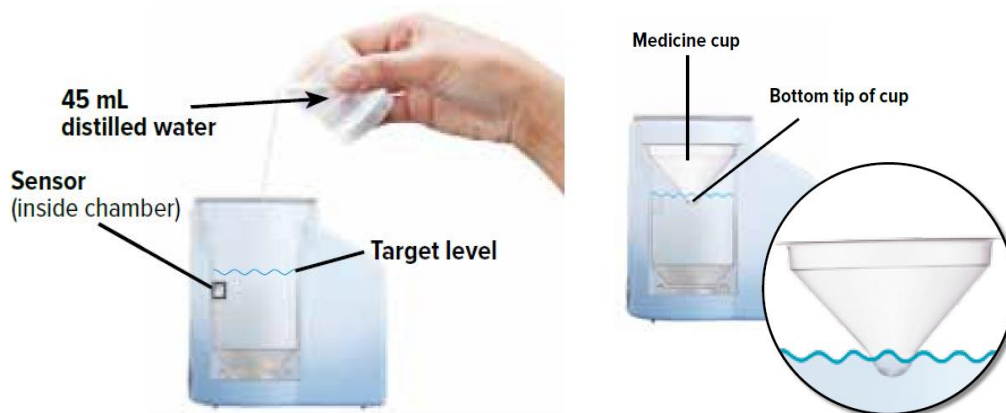


Figure 3. 3: Filling the water reservoir with 45 mL of distilled water and inserting the medicine cup. [41]

The water interface is greatly advantageous to protect the active drug compounds in the medicine solution from occurring heat in the ultrasonic nebulizer as the drug solution is not in direct contact with the ultrasound producer.

A volume of 3.0 mL H_2O_{bidest} was used for nebulization testing instead of medicine solution. The Optineb®-ir does not work continuously but in intervals. When the device is assembled correctly and connected with the power supply it can be switched on by pressing the ON/OFF button. To start the nebulization process the START/STOP button has to be pressed once. Acoustic and optical signals indicate the nebulization. Each cycle consists of three boosts. (see Figure 3. 4)

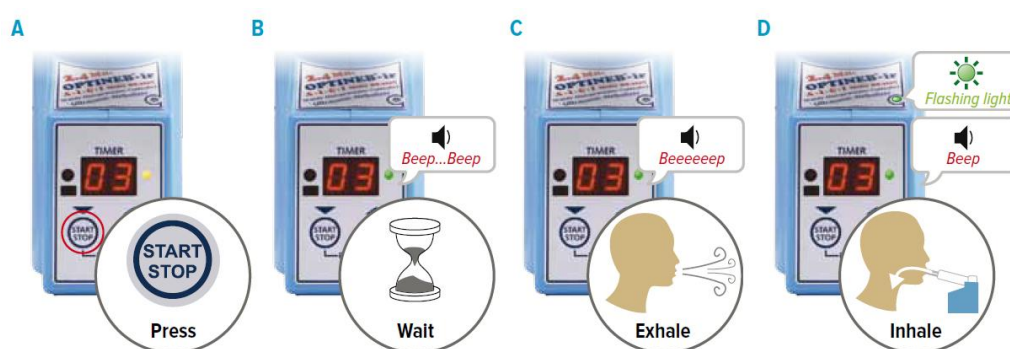


Figure 3. 4: Boost signaling for the patient's inhalation pattern. (A) button to start the inhalation process, (B) waiting interval, (C) exhalation time, the aerosol is generated, (D) inhalation time, the aerosol is produced. [41]

For the first condensation testing a volume of 3.0 mL of H_2O_{bidest} was used. The device was restarted for 13 times (13 cycles) with a total number of 39 boosts. As the production of the aerosol cloud inside the inhaler is very statically and the mist has to be inhaled actively by the patient, a breathing simulation had to be developed. For this reason active breathing against the inhalation filter (back filter) was carried out each time the inhalation period started. (see Figure 3. 4)

Despite the transport of some mist out of the nebulizer chamber, there was no significant condensation in the collection tube. Mainly the condensation occurred at the exhalation filter and in the nebulizer chamber itself.

The experimental set-up was altered. The exhalation filter was exchanged with a 15 mL Falcon tube to directly collect the aerosol right at the exit. Again 10 cycles were performed but no visible condensation occurred.

Therefore the set-up was altered again. This time the tubing coming from the nebulizer was directly led into a Falcon tube, which was sealed with Parafilm. The sealing should prevent mist from flowing outside. Again there is almost no visible or measurable condensation.

Another try was done with a 4 mL glass vial instead of a Falcon tube to condensate the mist. This glass vial was put into the ice bath and connected to the tubing coming from the inhaler. The occurring condensation was already visible. This experiment worked significantly better than the others before. Nevertheless there was not enough condensed aerosol to enable analysis steps afterwards.

3.1.2 MicroDrop® Pro

Because the condensation trials did not lead to the desired results with the Optineb®-ir, the second nebulizer was tested. This was the MicroDrop® Pro (air-jet), which had a much higher mass output than the other two nebulizers due to the fact that it was compressor driven. The compressor was connected to the nebulizer itself, which in turn was linked to a tubing system that led into an ice cooled Pyrex tube. (see Figure 3. 5)

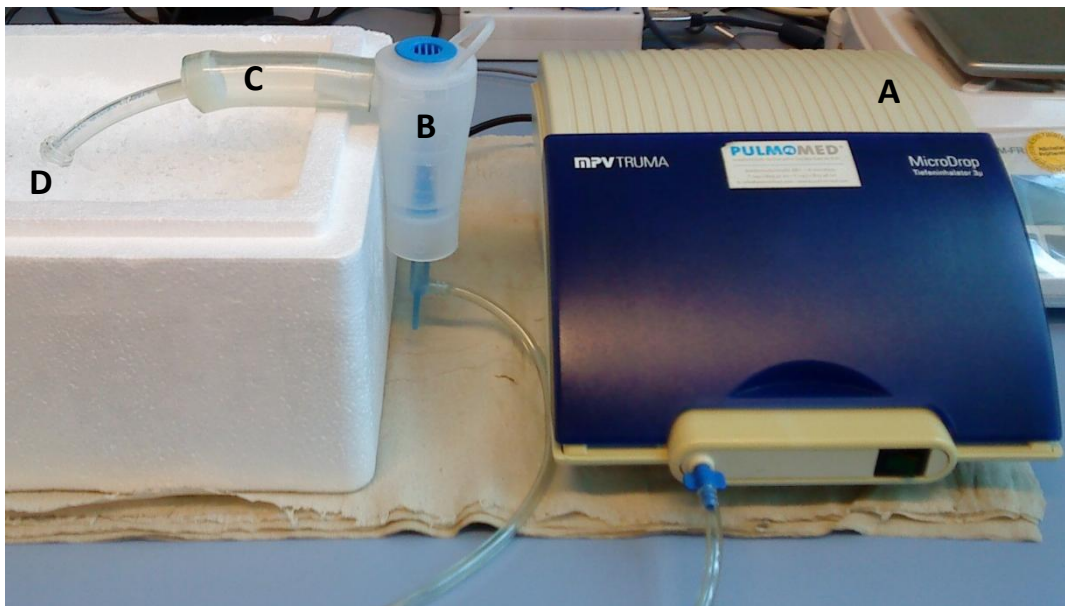


Figure 3. 5: Experimental set-up for the condensation experiments with the MicroDrop® Pro nebulizer. (A) compressor, (B) air-jet nebulizer chamber, (C) connection tubing system and (D) Pyrex tube in ice bath.

For the first nebulization process a volume of 6.0 mL H_2O_{bidest} was used. This water was filled into the nebulization chamber and the inhaler was closed. The compressor

was turned on and worked for 6 min before it was turned off again. There was significant condensation observable. The volumes of the remaining solution in the nebulization chamber as well as of the condensed liquid were measured. An amount of 4.9 mL remained in the chamber, 550 μL could be collected in the condensation tube, which means that approximately 550 μL were either lost in the tubing system, at chamber surfaces or simply escaped.

The same experimental set-up was repeated for another two times to assure its reproducibility. Again 6.0 mL $\text{H}_2\text{O}_{\text{bidest}}$ were used and the compressor worked for 6 min. The collected volume was 530 μL and 560 μL , respectively. Also the remaining liquid volume and the lost part were approximately the same. So this experimental set-up allows the collection of an appropriate amount of liquid to do analysis steps afterwards.

But for the experiments using liposomal samples a lower sample volume will be taken due to limited resources. That was the reason for further testing with lower sample volumes.

The first was done with 2.0 mL $\text{H}_2\text{O}_{\text{bidest}}$ in the nebulization chamber and 6 min compressor time. A total amount of 360 μL could be collected, which is much lower than for the experiments with 6.0 mL starting volume. The ground of the nebulization chamber is only partially covered with liquid after 6 min. This indicates that the sample volume is too low for a nebulization of 6 min.

So the sample volume was increased to 3.0 mL $\text{H}_2\text{O}_{\text{bidest}}$ in the nebulization chamber. The compressor was turned on for 6 min. This time the ground of the chamber is still covered with liquid. Sample volume of 600 μL could be collected. The experiment was repeated and again 530 μL could be collected.

Further testing was done with a significantly increased sample volume of 12.0 mL $\text{H}_2\text{O}_{\text{bidest}}$. The compressor was again turned on for 6 min. Despite the significantly higher starting volume, the condensed part could not be increased and was 530 μL .

To sum up it could be shown that for a sample volume below 3.0 mL the nebulization is incomplete and due to this fact the collected amount of liquid decreases. The amount of collected liquid remains unchanged, whether the starting volume is 3.0 mL, 6.0 mL or 12.0 mL. Thus the increase of starting liquid over 3.0 mL is not necessary.

3.1.3 eFlow® rapid

The third tested nebulizer was the eFlow® rapid (vibrating mesh). The mass output intensity is lower than those of the air-jet nebulizer, but still more intensive than for the ultrasonic inhaler. Due to its working mechanism the aerosol is pushed through the vibrating mesh and thus has a proper motion.

To condense this slow velocity vapor a direct connection between the nebulizer and the collection Pyrex tube was set up. The nebulizer's opening almost completely covered the Pyrex tube, and almost no mist could escape. For the first trial a sample volume of 2.0 mL H₂O_{bidest} was used. The nebulizer automatically stops its working process in case the liquid level decreases to a level where it does not cover the mesh completely. This is a safety function to protect the mesh and to avoid overdosing when applied for medical solutions. After 4 min 22 sec the nebulizer stopped working and a total volume of 75 µL could be collected in the Pyrex tube. A major part of the mist condensed in the aerosol chamber directly after the mesh. This is due to the mist's relatively low velocity and the high probability of getting in contact with the chamber walls when having no active inhalation. (see Figure 3. 6)

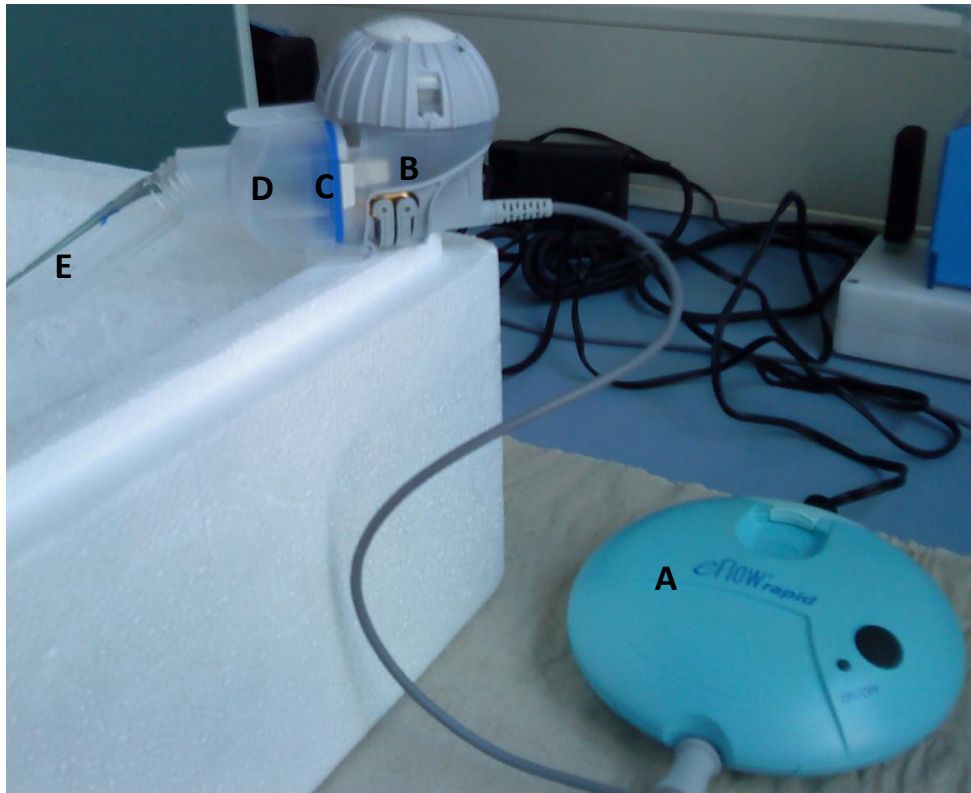


Figure 3. 6: Experimental set-up for the condensation experiments with the eFlow® rapid nebulizer. (A) operating unit connected to electrical supply, (B) nebulizer unit – liquid reservoir chamber, (C) vibrating mesh, (D) nebulizer unit – aerosol chamber after mesh and (E) Pyrex tube in ice bath.

The starting volume was altered to 3.0 mL H₂O_{bidest}, but this had no significant effect on the collectable volume. The volume in the Pyrex tube was again approx. 50 µL and the major part (approx. 500 µL) condensed directly in the nebulizer.

In total this would give a volume of about 550 µL and this is sufficient for further analysis. Following experiments showed that there is no difference between the liquids collected in the Pyrex tube or directly in the nebulizer after the mesh. The liquid underwent the same nebulization process and therefore shows same characteristics independent from the site of condensation.

3.2 Adaption of breathing air condenser for nebulizers

A breathing air condenser and additional equipment for the operation of the machine was provided by the Division of Pulmonology, Medical University of Graz, Austria. With this new device the condensation trials were repeated and improved. The general assembly remained constant, but the ice bath was replaced by the breathing air condenser. This machine gave the possibility of precise and reproducible cooling. It was set to a temperature of 4°C and provided a cooled chamber (50 mL Falcon tube) where the aerosol was condensed.

3.2.1 Optineb®-ir

For the Optineb®-ir a few improvements had to be made. As the condensation process absolutely did not work with the ice bath and the external breathing against the inhalation filter, a different way of inhalation had to be found. For this reason a lung simulator (Lifecare Beatmungsgerät PLV-100, Breas Medical GmbH, Herrsching, Germany) with a corresponding compressor (DeVO/MC 29, DeVILBISS GmbH Medical Products, Dietzenbach, Germany) was available. This instrument was capable of synchronizing a breathing pattern to the operation mode of the Optineb®-ir. Each time the nebulizer requests the patient for inhalation, the instrument simulates an inhalation and subsequent exhalation of the produced mist.

The problem was that the lung simulator collected the aerosol on filters, which was unfavorable for the analysis steps to be done afterwards. (see Figure 3. 7)

Because of this the lung simulator was bypassed and the nebulizer was directly connected to the compressor. The compressor worked continuously and had an inhalation and exhalation tube. The inhalation tube was connected with the breathing

air condenser and this in turn with the Optineb®-ir to produce a continuous inhalation flow. As the inhalation air flow was very powerful its intensity had to be regulated to a lower level. Otherwise the nebulizer's produced mist would be immediately sucked out of the chamber and would not have enough time to condense in the cooling trap. This regulation was done with another intake valve after the breathing air condenser.

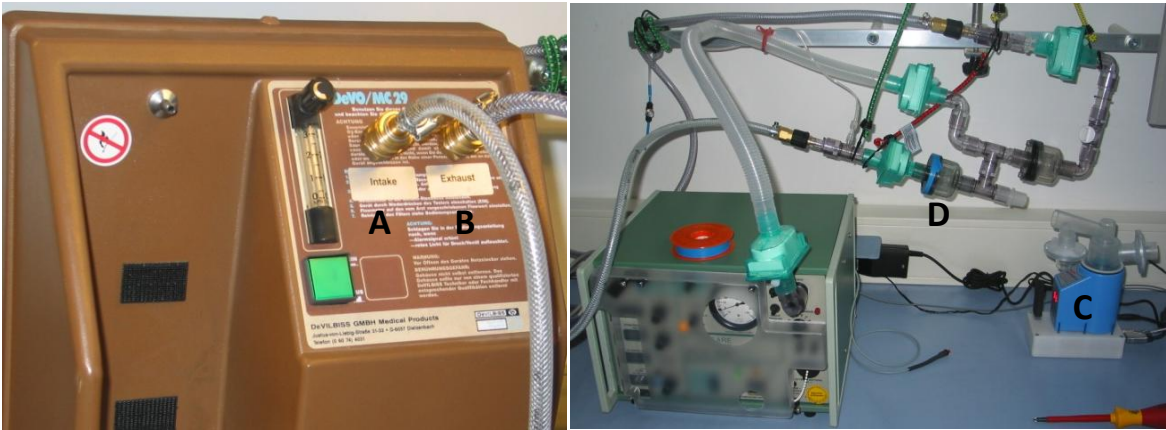


Figure 3. 7: Photos of the compressor (left) and the lung simulator (right). (A) Intake valve simulating inhalation, (B) exhaust valve simulating exhalation, (C) nebulizer, (D) collection filter.

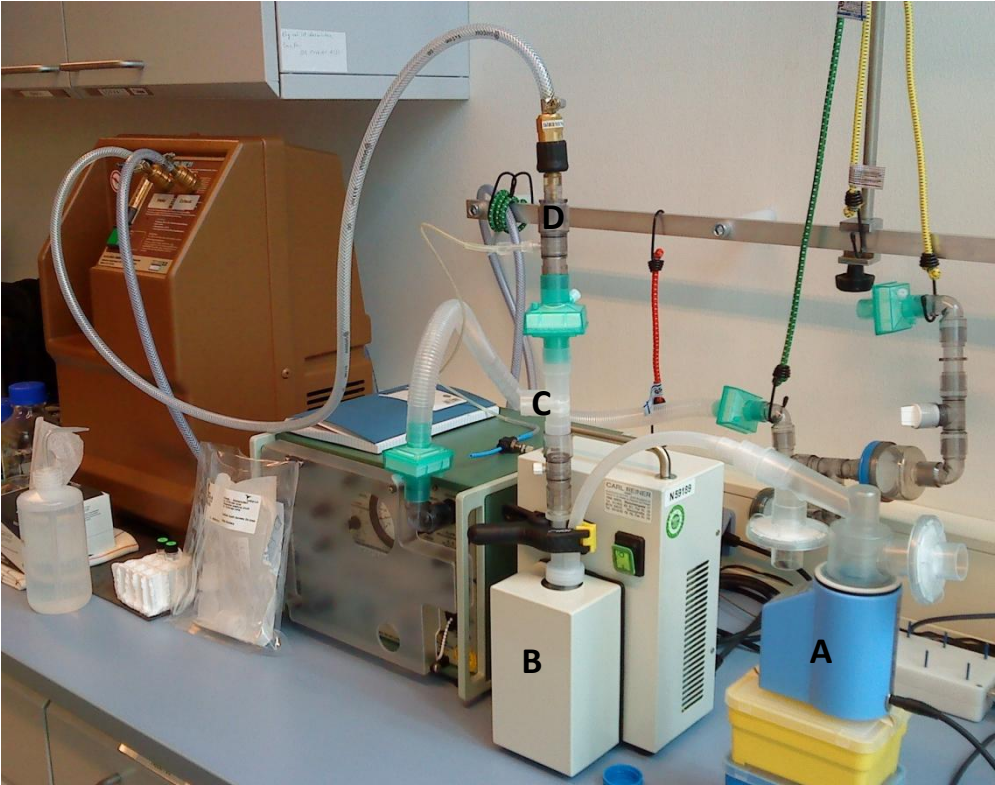


Figure 3. 8: Final assembly of the condensation equipment for the Optineb®-ir. (A) nebulizer, (B) breathing air condenser, (C) regulatory intake valve, (D) connection to compressor intake.

So the nebulizer was connected to the inlet opening of the breathing air condenser and this in turn via the outlet opening to the compressor. (see Figure 3. 8) The liquid was filled into the nebulization chamber of the Optineb®-ir and aerosolized. The compressor was already turned on and produced a continuous and moderate air flow from the nebulizer to the cooling trap. Because of this mild air stream the aerosol had enough time to remain in the cooling trap and to generate a condensate. To get enough condensed mist, the nebulizer was started for 15 times to produce 75 boosts in total.

3.2.2 MicroDrop® Pro

Because the air-jet nebulizer produced a strong active air stream, no further improvement of the system was necessary. The only adjustment made was the exchange of the ice bath with the more accurate breathing air condenser. Also for the experiments with the MicroDrop® Pro the temperature was set to 4°C. With this experimental set-up the optimal amount of liquid could be collected after nebulization.

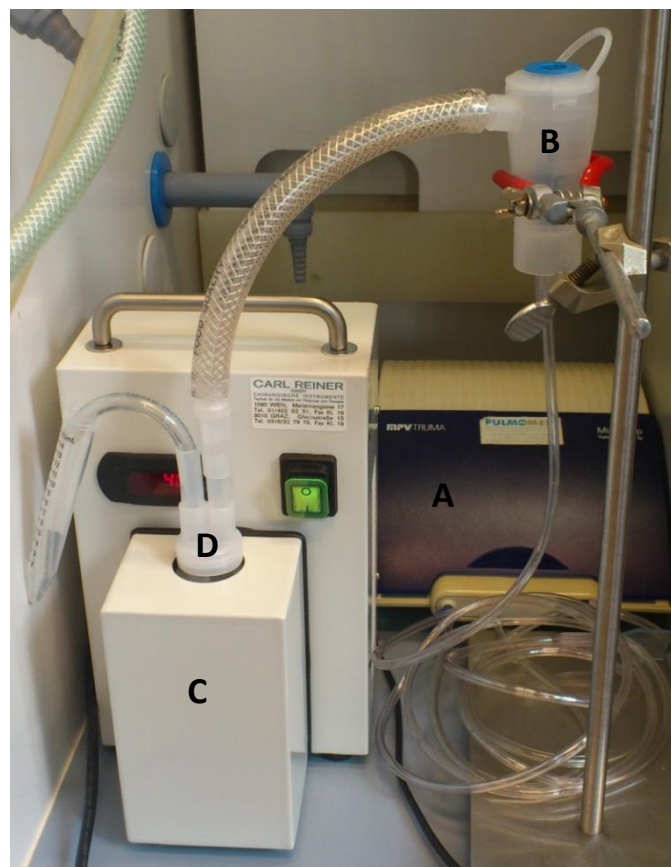


Figure 3. 9: Final experimental set-up of the condensation equipment for the MicroDrop® Pro. (A) MicroDrop® compressor, (B) nebulizer chamber, (C) breathing air condenser, (D) sample collection tube.

3.2.3 eFlow® rapid

The same improvements as done for the MicroDrop® *Pro* were done for the eFlow® rapid. The ice bath was exchanged with the breathing air condenser and the mouthpiece of the nebulizer adapted to a tubing system, which led to the cooling trap. With this improved version it was possible to collect enough aerosol for further analysis.

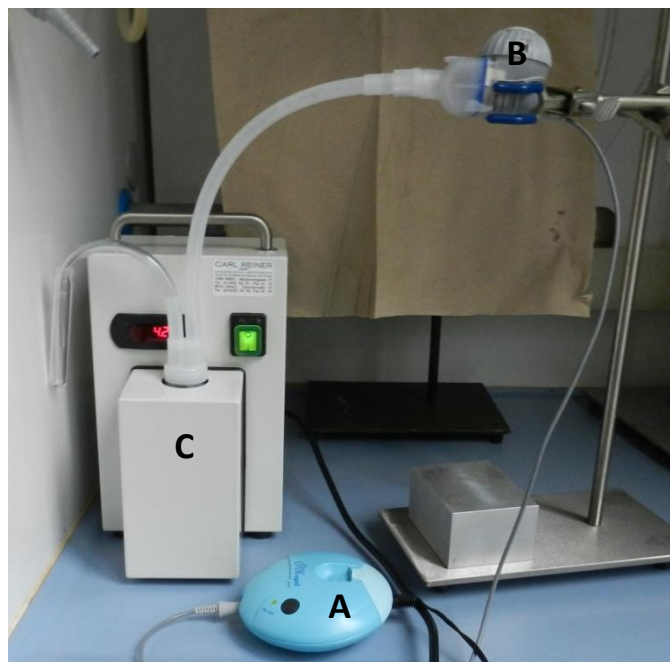


Figure 3. 10: Final experimental set-up of the condensation equipment for the eFlow® rapid. (A) eFlow® rapid operating unit, (B) nebulizer unit connected to operating unit, (C) breathing air condenser.

So the condensation equipment was set-up successfully for all three nebulizers and was ready to use for the nebulization trials with liposomal emulsions.

3.3 Nebulization trials with empty liposomes L-1 and L-2

3.3.1 MicroDrop® *Pro*

The experimental set-up was used exactly as described before in chapter 3.2. As a first step the experiments were done with the air-jet nebulizer MicroDrop® *Pro* and the empty liposomal formulations L-1 and L-2. The empty liposomes were prepared analogously to those with iloprost, but no active drug was added before evaporation of the organic solvent. The exact liposomal composition can be seen in Table 3. 1.

Table 3. 1: Liposomal composition for L-1 and L-2.

Component [mol%]	L-1	L-2
POPC	87	87
Stearylamine	10	10
DPPE-PEG2000	3	-
Kollidon® 17 PF (PVP)	-	3

The liposomes were prepared at concentrations of 6.0 mg/mL total lipid amount. After their final extrusion they were diluted to a final lipid concentration of 3.0 mg/mL and 0.6 mg/mL with Tris/HCl buffer 10 mM pH 7.0. The size of liposomes in the sample and their PDI was measured before the nebulization (start) and after the procedure (aerosol and remainder), as well as the liposomal concentration for the 3.0 mg/mL samples.

For all nebulization procedures 3.0 mL sample were used. The compressor was turned on for exactly 6 min. In Table 3. 2 the volumes of the various samples before and after nebulization are summarized. The table afterwards provides an overview of all DLS measurements done before and after nebulization.

Table 3. 2: Volumes of the samples before and after nebulization with MicroDrop® Pro for L-1 and L-2.

Volumes [µL]	start	aerosol	remainder	loss
L-1 3.0 mg/mL	3000	550	1300	1150
L-2 3.0 mg/mL	3000	400	1300	1300
L-1 0.6 mg/mL	3000	370	1650	980
L-2 0.6 mg/mL	3000	170	1650	1180

Table 3. 3: Size and PDI results from the liposomes L-1 and L-2 before and after nebulization with MicroDrop® Pro.

	start		aerosol		remainder	
	size [nm]	PDI	size [nm]	PDI	size [nm]	PDI
L-1 3.0 mg/mL	164.2	0.116	225.4	0.528	150.3	0.200
L-2 3.0 mg/mL	168.8	0.123	165.8	0.124	159.7	0.117
L-1 0.6 mg/mL	164.5	0.143	293.9	0.759	149.9	0.217
L-2 0.6 mg/mL	168.8	0.123	206.5	0.270	161.0	0.136

The nebulization worked well for both formulations. The aerosol stream could be observed but unfortunately the non-condensed mist was lost during nebulization because of the compressor's relatively powerful air stream. After 6 min the produced aerosol amount decreased significantly due to lack of liquid in the nebulizer chamber. The dead volume of the nebulizer is approximately 1 mL. Moreover the occurrence of foam could be observed after 6 min of nebulization. Due to the strong shear forces and the low liquid level at the end more foam was generated. This may be also the reason for the significantly decreased aerosol production after 6 min.

The foam occurrence was decreased for the more diluted samples. This seems to be obvious as more liposomes can produce more foam. Another finding was that the amount of foam was lower with the L-2 formulation. So probably the PVP has an advantageous effect towards the reduction of emerging foam.

The following three figures exemplarily show DLS results from liposomes before and after nebulization. The size distribution obtained from a DLS measurement is based on intensity. These three figures show the size distribution as a function of % intensity. It is important to mind that bigger particles produce a higher scattering intensity.

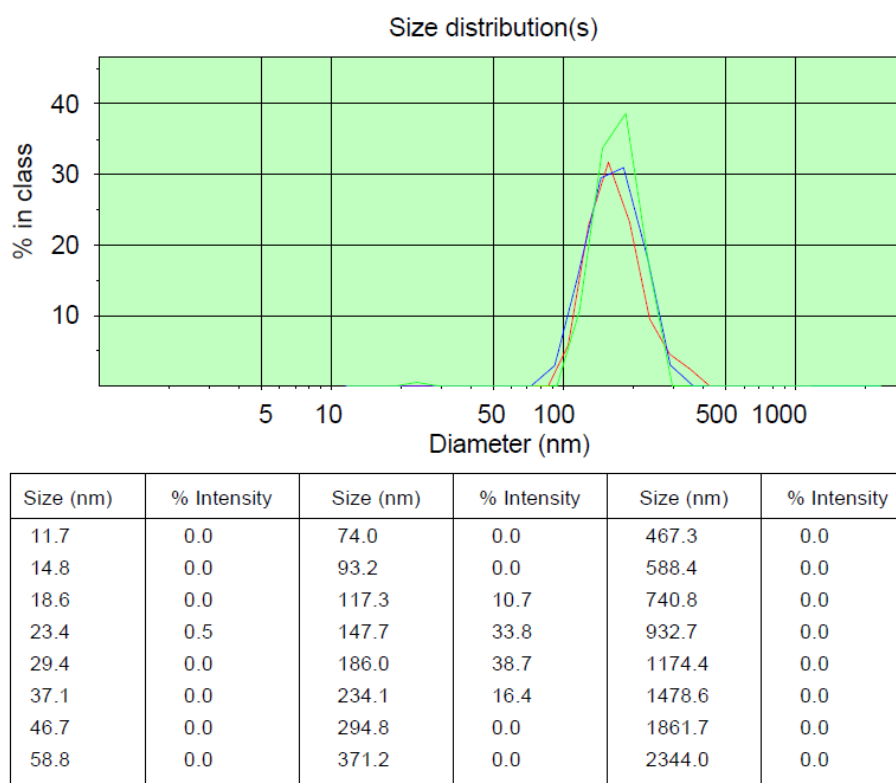


Figure 3. 11: L-1 before nebulization DLS result curve and table show size distribution vs. intensity.

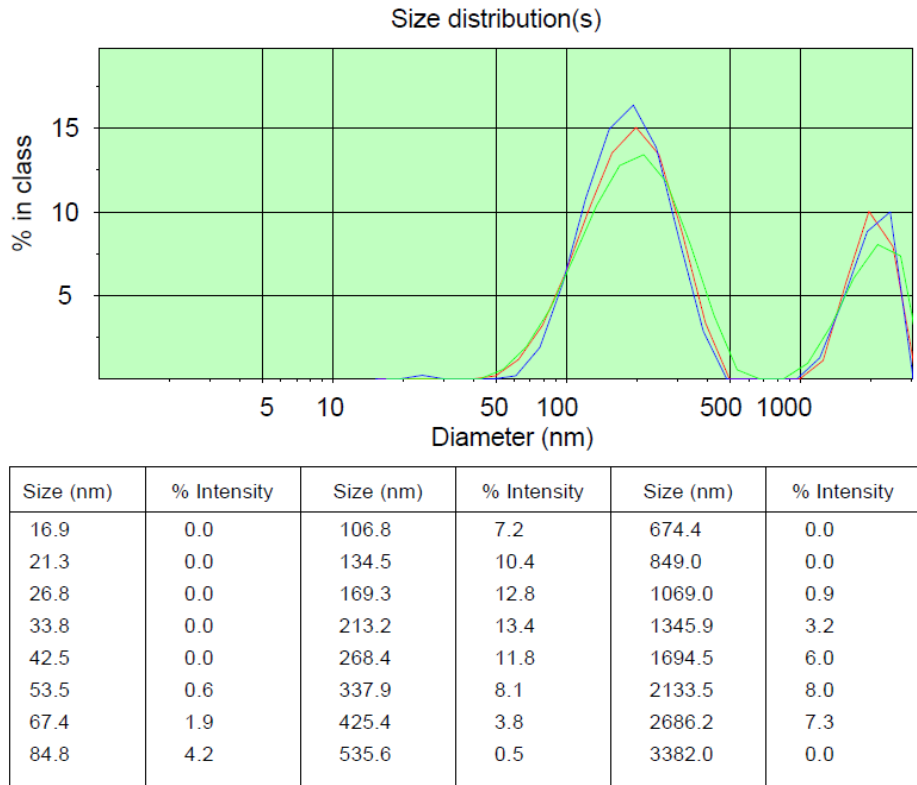


Figure 3. 12: L-1 aerosol after nebulization DLS result curve and table show size distribution vs. intensity.

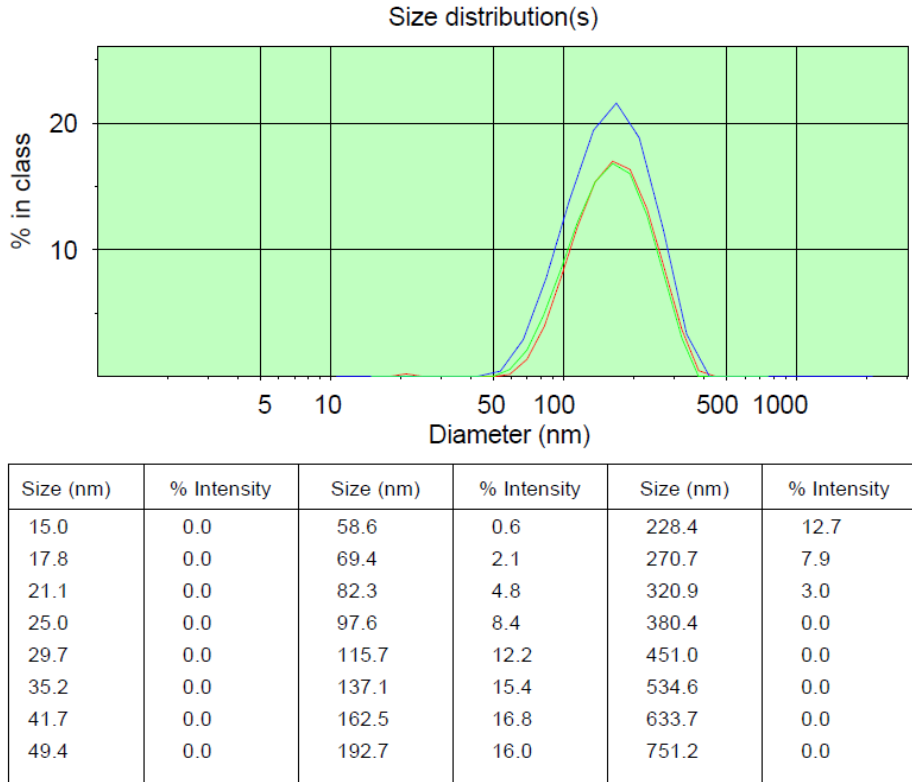


Figure 3. 13: L-1 remainder after nebulization DLS result curve and table show size distribution vs. intensity.

In this particular case for L-1 with 3.0 mg/mL shown in the figures before, the starting solution has an average size of 164.2 nm with a PDI of 0.116. This PDI is extremely low and indicates a very homogeneous size distribution among prepared liposomes. After nebulization the average size of the aerosol is 225.4 nm with a PDI of 0.528. This would immediately lead to the conclusion that the average size has increased and the size distribution is much wider than before. But this is not absolutely correct. When checking the real size distribution as a function of intensity (see Figure 3. 12) one can see that the main size distribution is approximately the same and only some very large particles have this big influence on average size. Moreover it has to be considered that intensity correlates to diameter to the power of 6 (d^6). This means that one single very large particle gives a 10^6 higher intensity than a small particle. This leads to the conclusion that only some larger particles are actually produced in the aerosol, but give a relatively high intensity peak.

The remainder after nebulization has an average size of 150.3 nm and a PDI of 0.200, which is also very low. The size distribution is comparable to the starting solution and the PDI only slightly increased. So the liposomes seem to be quite stable during the nebulization process.

The same is true for L-2, which was even more stable than L-1 concerning size and PDI changes.

Another observation was that the more diluted the samples were the less stable they seemed to be during nebulization. The size and PDI changes were more significant in samples with lower concentration. (see Table 3. 3)

Table 3. 4: Liposomal concentration in samples without iloprost when nebulized with MicroDrop® Pro (n=1).

POPC [mg/mL]	start	aerosol	remainder
L-1	2,58	1,87	2,92
L-2	2,07	1,41	2,81

As already mentioned before, the liposomal concentration was also determined in the samples with a phospholipid assay. From the results presented in Figure 3. 14 one can nicely see that the liposomal concentration in the aerosol is lower than in the starting solution. On the contrary the concentration was increased in the remainder. This indicates that a lower amount of liposomes is transported to the aerosol via nebulization than remains in the reservoir liquid. This may be due to inertia of the liposomal particles and therefore developed nebulization gradient.

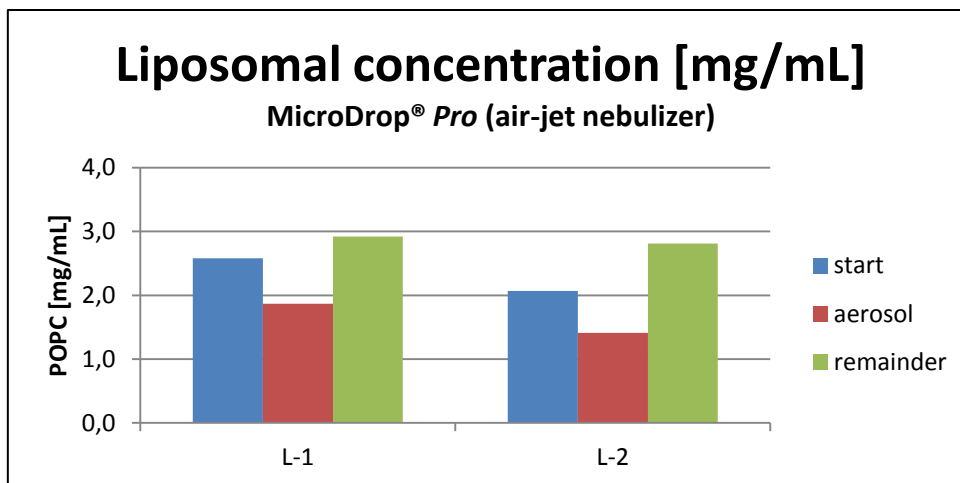


Figure 3. 14: Liposomal concentration in samples without iloprost when nebulized with MicroDrop® Pro (n=1).

3.3.2 Optineb®-ir

The second tested nebulizer was the Optineb®-ir. The same empty liposomal formulations L-1 and L-2 were used. Again the samples were diluted to final lipid concentrations of 3.0 mg/mL and 0.6 mg/mL with Tris/HCl buffer 10 mM pH 7.0. The size of liposomes in the sample and their PDI was measured before the nebulization (start) and after the procedure (aerosol and remainder), as well as the liposomal concentration for the 3.0 mg/mL samples.

For all nebulization procedures 2.0 mL sample were used. For each experiment the nebulizer was started for 15 cycles to produce a total number of 75 boosts. The following two tables provide an overview of sample volumes and DLS measurements for the experiments with the ultrasonic nebulizer.

Table 3. 5: Volumes of the samples before and after nebulization with Optineb®-ir for L-1 and L-2.

Volumes [μ L]	start	aerosol	remainder	loss
L-1 3.0 mg/mL	2000	310	420	1270
L-2 3.0 mg/mL	2000	250	850	900
L-1 0.6 mg/mL	2000	230	450	1320
L-2 0.6 mg/mL	2000	220	780	1000

The significant loss of sample for the different experiments was relatively high compared to the collected aerosol. This is due to the experimental set-up and was further optimized by reducing the inhalation intensity of the compressor. With this

change the loss of aerosol passing through the cooling trap without condensing was reduced.

Table 3. 6: Size and PDI results from the liposomes L-1 and L-2 before and after nebulization with Optineb®-ir.

	start		aerosol		remainder	
	size [nm]	PDI	size [nm]	PDI	size [nm]	PDI
L-1 3.0 mg/mL	158.9	0.094	176.9	0.221	168.1	0.186
L-2 3.0 mg/mL	172.0	0.079	170.5	0.101	174.1	0.114
L-1 0.6 mg/mL	158.9	0.094	*	*	198.1	0.310
L-2 0.6 mg/mL	172.0	0.079	*	*	178.8	0.223

*polydisperse PDI 1.000

As already discussed for the air-jet nebulizer, the more diluted samples showed a drastically decreased stability during nebulization, which was even more pronounced with the ultrasonic nebulizer. The 3.0 mg/mL samples were very stable and showed almost no significant changes in size or PDI. This was completely different for the 0.6 mg/mL samples. The collected aerosols of L-1 and L-2 were polydisperse and no average size could be determined, the PDI was about 1.0.

As already shown for the air-jet nebulizer, also for the ultrasonic device the L-2 formulation was more stable than L-1, since size and PDI change was lower.

There was no foam generation during the nebulization process. Moreover it was undoubtedly observable that the remainder had a more opalescent appearance compared to the collected aerosol, which was a completely clear liquid. This was a distinct indication that the liposomes were concentrated in the remainder and only partially transported to the aerosol. And it was approved by the phospholipid assay to determine the liposomal concentration.

As the results in Figure 3. 15 show, the transport of liposomes to the aerosol was very incomplete. The ultrasonic device was not capable of transporting the liposomal particles to the inhalable aerosol. This may be due to the technique of producing an ultrasonic wave, which first pervades the liquid to the surface and then carries liquid droplets from the surface along to the air. Inertia may play an even more important role in this nebulization technique than for the air-jet inhaler.

Table 3. 7: Liposomal concentration in samples without iloprost before and after nebulization with Optineb®-ir (n=1).

POPC [mg/mL]	start	aerosol	remainder
L-1	2,58	0,50	3,71
L-2	2,07	0,23	2,69

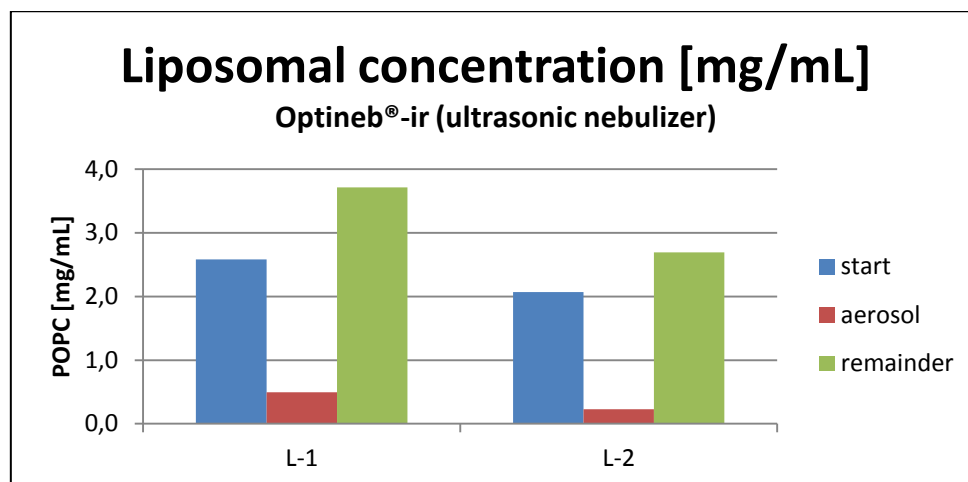


Figure 3. 15: Liposomal concentration in samples without iloprost before and after nebulization with Optineb®-ir (n=1).

3.3.3 eFlow® rapid

The third tested nebulizer was the eFlow® rapid. The same empty liposomal formulations L-1 and L-2 were used and diluted to final lipid concentrations of 3.0 mg/mL and 0.6 mg/mL with Tris/HCl buffer 10 mM pH 7.0. The size of liposomes in the sample and their PDI was measured before the nebulization (start) and after the procedure (aerosol and remainder), as well as the liposomal concentration for the 3.0 mg/mL samples.

For all nebulization procedures 3.0 mL sample were used. For each experiment the nebulizer worked until it automatically stopped. The following two tables provide an overview of sample volumes and DLS measurements.

Table 3. 8: Volumes of the samples before and after nebulization with eFlow® rapid for L-1 and L-2.

Volumes [μ L]	start	aerosol	remainder	loss
L-1 3.0 mg/mL	3000	1300	900	800
L-2 3.0 mg/mL	3000	950	1060	990
L-1 0.6 mg/mL	3000	1450	1000	550
L-2 0.6 mg/mL	3000	1150	1000	850

The results clearly show that L-2 is again more resistant and more stable during nebulization than L-1. The size and PDI values for L-1 increased considerably more in the aerosol than for L-2, which had almost constant values. Moreover it could be observed that the samples with lower liposome concentration were less stable than for the higher concentration, which was already observed for the other two nebulizers as well.

Table 3. 9: Size and PDI results from the liposomes L-1 and L-2 before and after nebulization with eFlow® rapid.

	start		aerosol		remainder	
	size [nm]	PDI	size [nm]	PDI	size [nm]	PDI
L-1 3.0 mg/mL	155.7	0.097	194.7	0.425	148.0	0.121
L-2 3.0 mg/mL	167.9	0.111	164.4	0.122	164.2	0.102
L-1 0.6 mg/mL	155.7	0.097	273.1*	0.645*	148.1	0.220
L-2 0.6 mg/mL	165.4	0.116	170.3	0.152	168.4	0.127

* bimodal distribution – average size and PDI not significant

Foam was generated during nebulization in the reservoir chamber, but had no effect on the nebulization efficiency. The opalescence of the collected aerosol and the remainder were approximately the same, which was approved by the similar concentration determined with the phospholipid assay. The results point out that liposomal transport is clearly most efficient with the eFlow® rapid inhaler. The concentration of liposomes in the collected aerosol is almost the same as in the starting solution. The minor increase in concentration of the remainder may be due to loss of liquid without liposomes and a subsequent accumulation.

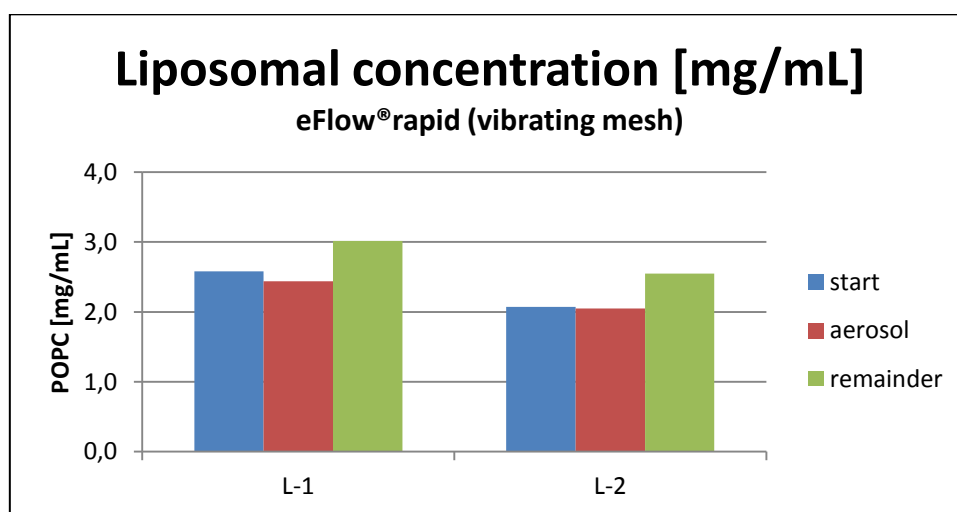


Figure 3. 16: Liposomal concentration in samples without iloprost before and after nebulization with eFlow® rapid (n=1).

Table 3. 10: Liposomal concentration in samples without iloprost before and after nebulization with eFlow® rapid (n=1).

POPC [mg/mL]	start	aerosol	remainder
L-1	2,58	2,44	3,02
L-2	2,07	2,05	2,55

3.4 Nebulization trials with iloprost loaded liposomes LI-1 and LI-2

The experimental set-up was used as described before in chapter 3.2. The experiments were done with iloprost loaded liposomes LI-1 and LI-2. The liposomal composition can be seen in Table 3. 1. The trials were executed again for all three nebulizers and with the same concentrations of 3.0 mg/mL and 0.6 mg/mL and each with a starting volume of 3.0 mL sample. The nebulization of the 3.0 mg/mL samples was made in triplicate. The average size, the PDI and the phospholipid concentration were determined for all samples. Moreover the iloprost encapsulation efficiency was determined for the 3.0 mg/mL samples before and after nebulization.

3.4.1 MicroDrop® Pro

The first two figures show the results of the phospholipid determination for nebulized LI-1 and LI-2. The first one illustrates the absolute POPC concentrations comparing the start with the aerosol and the remainder. The second figure depicts the same results in percent to enable a comparison among the two formulations and different nebulizer devices. The starting concentration is assumed as 100% and the other concentrations shown in relation to this value.

Analyzing the results it can be seen that the liposomal transport efficiencies are very similar for both formulations. The nebulizer delivers less than half of the liposomes to the aerosol, 40% and 46% respectively. For both formulations this in turn leads to an enrichment of liposomes in the remainder, 119% and 113% respectively. So the results demonstrate that the MicroDrop® Pro has the ability of transporting liposomes to the aerosol but with a relatively high loss of more than 50%. (see Figure 3. 17 and Figure 3. 18)

Table 3. 11: Liposomal concentration [mg/mL] in samples with iloprost before and after nebulization with MicroDrop® Pro (mean ± S.D., n=3).

POPC [mg/mL]	start	+/-	aerosol	+/-	remainder	+/-
LI-1	2,58	0,13	1,03	0,41	3,07	0,13
LI-2	2,07	0,10	0,94	0,20	2,34	0,06

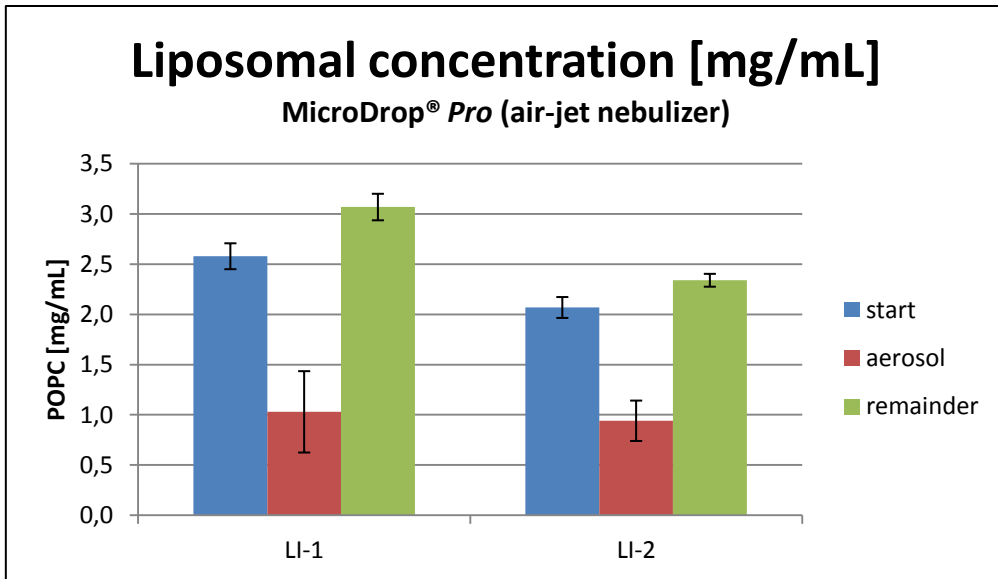


Figure 3. 17: Liposomal concentration [mg/mL] in samples with iloprost before and after nebulization with MicroDrop® Pro (mean ± S.D., n=3).

Table 3. 12: Liposomal concentration [%] in samples with iloprost before and after nebulization with MicroDrop® Pro (mean ± S.D., n=3).

POPC [%]	start	+/-	aerosol	+/-	remainder	+/-
LI-1	100,0	5,0	40,0	15,7	119,0	5,1
LI-2	100,0	5,0	45,5	9,7	113,1	3,1

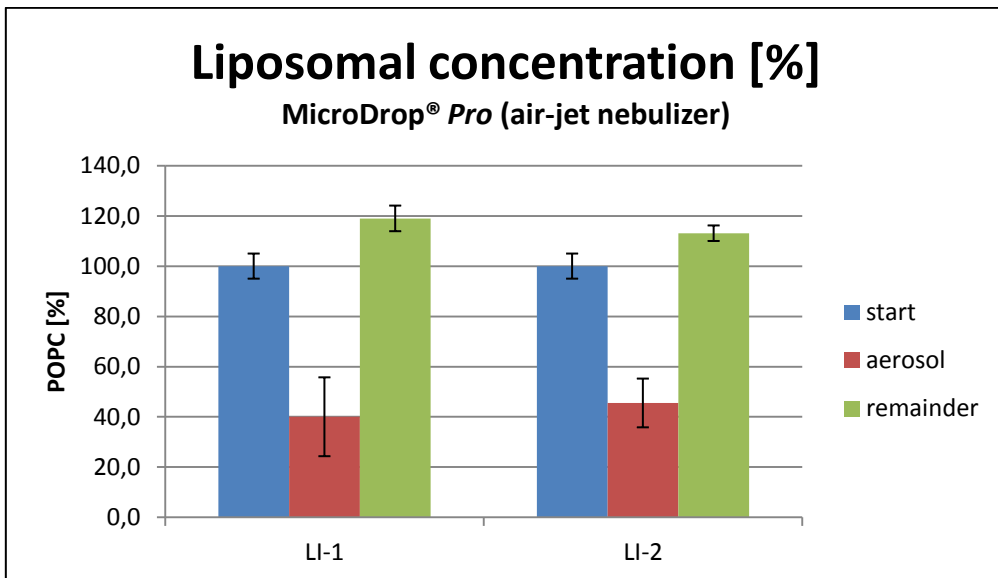


Figure 3. 18: Liposomal concentration [%] in samples with iloprost before and after nebulization with MicroDrop® Pro (mean ± S.D., n=3).

The next two figures depict size and PDI analyses before and after nebulization. From these measurements it can be seen that the particle size is only slightly influenced by nebulization.

Table 3. 13: Liposomal particle size in samples with iloprost before and after nebulization with MicroDrop® Pro (mean ± S.D., n=3).

size [nm]	start	+/-	aerosol	+/-	remainder	+/-
LI-1	166,5	2,0	178,0	8,8	153,3	4,7
LI-2	169,3	2,8	165,8	6,1	151,1	2,0

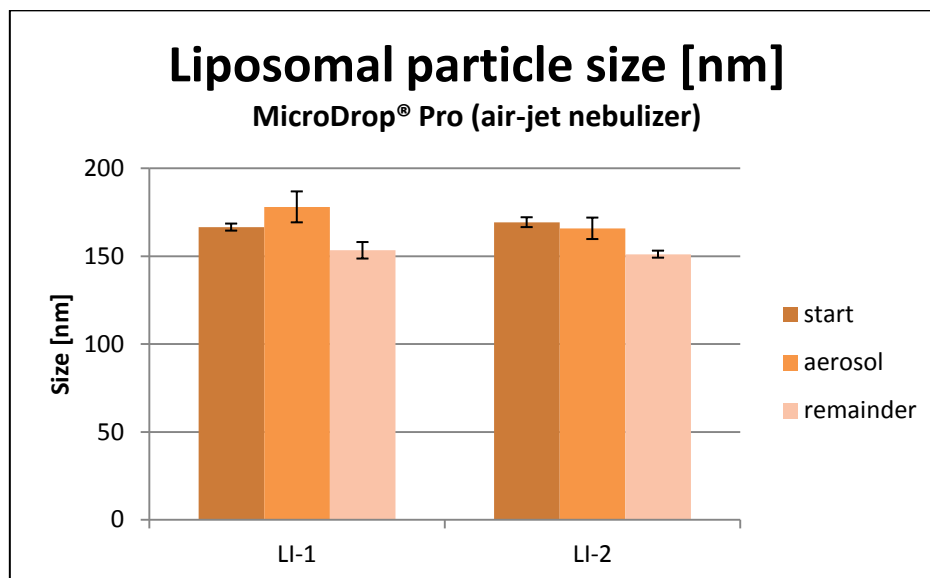


Figure 3. 19: Liposomal particle size in samples with iloprost before and after nebulization with MicroDrop® Pro (mean ± S.D., n=3).

Table 3. 14: Liposomal particle PDI in samples with iloprost before and after nebulization with MicroDrop® Pro (mean ± S.D., n=3).

PDI	start	+/-	aerosol	+/-	remainder	+/-
LI-1	0,124	0,027	0,275	0,041	0,191	0,016
LI-2	0,143	0,025	0,190	0,007	0,168	0,017

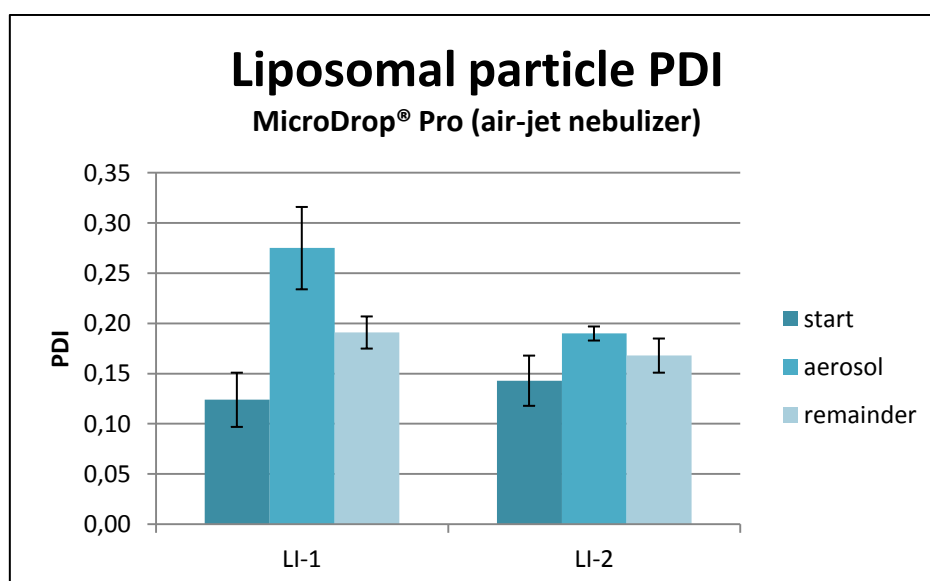


Figure 3. 20: Liposomal particle PDI in samples with iloprost before and after nebulization with MicroDrop® Pro (mean ± S.D., n=3).

The particle size slightly increases only in the aerosol of LI-1. In all other samples the average size decreases a little bit. These decreases are quite similar for both remainders, 167 nm to 153 nm and 169 nm to 151 nm for LI-1 and LI-2, respectively. When considering the PDI values for the measurements, it is clear that nebulization has an influence on particle size distribution. But the PDI of all samples increased only very slightly. The only sample with a higher PDI increase is the LI-1 aerosol, which was the only sample with an average liposome size increase. This leads to the conclusion that LI-1 is less stable during nebulization than LI-2.

All in all the nebulizer does not destroy the liposomes; none of the formulations shows significant changes in size or PDI. Merely the transport efficiency is limited due to the technology.

The experiment was also carried out once with a lower liposomal concentration of 0.6 mg/mL and those results are summarized in the following figure. The results are very similar to those of the higher concentration. Approximately 40% of the liposomes are transported for both LI-1 and LI-2. So the relative nebulization efficiency is independent from the initial concentration.

Table 3. 15: Liposomal concentration [mg/mL] in samples with iloprost before and after nebulization with MicroDrop® Pro (n=1).

POPC [mg/mL]	start	aerosol	remainder
LI-1	0,52	0,20	0,42
LI-2	0,41	0,15	0,34

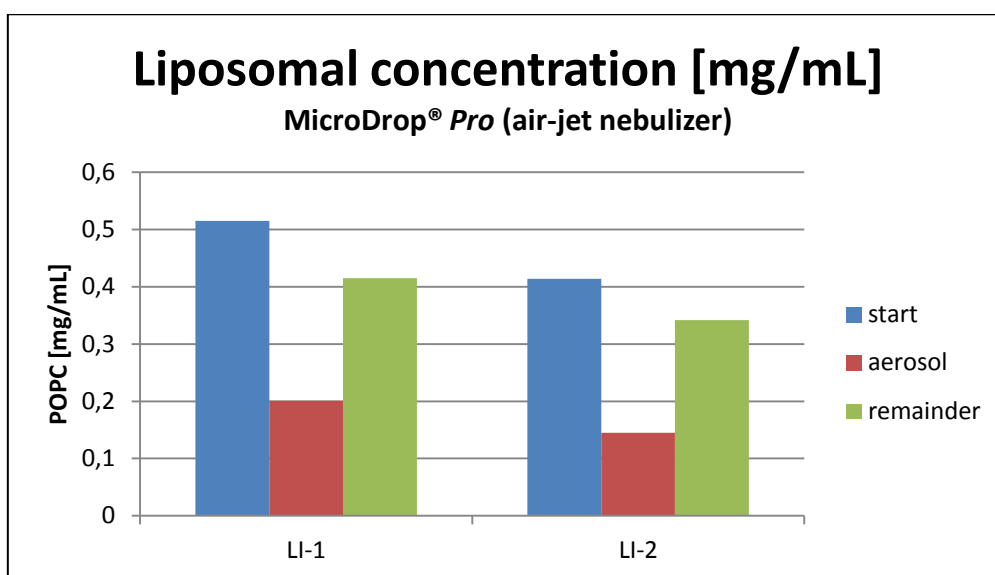


Figure 3. 21: Liposomal concentration [mg/mL] in samples with iloprost before and after nebulization with MicroDrop® Pro (n=1).

3.4.2 Optineb®-ir

The results for the Optineb®-ir are summarized in the following figures. In contrast to the MicroDrop® *Pro* is the nebulizer's efficiency of transporting liposomes significantly worse. Figure 3. 22 shows the absolute POPC amounts where a significant lack of transport is evident. The second figure summarized the relative amounts in percent. From these results one can say that transport is even worse than for the air-jet nebulizer. Transported liposomes are only 17% and 12% for LI-1 and LI-2 respectively. Again the remainder showed an increased concentration of about 122% of the initial one. To sum up, the ultrasonic nebulizer shows extremely poor transport efficiencies for liposomes, independent from the formulation.

Table 3. 16: Liposomal concentration [mg/mL] in samples with iloprost before and after nebulization with Optineb®-ir (mean ± S.D., n=3).

POPC [mg/mL]	start	+/-	aerosol	+/-	remainder	+/-
LI-1	2,58	0,13	0,44	0,01	3,15	0,22
LI-2	2,07	0,10	0,25	0,03	2,51	0,17

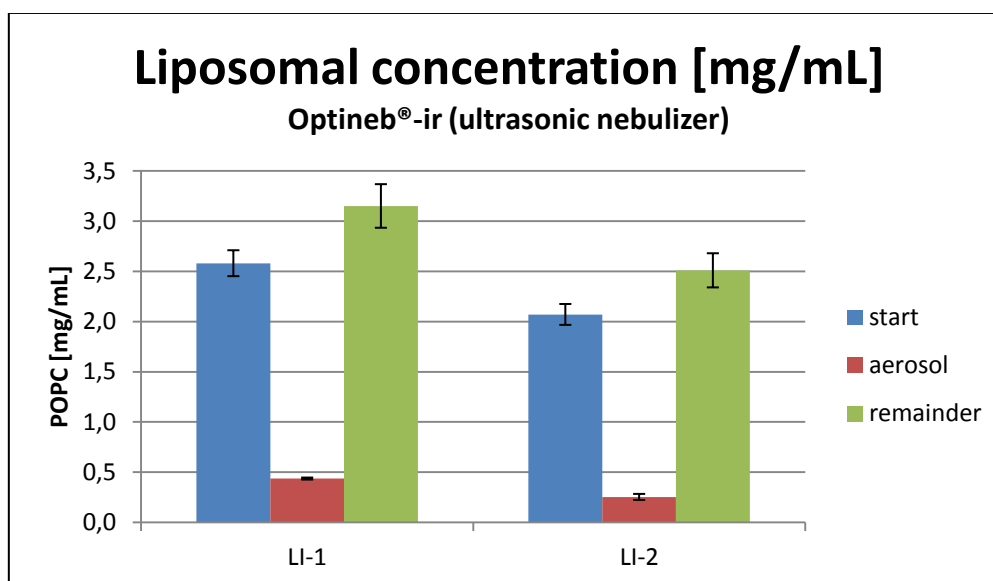


Figure 3. 22: Liposomal concentration [mg/mL] in samples with iloprost before and after nebulization with Optineb®-ir (mean ± S.D., n=3).

Table 3. 17: Liposomal concentration [%] in samples with iloprost before and after nebulization with Optineb®-ir (mean ± S.D., n=3).

POPC [%]	start	+/-	aerosol	+/-	remainder	+/-
LI-1	100,0	5,0	16,9	0,4	122,1	8,4
LI-2	100,0	5,0	12,2	1,4	121,2	8,2

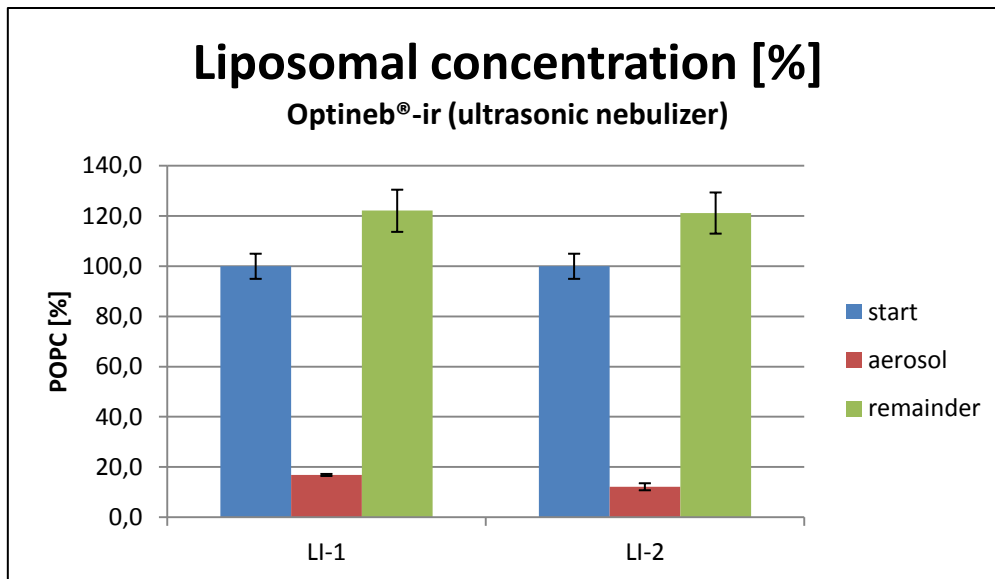


Figure 3. 23: Liposomal concentration [%] in samples with iloprost before and after nebulization with Optineb®-ir (mean \pm S.D., n=3).

The size and PDI analyses showed almost unchanged liposomal sizes and relatively small PDI changes. The aerosol of LI-1 had the largest increase in size and the highest standard deviation, which is also reflected in its very high and variable PDI.

Table 3. 18: Liposomal particle size in samples with iloprost before and after nebulization with Optineb®-ir (mean \pm S.D., n=3).

size [nm]	start	+/-	aerosol	+/-	remainder	+/-
LI-1	164,8	3,7	178,2	11,0	166,1	0,7
LI-2	168,6	3,6	170,4	6,1	171,2	6,6

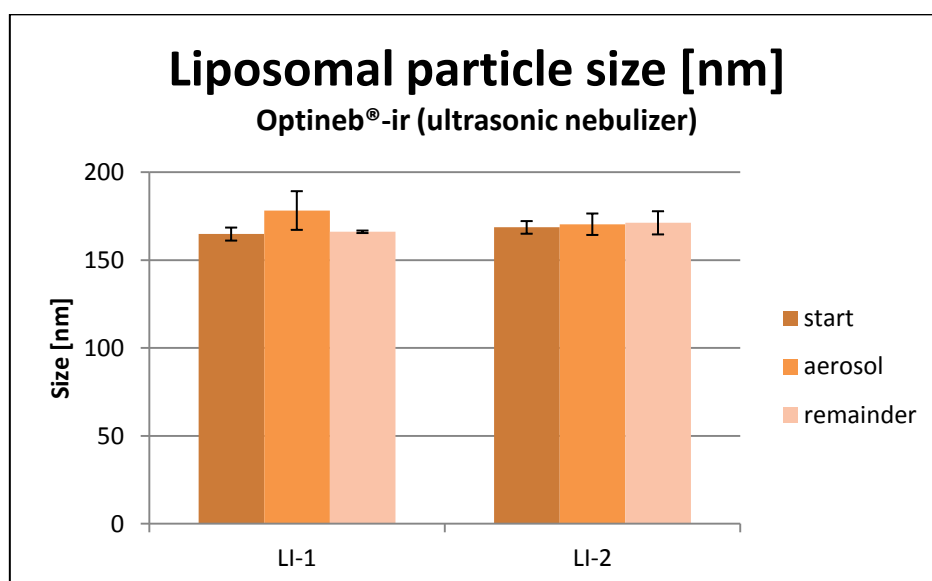


Figure 3. 24: Liposomal particle size in samples with iloprost before and after nebulization with Optineb®-ir (mean \pm S.D., n=3).

Table 3. 19: Liposomal particle PDI in samples with iloprost before and after nebulization with Optineb®-ir (mean ± S.D., n=3).

PDI	start	+/-	aerosol	+/-	remainder	+/-
LI-1	0,101	0,009	0,248	0,097	0,158	0,040
LI-2	0,088	0,003	0,170	0,037	0,126	0,023

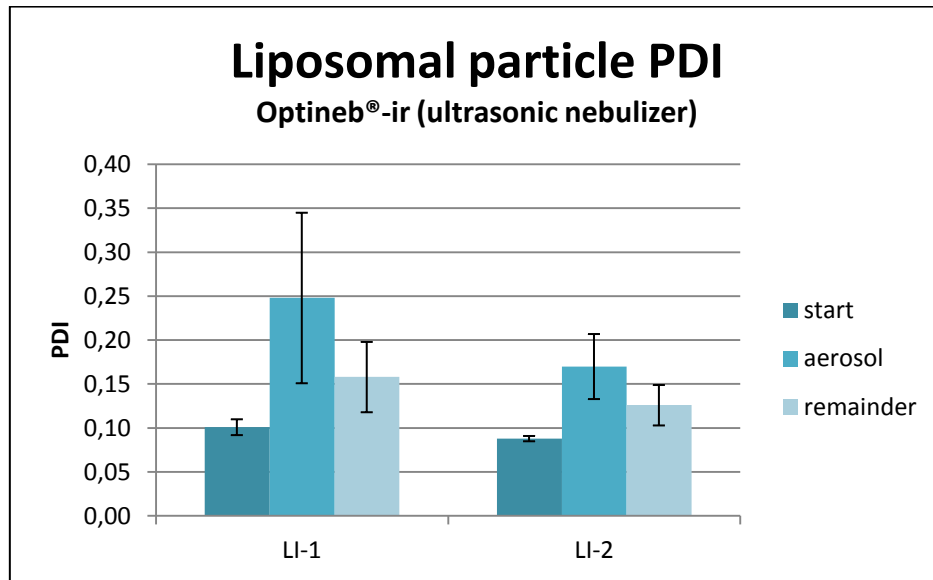


Figure 3. 25: Liposomal particle PDI in samples with iloprost before and after nebulization with Optineb®-ir (mean ± S.D., n=3).

In contrast to this size variation of LI-1, the second formulation LI-2 had an absolutely unchanged average size and only very small PDI changes. This indicates that LI-2 is a bit more stable than LI-1.

All in all these changes are not very prominent, and both formulations are suitable for the ultrasonic nebulizer. But the technology itself may have limitations for liposomal transport and due to this may be uneconomical.

Also for this nebulizer a lower concentration was tested. The result absolutely reflects those of the higher concentrations. The transport of liposomes is almost identical with 17% and 14% respectively. So the technology is unsuitable for the nebulization of liposomes independent of the applied concentration.

Table 3. 20: Liposomal concentration [mg/mL] in samples with iloprost before and after nebulization with Optineb®-ir (n=1).

POPC [mg/mL]	start	aerosol	remainder
LI-1	0,52	0,09	0,69
LI-2	0,41	0,06	0,49

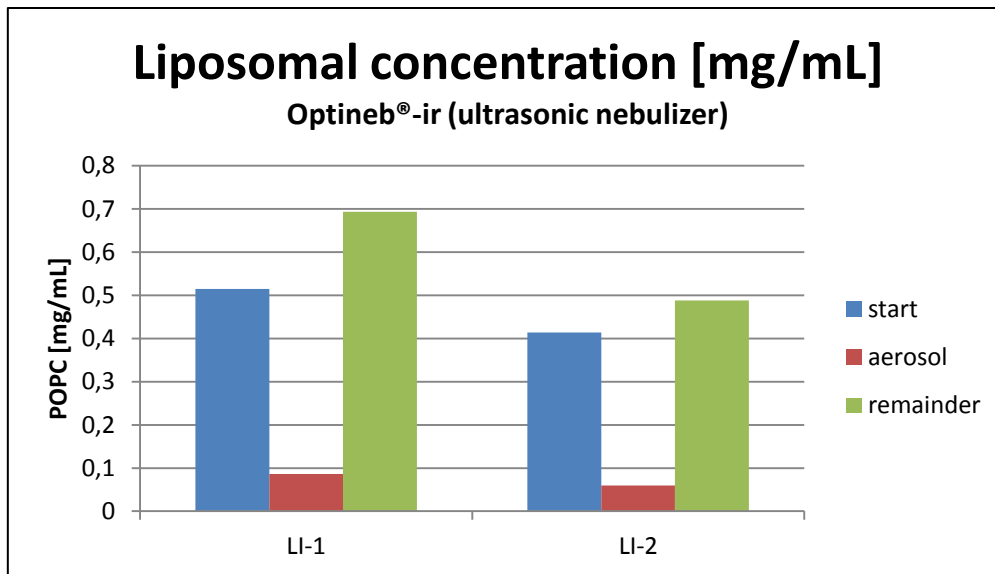


Figure 3. 26: Liposomal concentration [mg/mL] in samples with iloprost before and after nebulization with Optineb®-ir (n=1).

3.4.3 eFlow® rapid

The results for the vibrating mesh nebulizer are summarized in the following figures.

Table 3. 21: Liposomal concentration [mg/mL] in samples with iloprost before and after nebulization with eFlow® rapid (mean ± S.D., n=3).

POPC [mg/mL]	start	+/-	aerosol	+/-	remainder	+/-
LI-1	2,58	0,13	2,40	0,52	2,56	0,48
LI-2	2,07	0,10	2,06	0,12	2,22	0,25

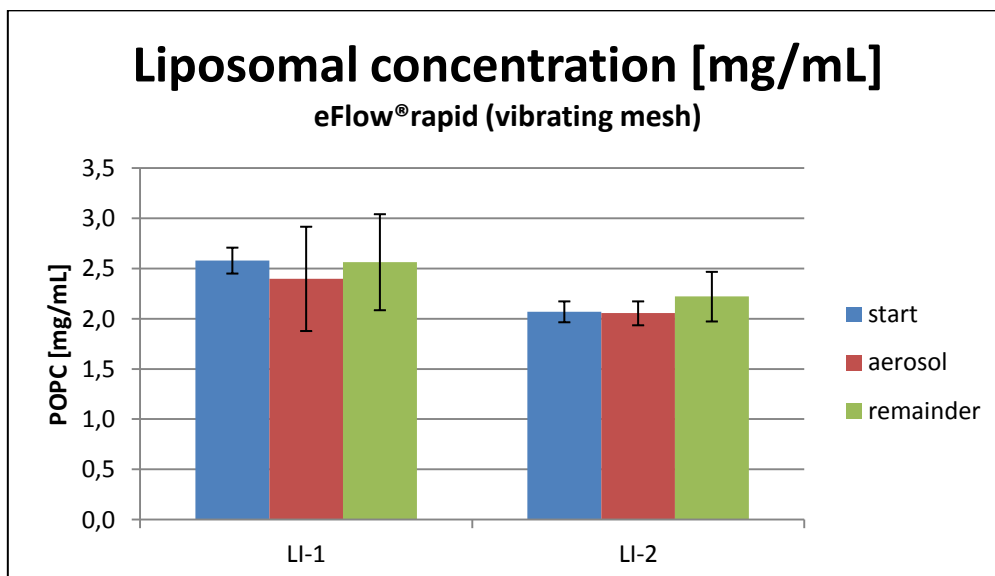


Figure 3. 27: Liposomal concentration [mg/mL] in samples with iloprost before and after nebulization with eFlow® rapid (mean ± S.D., n=3).

Again the liposome concentration was measured and interestingly it gave completely different results compared to the other two nebulizers. The aerosol's concentration was almost completely the same as the initial one, which indicates that almost all liposomes are getting transported and no concentration gradient emerges. With a transported amount of 93% and 99% respectively this is ideal for a liposomal application. (see Table 3. 22)

Table 3. 22: Liposomal concentration [%] in samples with iloprost before and after nebulization with eFlow® rapid (mean ± S.D., n=3).

POPC [%]	start	+/-	aerosol	+/-	remainder	+/-
LI-1	100,0	5,0	92,9	20,1	99,4	18,5
LI-2	100,0	5,0	99,3	5,8	107,3	11,9

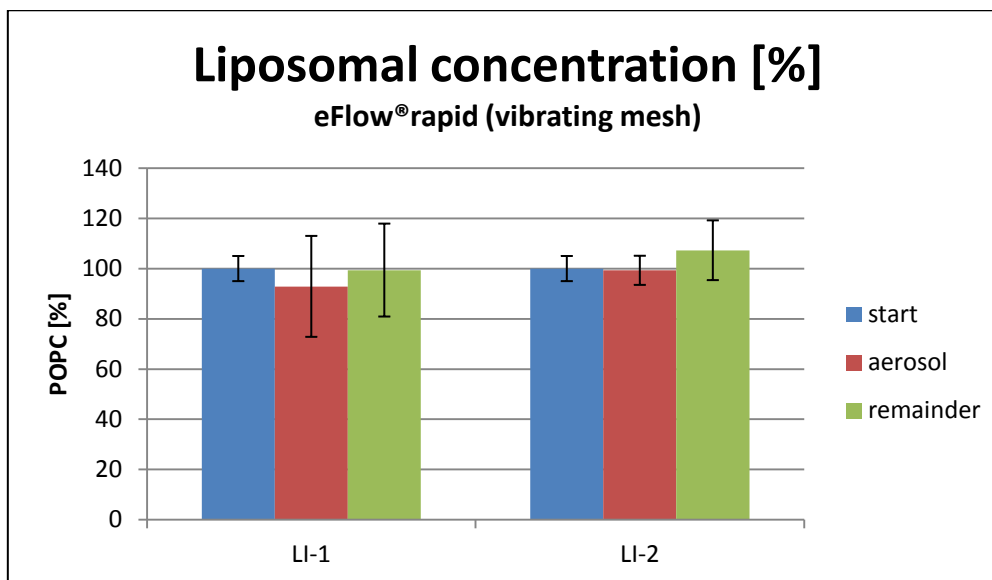


Figure 3. 28: Liposomal concentration [%] in samples with iloprost before and after nebulization with eFlow® rapid (mean ± S.D., n=3).

Also the measured size and PDI values gave promising results. The changes in size were a bit larger for LI-1, whereas LI-2 stayed almost completely stable. This is also reflected in the PDI values where the changes for LI-1 are significantly higher than for LI-2. In particular the aerosol's PDI of LI-1 has a very high and variable value, which indicates that those particles were strongly influenced by the nebulization process. So again it can be said that LI-2 is drastically more stable than LI-1.

To sum up, the technology is optimally suitable for the nebulization of liposomes, as the transport efficiency is almost 100%. The technology has a low impact on liposomes' size and PDI values.

Table 3. 23: Liposomal particle size in samples with iloprost before and after nebulization with eFlow® rapid (mean ± S.D., n=3).

size [nm]	start	+/-	aerosol	+/-	remainder	+/-
LI-1	172,8	4,3	183,8	15,2	151,5	4,6
LI-2	171,6	0,5	169,7	5,6	164,4	2,4

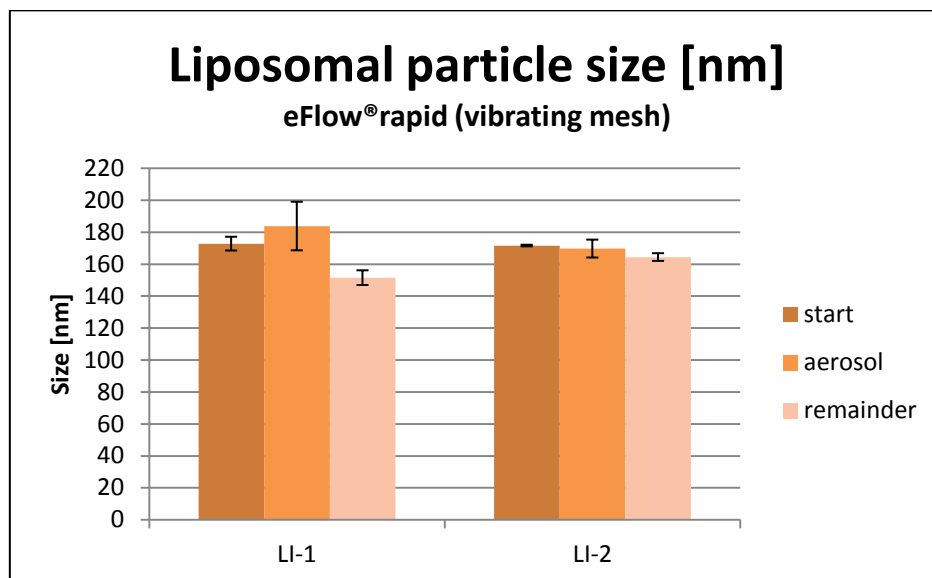


Figure 3. 29: Liposomal particle size in samples with iloprost before and after nebulization with eFlow® rapid (mean ± S.D., n=3).

Table 3. 24: Liposomal particle PDI in samples with iloprost before and after nebulization with eFlow® rapid (mean ± S.D., n=3).

PDI	start	+/-	aerosol	+/-	remainder	+/-
LI-1	0,102	0,015	0,401	0,074	0,163	0,023
LI-2	0,106	0,013	0,215	0,049	0,115	0,012

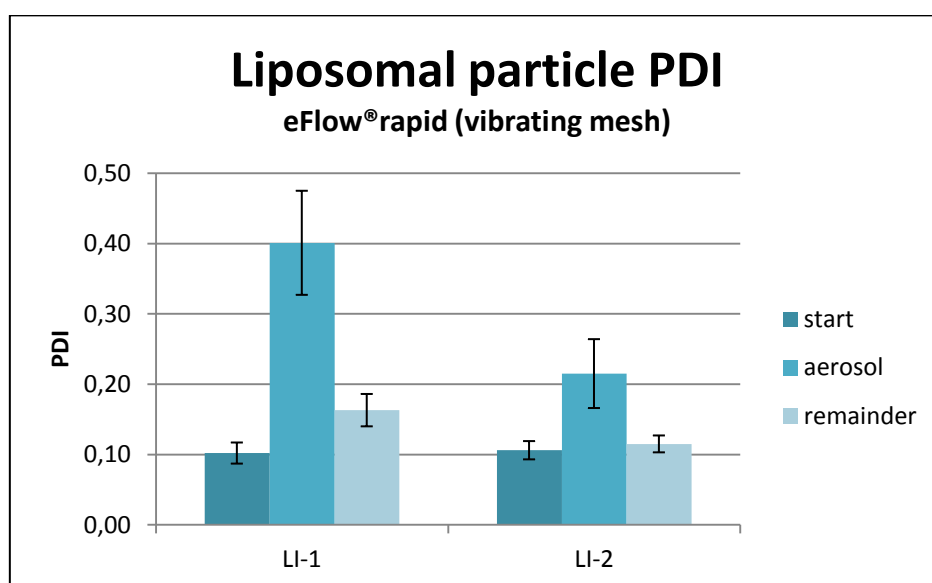


Figure 3. 30: Liposomal particle PDI in samples with iloprost before and after nebulization with eFlow® rapid (mean ± S.D., n=3).

The low liposomal concentration was tested again with the vibrating mesh nebulizer. The result is not completely the same as for the higher concentration, but has to be analyzed with care. For LI-2 the transport efficiency was again about 90% of initial concentration. For LI-1 this amount was decreased to about 52%. This could be because of concentration dependent effects during nebulization (e.g. a certain amount of liposomes is lost in the reservoir and the mesh), which are rather noticeable at a lower initial concentration.

All in all the vibrating mesh nebulizer is the device of choice for the transport of liposomes.

Table 3. 25: Liposomal concentration [mg/mL] in samples with iloprost before and after nebulization with eFlow® rapid (n=1).

POPC [mg/mL]	start	aerosol	remainder
LI-1	0,52	0,27	0,42
LI-2	0,41	0,37	0,41

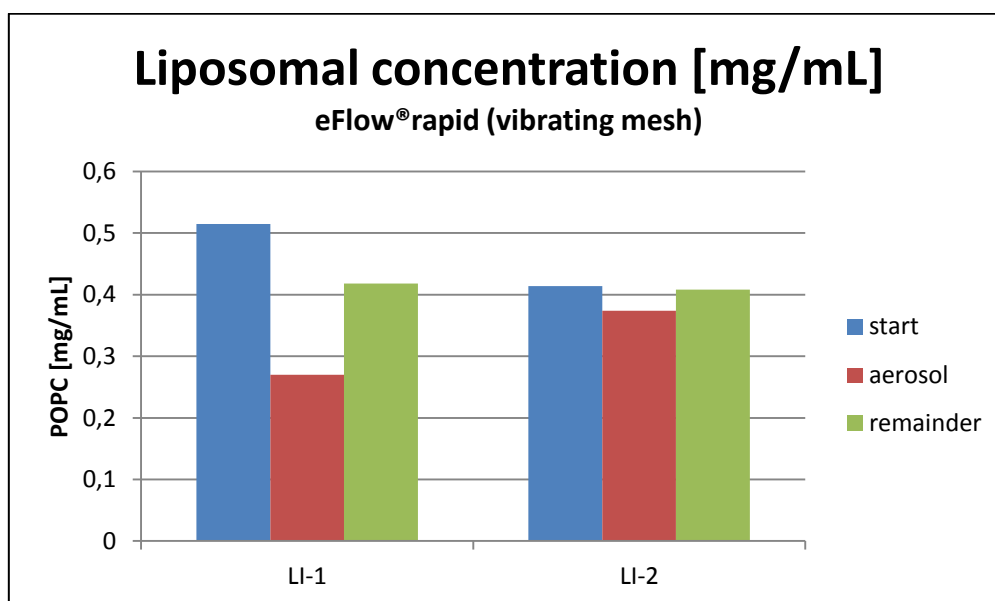


Figure 3. 31: Liposomal concentration [mg/mL] in samples with iloprost before and after nebulization with eFlow® rapid (n=1).

3.5 Iloprost encapsulation after nebulization – TLC results

The liposomes' iloprost encapsulation efficiency was checked before and after nebulization with TLC semi quantitatively and with MS quantitatively. The results are shown in the following figures.

3.5.1 MicroDrop® Pro

The first figure depicts the starting conditions for LI-1 and LI-2. The EE was determined directly after preparation without purification of the liposomes. The EE for LI-1 was 70-80%, whereas the EE for LI-2 was 80-90%.

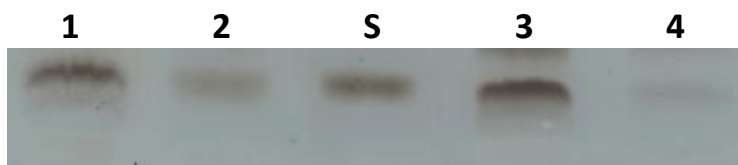


Figure 3. 32: Iloprost encapsulation efficiency before nebulization with MicroDrop® Pro, (1) LI-1 liposomal iloprost EE 70-80%, (2) LI-1 free iloprost, (S) iloprost standard, (3) LI-2 liposomal iloprost EE 80-90%, (4) LI-2 free iloprost. LI-1 and LI-2 samples contain in each case both bands together 4 µg of iloprost. The standard was 2 µg of iloprost.

The collected aerosol and the remainder were analyzed after nebulization. Based on the initial EE of the liposomes a release of iloprost could be observed. For LI-1 the ratio of encapsulated to free iloprost was altered in the aerosol. The EE of the aerosol after nebulization is about 50% (see Figure 3. 33, bands 1 and 2), which means a decline from the initial 70-80%. The remainder has approximately 70% EE and thus is unchanged. (see Figure 3. 33, bands 3 and 4).



Figure 3. 33: LI-1 iloprost encapsulation efficiency after nebulization with MicroDrop® Pro, (1) aerosol liposomal iloprost EE ~50%, (2) aerosol free iloprost, (S) iloprost standard, (3) remainder liposomal iloprost EE ~70%, (4) remainder free iloprost. Aerosol and remainder samples contain in each case both bands together 4 µg of iloprost. The standard was 2 µg of iloprost.

Similar results can be observed for LI-2. The aerosol's EE is about 70%, which is slightly decreased from the initial 80-90% (see Figure 3. 34, bands 1 and 2), whereas the remainder shows exactly the same 80-90% EE from the start.



Figure 3. 34: LI-2 iloprost encapsulation efficiency after nebulization with MicroDrop® Pro, (1) aerosol liposomal iloprost EE ~70%, (2) aerosol free iloprost, (S) iloprost standard, (3) remainder liposomal iloprost EE ~80-90%, (4) remainder free iloprost. Aerosol and remainder samples contain in each case both bands together 4 µg of iloprost. The standard was 2 µg of iloprost.

So these results indicate that aerosolized liposomes have a decreased EE compared to the initial EE. But those liposomes remaining in the reservoir are mainly unaltered in their EE. So the process of aerosol formation must have an influence on the liposomes integrity during air-jet nebulization.

Moreover it could be shown that LI-2 is superior in terms of iloprost EE than LI-1.

3.5.2 Optineb®-ir

The first figure depicts the starting EE for LI-1 and LI-2. The EE for LI-1 was 50-60%, whereas the EE for LI-2 was 80-90%. The low initial EE for LI-1 may be due to the preparation process and has to be minded during analysis of further results.



Figure 3. 35: Iloprost encapsulation efficiency before nebulization with Optineb®-ir, (1) LI-1 liposomal iloprost EE 50-60%, (2) LI-1 free iloprost, (S) iloprost standard, (3) LI-2 liposomal iloprost EE 80-90%, (4) LI-2 free iloprost. LI-1 and LI-2 samples contain in each case both bands together 4 µg of iloprost. The standard was 2 µg of iloprost.

The aerosol's EE of LI-1 is very low and only about 20%, whereas the remainder shows an EE of about 80%, which is higher than the initial value (see Figure 3. 36, bands 1,2 and 3,4). The problem could be a mistake during TLC separation process. It is obvious that the initial EE of LI-1 should be higher. Moreover it has to be mentioned that for the aerosol bands only a decreased volume of sample was available and due to this fact the bands are lighter than the others. This could also be a reason why the estimated EE is so low.



Figure 3. 36: LI-1 iloprost encapsulation efficiency after nebulization with Optineb®-ir, (1) aerosol liposomal iloprost EE ~20%, (2) aerosol free iloprost, (S) iloprost standard, (3) remainder liposomal iloprost EE ~80%, (4) remainder free iloprost. Aerosol and remainder samples contain in each case both bands together 4 µg of iloprost. The standard was 2 µg of iloprost. *The sample bands contain together only 1.7 µg iloprost due to insufficient sample volume.

The results for LI-2 are more precise. The aerosol's EE is extremely low and only about 10%, whereas the remainder's EE is about 70-80%. This means the transported liposomes release almost all of their encapsulated iloprost, while the remainder is mainly unchanged.



Figure 3. 37: LI-2 iloprost encapsulation efficiency after nebulization with Optineb®-ir, (1) aerosol liposomal iloprost EE ~10%, (2) aerosol free iloprost, (S) iloprost standard, (3) remainder liposomal iloprost EE ~70-80%, (4) remainder free iloprost. Aerosol and remainder samples contain in each case both bands together 4 µg of iloprost. The standard was 2 µg of iloprost. *The sample bands contain together only 0.9 µg iloprost due to insufficient sample volume.

The results show that the remainder is mainly unchanged for ultrasonic nebulizers, but the aerosol is highly influenced by the nebulization process. Moreover the TLC determination was hard to perform with aerosol samples, due to the extremely low amount of delivered liposomes (see chapter 3.4). The ultrasonic technology is not suitable for the transport of iloprost encapsulating liposomes.

3.5.3 eFlow® rapid

The first figure depicts the starting EE for LI-1 and LI-2. The EE for LI-1 was 70-80%, whereas the EE for LI-2 was 80-90%.

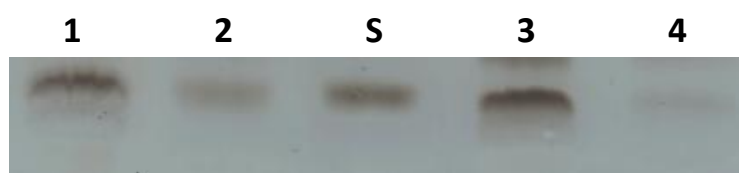


Figure 3. 38: Iloprost encapsulation efficiency before nebulization with eFlow® rapid, (1) LI-1 liposomal iloprost EE 70-80%, (2) LI-1 free iloprost, (S) iloprost standard, (3) LI-2 liposomal iloprost EE 80-90%, (4) LI-2 free iloprost. LI-1 and LI-2 samples contain in each case both bands together 4 µg of iloprost. The standard was 2 µg of iloprost.

The aerosol's EE for LI-1 is about 60-70%, the same is true for the remainder's EE. So both, the aerosol and the remainder behave the same concerning EE after nebulization. This means that for both aerosol and remainder only a slight decrease of about 10-20% occurred (see Figure 3. 39).

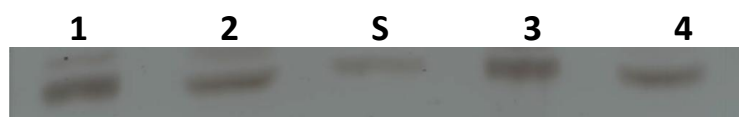


Figure 3. 39: LI-1 iloprost encapsulation efficiency after nebulization with eFlow® rapid, (1) aerosol liposomal iloprost EE ~60-70%, (2) aerosol free iloprost, (S) iloprost standard, (3) remainder liposomal iloprost EE ~60-70%, (4) remainder free iloprost. Aerosol and remainder samples contain in each case both bands together 4 µg of iloprost. The standard was 2 µg of iloprost.

More promising results come from the second formulation LI-2. From an initial EE of about 80-90% no significant decrease is observable for both aerosol and remainder. Again the aerosol and the remainder seem to behave similar. Both have an estimated EE of 80-90% after nebulization, which means they have the starting conditions (see Figure 3. 40).



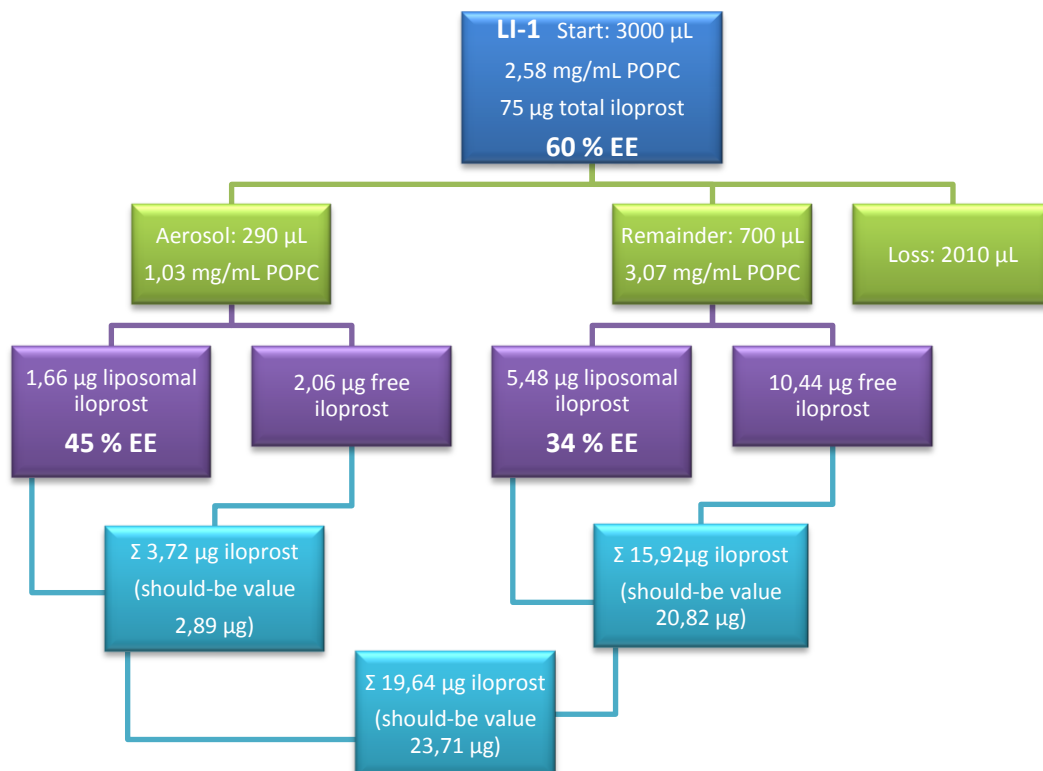
Figure 3. 40: LI-2 iloprost encapsulation efficiency after nebulization with eFlow® rapid, (1) aerosol liposomal iloprost EE ~80-90%, (2) aerosol free iloprost, (S) iloprost standard, (3) remainder liposomal iloprost EE ~80-90%, (4) remainder free iloprost. Aerosol and remainder samples contain in each case both bands together 4 µg of iloprost. The standard was 2 µg of iloprost.

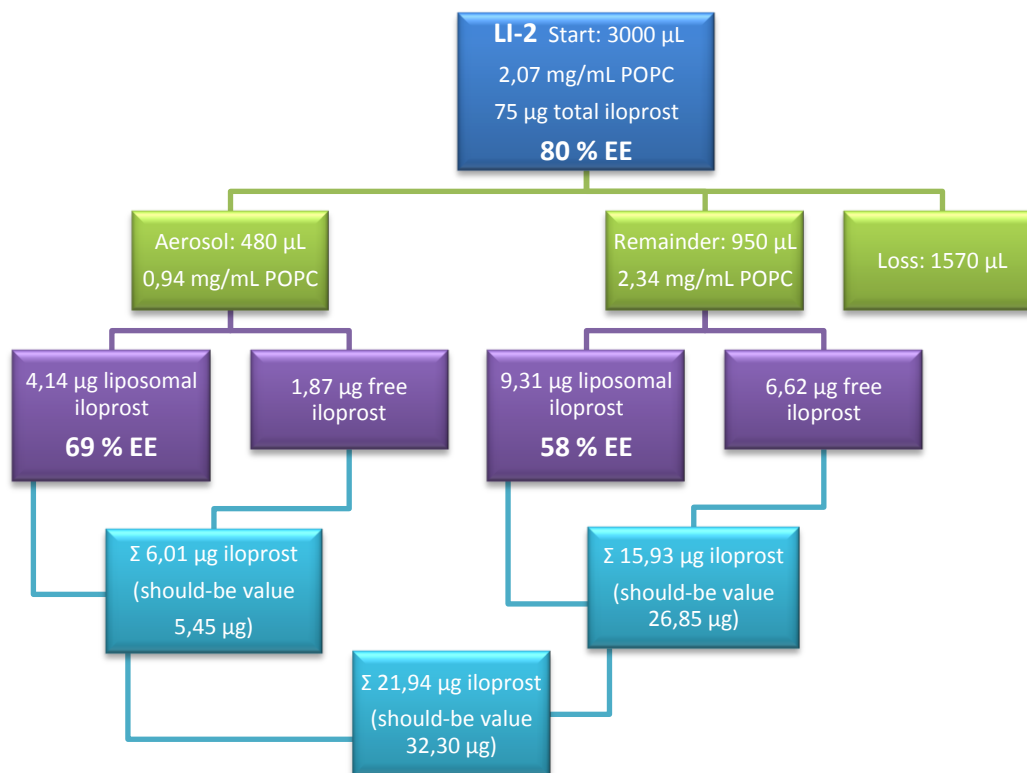
To sum up, the EE of liposomes nebulized with the vibrating mesh device remains almost the same and this technology obviously has the least impact on the EE compared with the other two.

3.6 Iloprost encapsulation after nebulization – MS results

The iloprost encapsulation after nebulization was also checked with MS. The samples were prepared appropriately and the obtained results were analyzed.

3.6.1 MicroDrop® Pro





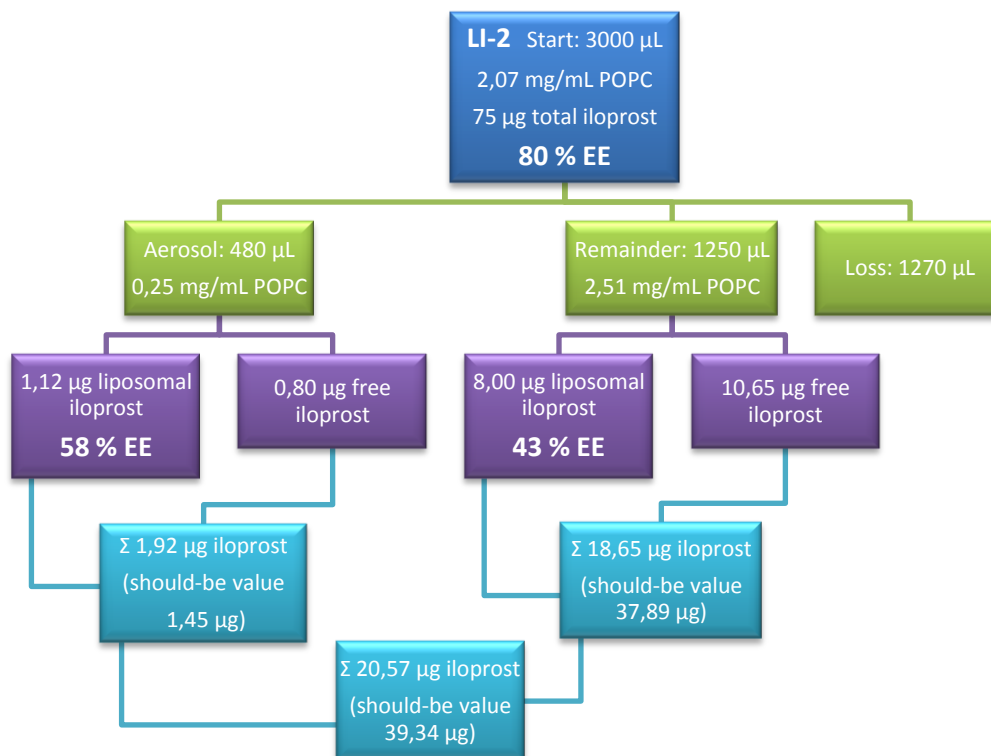
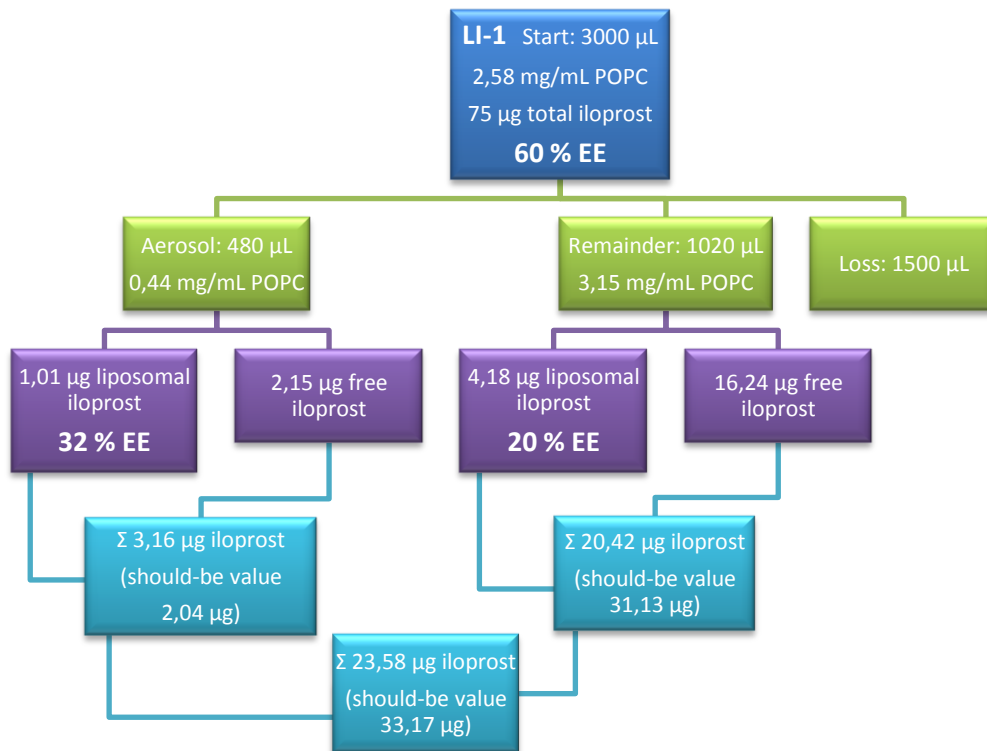
The first tree diagram depicting the MS results for LI-1 shows that the EE was reduced from initially 60% to about 45% in the aerosol. The remainder underwent an even higher reduction to 34% EE. The LI-2 results are shown in the second diagram and illustrate that the reduction of EE for LI-2 was clearly less. All in all the results fit quite well to the TLC estimations. The LI-1 aerosol EE was estimated with TLC to be 50% and with MS 45%, the LI-2 aerosol EE gave 70% with TLC and 69% with MS. In contrast the remainders' EEs do not fit so well and are lower than TLC estimations (LI-1 70% vs. 34% and LI-2 80% vs. 58%).

As already discovered before is LI-2 more stable than LI-1 and the MS results emphasize this assumption.

3.6.2 Optineb®-ir

The Optineb®-ir MS results show an aerosol EE of 32% for LI-1 and 58% for LI-2. Compared to the TLC results (LI-1 20% and LI-2 10%) it must be mentioned that these TLC estimations may be vague due to the limited sample volume. Again LI-2 is more stable after nebulization than LI-1. The remainders' EE were overestimated during TLC (both 80% EE) and much lower for MS (LI-1 20% and LI-2 43%).

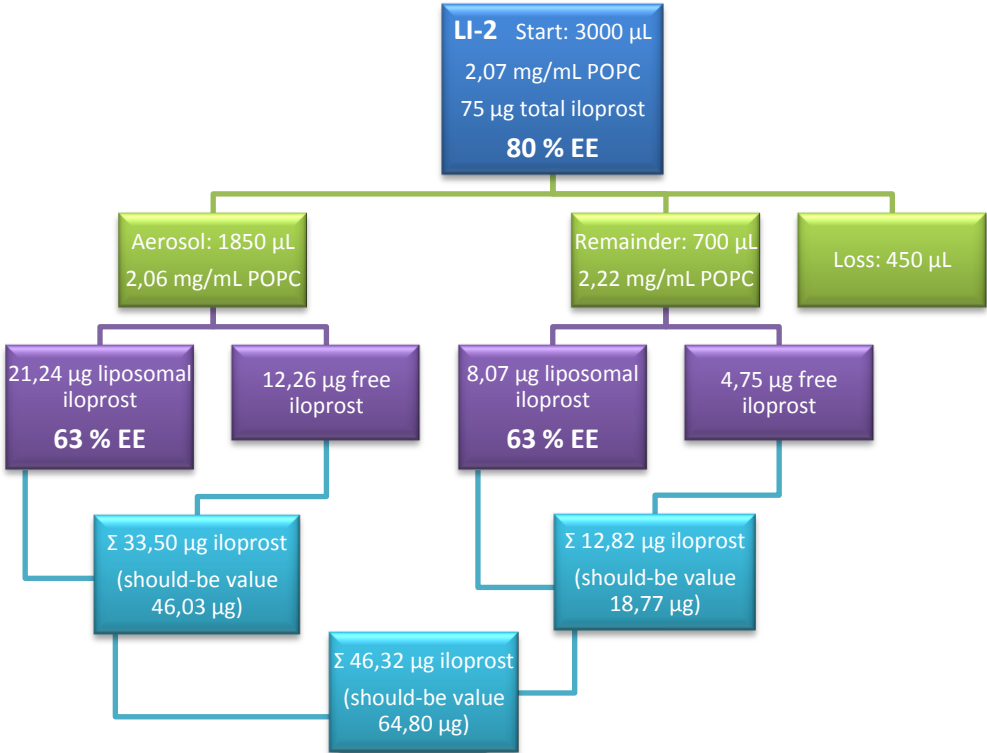
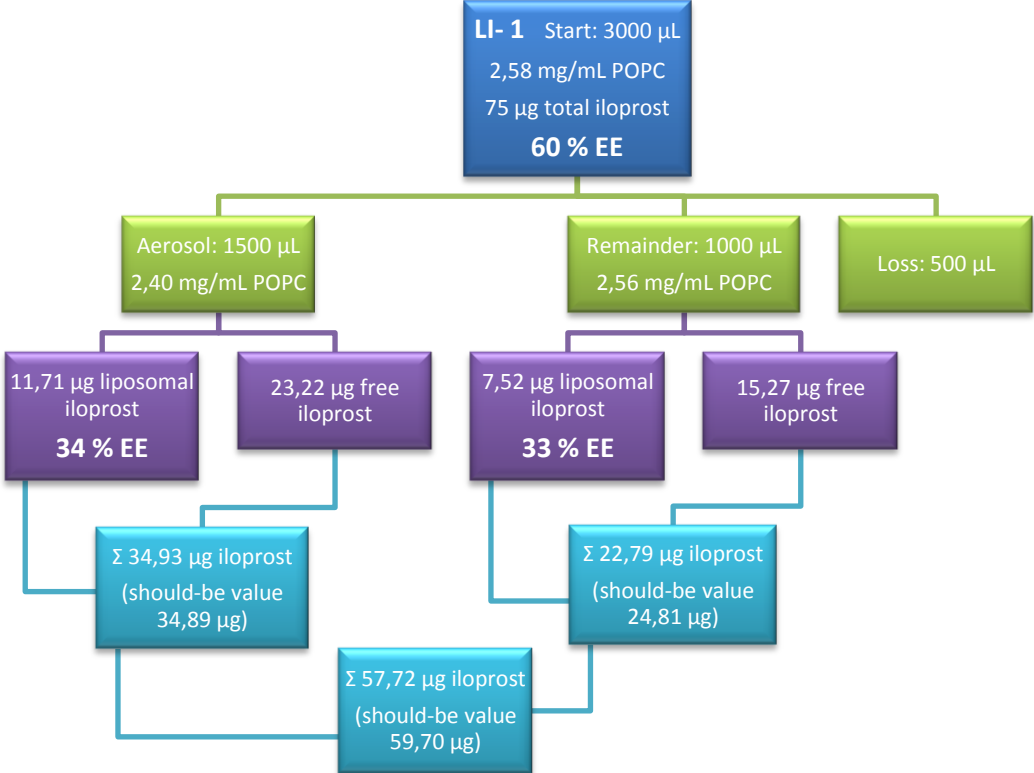
Generally the ultrasonic nebulizer yields aerosols with lower EEs than the vibrating mesh nebulizer.



3.6.3 eFlow® rapid

Interestingly the results for the eFlow® rapid are quite dissimilar. On the one hand is the EE for LI-1 with about 34% and on the other hand the EE for LI-2 with about 63% after nebulization (TLC results 60% for LI-1 and 80% for LI-2). Again LI-2 is more

stable than LI-1. Another interesting fact is that the EEs of the aerosol and the remainder are completely the same for both samples. The same fact was already observed with the TLC results.



Generally it can be stated, that almost all results of the MS are below TLC estimations. So obviously TLC results are easily overestimated and not very accurate. The MS results made it possible to investigate the EE of collected samples more precisely.

All in all the LI-2 formulation is definitely more stable during nebulization than LI-1. Its encapsulated iloprost undergoes a smaller reduction than for the LI-1 formulation. The vibrating mesh's superiority was reduced in terms of encapsulation, as it has a relatively low EE for LI-1 and the air-jet nebulizer had the highest EE after nebulization for LI-2. The worst nebulizer in terms of EE was the ultrasonic device. It had the lowest EE values for LI-1 and LI-2 after nebulization.

3.7 Zeta potential of liposomes

The zeta potential of the investigated liposomes was measured. The zeta potential was determined for empty liposomes (L-1 and L-2), for the same formulations containing iloprost (LI-1 and LI-2) and for liposomes containing iloprost after they were separated from non-encapsulated iloprost via Amicon-centrifugation (LI-1 sep. and LI-2 sep.). The following table summarizes the results.

Table 3. 26: Zeta potential of the investigated liposomes.

Sample	Zeta potential [mV]	SD +/- [mV]
L-1	11,3	0,88
LI-1	12,9	1,01
LI-1 sep.	12,7	1,00
L2	35,6	2,79
LI-2	36,0	2,82
LI-2 sep.	36,6	2,87

There is almost no change of zeta potential within the same formulation independent of iloprost. But the two formulations strongly differ in their zeta potential in which the second has the threefold higher potential. This is caused by the different polymer shield used for the formulations. PVP used for the second one is a polycation and due to this fact the zeta potential is highly increased.

3.8 Droplet size measurements with nebulizers

To investigate the influence of liposomes on droplet size and to get general information about droplet size distribution of the applied devices laser light scattering experiments were performed. Each nebulizer was tested with a buffer solution only and the buffer solution containing 3.0 mg/mL L-2 liposomes.

3.8.1 MicroDrop® Pro

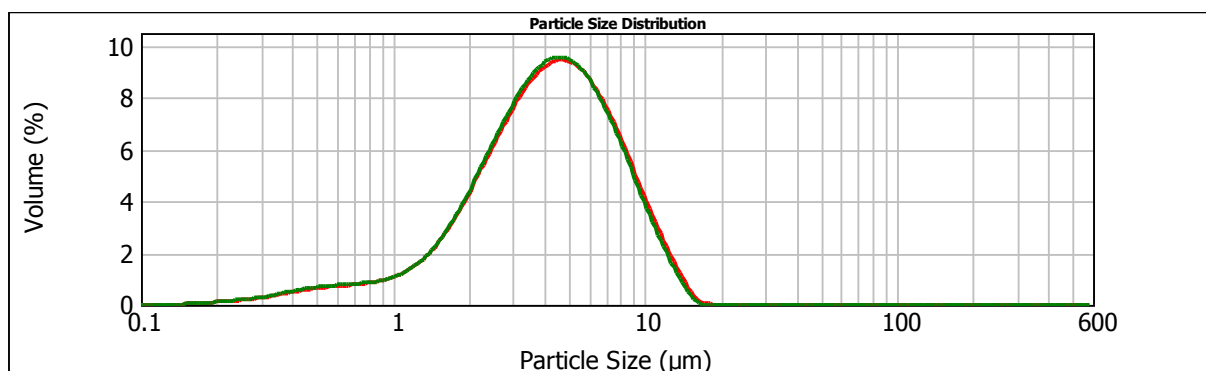


Figure 3. 41: Droplet size distribution of the MicroDrop® Pro measured with laser light scattering. Droplet size distribution is plotted versus corresponding volume distribution. Red line represents Tris buffer 10 mM pH 7.0 only and green line represents the same buffer with L-2 liposomes 3.0 mg/mL (n=3).

The droplet size distribution for the MicroDrop® Pro shows a relatively high median of 4.15 µm, which is not absolutely ideal for lower lung deposition. The droplet size is not influenced by the presence of liposomes in the solution, as there is no significant change in size distribution between pure buffer and liposomal emulsion (see Table 3. 27).

Table 3. 27: Droplet size distribution of the MicroDrop® Pro defined by d(0.1), d(0.5) and d(0.9). These values indicate droplet sizes with a certain percentage, i.e. 10%, 50% or 90% respectively, of droplets below this size (n=3).

[µm]	d(0.1)	d(0.5)	d(0.9)
Tris buffer 10 mM pH 7.0	1.562	4.225	8.889
L-2 3.0 mg/mL	1.533	4.149	8.657

3.8.2 Optineb®-ir

The droplet size distribution for the Optineb®-ir shows a lower median of 3.54 µm for the liposomal emulsion. The droplet size is only slightly influenced by the presence of liposomes in the solution, as the droplet size is a little shifted to smaller droplets, when liposomes are present (see Table 3. 28).

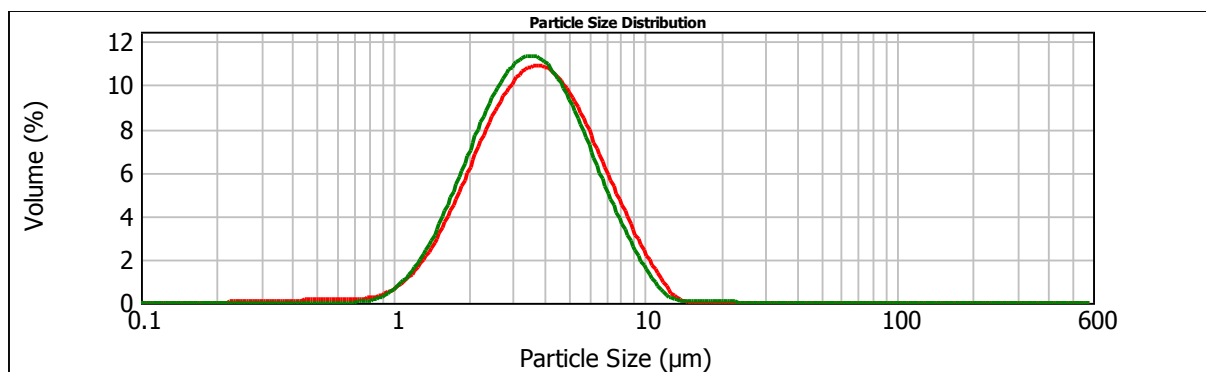


Figure 3. 42: Droplet size distribution of the Optineb®-ir measured with laser light scattering. Droplet size distribution is plotted versus corresponding volume distribution. Red line represents Tris buffer 10 mM pH 7.0 only and green line represents the same buffer with L-2 liposomes 3.0 mg/mL (n=3).

Table 3. 28: Droplet size distribution of the MicroDrop® Pro defined by d(0.1), d(0.5) and d(0.9). These values indicate droplet sizes with a certain percentage, i.e. 10%, 50% or 90% respectively, of droplets below this size (n=3).

[µm]	d(0.1)	d(0.5)	d(0.9)
Tris buffer 10 mM pH 7.0	1.829	3.730	7.395
L-2 3.0 mg/mL	1.807	3.535	6.874

3.8.3 eFlow® rapid

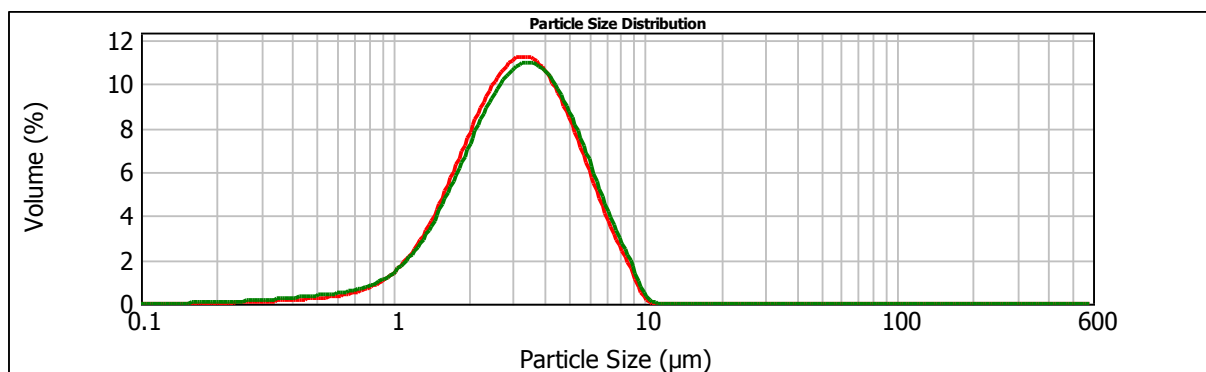


Figure 3. 43: Droplet size distribution of the eFlow® rapid measured with laser light scattering. Droplet size distribution is plotted versus corresponding volume distribution. Red line represents Tris buffer 10 mM pH 7.0 only and green line represents the same buffer with L-2 liposomes 3.0 mg/mL (n=3).

The droplet size distribution for the eFlow® rapid shows an even smaller median of 3.24 µm for the liposomal emulsion, which is ideal for lower lung deposition. The droplet size is not influenced by the presence of liposomes in the solution either, as there is no significant change in size distribution between pure buffer and liposomal emulsion (see Table 3. 29).

Table 3. 29: Droplet size distribution of the MicroDrop® Pro defined by d(0.1), d(0.5) and d(0.9). These values indicate droplet sizes with a certain percentage, i.e. 10%, 50% or 90% respectively, of droplets below this size (n=3).

[μm]	d(0.1)	d(0.5)	d(0.9)
Tris buffer 10 mM pH 7.0	1.516	3.168	6.014
L-2 3.0 mg/mL	1.480	3.243	6.204

3.8.4 Comparison

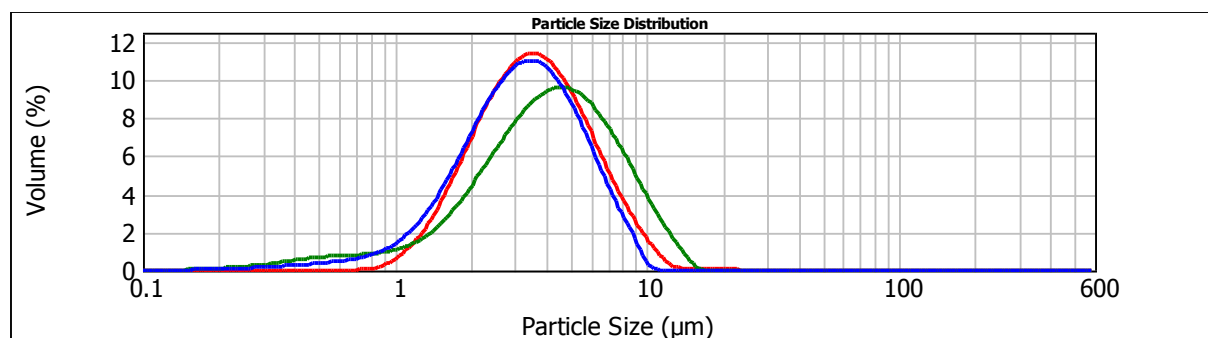


Figure 3. 44: Compared droplet size distribution among all three tested nebulizers. Droplet size distribution is plotted versus corresponding volume distribution. Red line represents Optineb®-ir, the blue line represents eFlow® rapid and the green line MicroDrop® Pro. All shown results are for the L-2 liposomal emulsions 3.0 mg/mL (n=3).

Figure 3. 44 compares the results for the liposomal emulsions and nicely depicts the difference among applied nebulizers. While the droplet size distribution is quite similar for the Optineb®-ir and the eFlow® rapid, it is significantly shifted to larger droplets for the MicroDrop® Pro. But despite these slightly larger droplets it is still applicable for inhalation therapy.

3.9 Nebulization trials with mouse inhaler M-neb

The efficiency of liposomal transport was investigated for the M-neb (a prototype, kindly provided by NEBU-TEC, Elsenfeld, Germany) by nebulizing liposomal emulsions of LI-1 and LI-2 each with a concentration of 3.0 mg/mL. The phospholipid concentration was determined before and after nebulization. Moreover the liposomal size and PDI were measured each time. The results are summarized in the following figures and tables.

Table 3. 30: Liposomal concentration [mg/mL] in samples with iloprost before and after nebulization with M-neb (n=1).

POPC [mg/mL]	start	aerosol	remainder
LI-1	2,58	2,17	2,46
LI-2	2,07	1,92	2,40

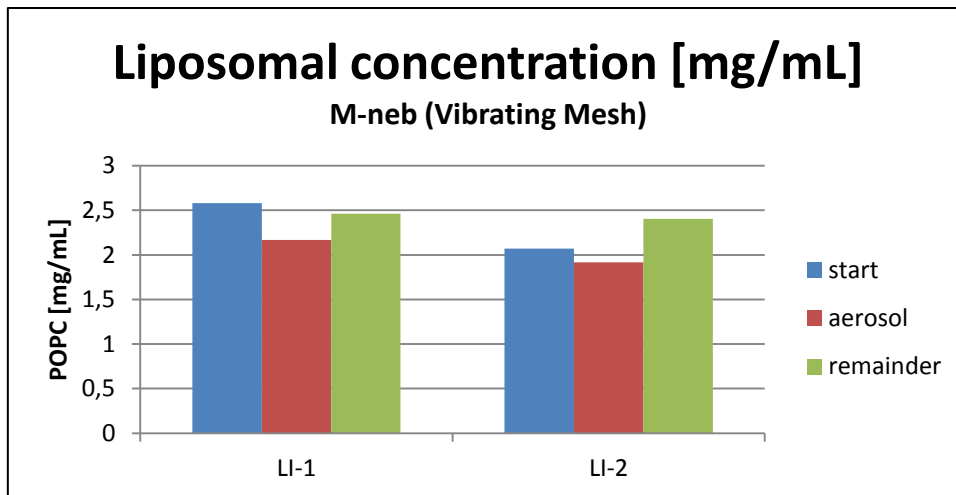


Figure 3. 45: Liposomal concentration [mg/mL] in samples with iloprost before and after nebulization with M-neb (n=1).

The first figure depicts the POPC concentrations at the beginning and after nebulization. Expectedly the liposomal transport is very high. The M-neb uses vibrating mesh technology, which was the best working principle concerning liposomal transport when human inhalers were tested. The same could be shown for the mouse inhaler. The liposomal transport is about 84% and 93% in the mist, respectively. These values are comparable to the eFlow® rapid nebulizer (see Table 3. 31). So the liposomal transport is carried out efficiently by the M-neb.

Table 3. 31: Liposomal concentration [%] in samples with iloprost before and after nebulization with M-neb (n=1).

POPC [%]	start	aerosol	remainder
LI-1	100,0	84,0	95,3
LI-2	100,0	92,5	116,1

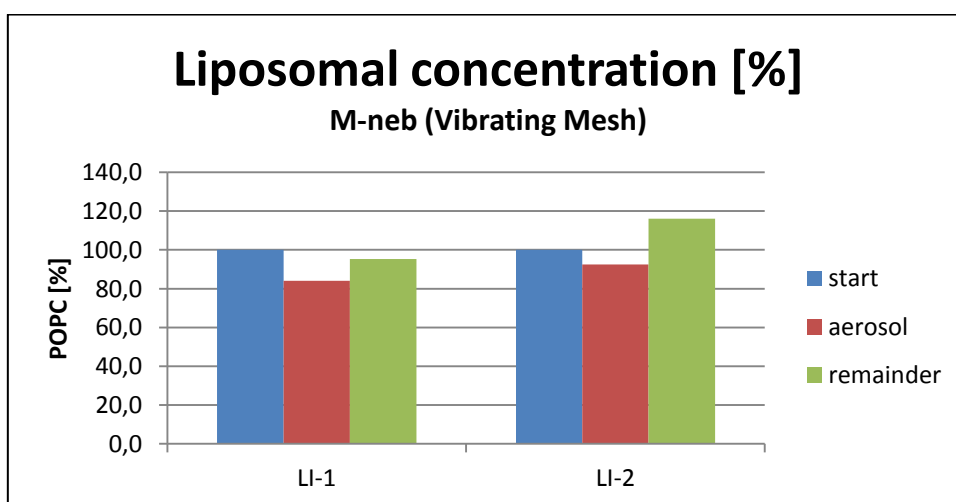


Figure 3. 46: Liposomal concentration [%] in samples with iloprost before and after nebulization with M-neb (n=1).

When measuring the liposomal size it could be shown that there is almost no change after nebulization. Both LI-1 and LI-2 were very stable, just the PDI increased a bit for LI-1. This indicates that LI-1 has a larger liposomal size distribution after nebulization than LI-2. This leads once more to the conclusion that LI-1 is less stable than LI-2, which showed almost no change in PDI.

Table 3. 32: Liposomal size and PDI in samples with iloprost before and after nebulization with M-neb (n=1).

	LI-1		LI-2	
	size [nm]	PDI	size [nm]	PDI
start	194,9	0,097	213,5	0,102
aerosol	187,1	0,199	209,5	0,127
remainder	183,2	0,189	205,9	0,124

3.10 Droplet size measurements with mouse inhaler M-neb

Laser light scattering experiments were performed to investigate the influence of liposomes on droplet size and to get general information about droplet size distribution of the M-neb mouse inhaler. The inhaler was tested with buffer solution 10 mM Tris, 155 mM NaCl, pH 7.0 and the same buffer containing 3.0 mg/mL L-1 or L-2 liposomes.

Interestingly the results show that the droplet size distribution is around very small sizes between 0.4 μm and 1.0 μm . This is true for the pure buffer and also for both tested liposomal emulsions. As already investigated for the other nebulizers the liposomes do not have any influence on droplet size with the M-neb either.

Table 3. 33: Droplet size distribution of the M-neb nebulizer defined by d(0.1), d(0.5) and d(0.9). These values indicate droplet sizes with a certain percentage, i.e. 10%, 50% or 90% respectively, of droplets below this size (n=3).

[μm]	d(0.1)	d(0.5)	d(0.9)
Tris buffer pH7.0	0.398	0.597	0.920
L-1 3.0 mg/mL	0.417	0.646	1.029
L-2 3.0 mg/mL	0.412	0.631	0.991

The following two figures show L-1 and L-2 (red line) each time compared to the pure buffer solution (green line). There is no significant size change observable.

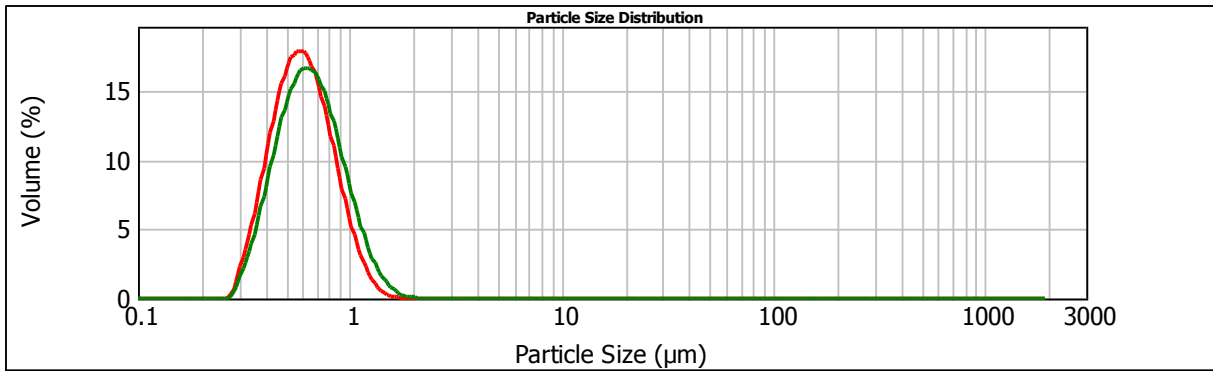


Figure 3. 47: Droplet size distribution of the M-neb nebulizer measured with laser light scattering. Droplet size distribution is plotted versus corresponding volume distribution. Red line represents the buffer 10 mM Tris, 155 mM NaCl, pH 7.0 and green line represents the same buffer with L-1 liposomes 3.0 mg/mL (n=3).

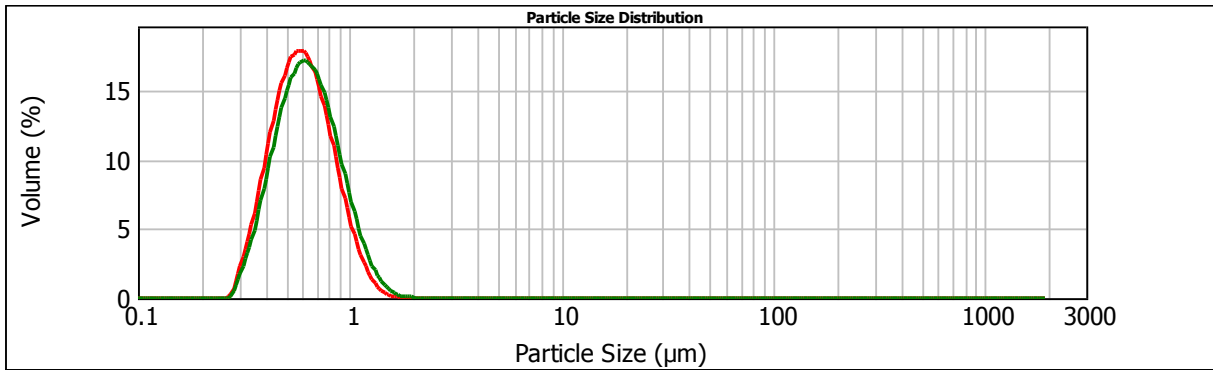


Figure 3. 48: Droplet size distribution of the M-neb nebulizer measured with laser light scattering. Droplet size distribution is plotted versus corresponding volume distribution. Red line represents the buffer 10 mM Tris, 155 mM NaCl, pH 7.0 and green line represents the same buffer with L-2 liposomes 3.0 mg/mL (n=3).

The next figure compares the droplet size distributions of L-1 (red line) and L-2 (green line) with each other. There is no observable difference between the two formulations, indicating that the inhaler behaves reproducibly independent of the applied formulation. The droplet size distribution comprises very small particles, which are suitable for mouse lung inhalation. For human applications, these particles are too small and would be immediately exhaled again.

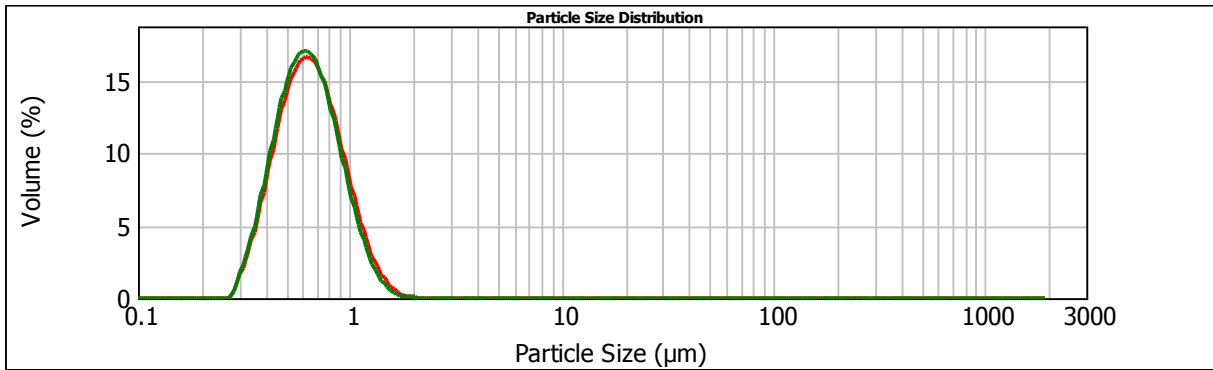
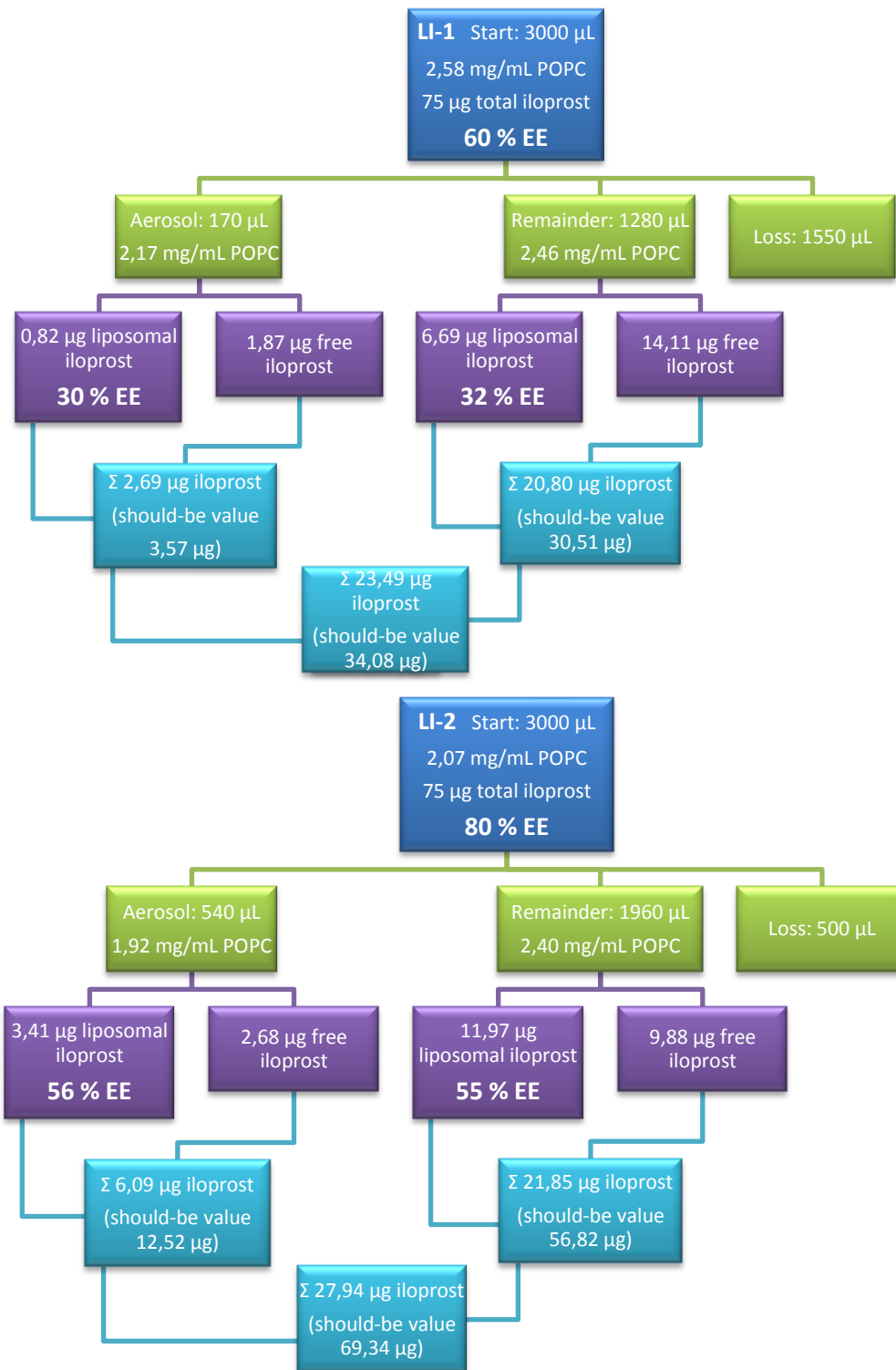


Figure 3. 49: Droplet size distribution of the M-neb nebulizer measured with laser light scattering. Droplet size distribution is plotted versus corresponding volume distribution. Red line represents the buffer 10 mM Tris, 155 mM NaCl, pH 7.0 with L-1 liposomes and green line represents the same buffer with L-2 liposomes 3.0 mg/mL (n=3).

3.11 Iloprost encapsulation after nebulization – MS results – M-neb



The MS analysis of M-neb's samples led to similar results as for the eFlow® rapid, both vibrating mesh nebulizers. The results nicely show the relatively high difference between LI-1 and LI-2, as already discovered for the other nebulizers. LI-2 again is more stable and shows a higher EE of iloprost.

When directly comparing the MS results for both vibrating mesh nebulizers, the obvious analogy becomes apparent. LI-1 when nebulized with eFlow® rapid had 34% and 33% encapsulation for aerosol and remainder, respectively. The M-neb has 30% and 32% after nebulization. LI-2 when nebulized with eFlow® rapid had 63% for aerosol and remainder. The M-neb showed approximately 56% for both samples. So this mouse inhaler behaved similar to the human vibrating mesh concerning iloprost encapsulation.

3.12 Nebulization of L-1 and L-2 containing ANTS/DPX with eFlow® rapid

L-1 and L-2 liposomes encapsulating ANTS/DPX were prepared, extruded and purified with a Sephadex G75 column. The purified liposomes were analyzed for their average size and homogeneity with DLS. The resulting emulsions were very homogenous. L-1 had an average size of 157.0 nm and a PDI of 0.070. L-2 had an average size of 199.9 nm and a PDI of 0.085.

The phospholipid concentration was determined after column purification. L-1 had a concentration of 3.41 mg/mL POPC and L-2 had a concentration of 2.79 mg/mL POPC. Then the encapsulation efficiency was measured with fluorescence spectroscopy. The whole experiment was carried out in duplicate (n=2) and each fluorescence measurement was done in quadruplicate.

The first table summarizes the measurement results of the undiluted samples right after column purification. Surprisingly the encapsulation factor is considerably higher for L-1 (2.55) in comparison to L-2 (1.55). This formulation may be more ideal for the encapsulation of ANTS/DPX. The same samples were again measured one week later to test the stability of encapsulation. The results show that the factor has only slightly increased (2.45 and 1.49, respectively), which means that the encapsulation is completely stable over a time period of a week.

Table 3. 34: Fluorescence measurements with undiluted L-1 (3.41 mg/mL POPC) and L-2 (2.79 mg/mL POPC) samples directly after preparation and one week later to test stability. For each sample the I_0 and I_∞ was measured.

	L-1	L-2	L-1 one week old	L-2 one week old
I_0 [cps]	190,141	156,799	207,087	162,469
I_∞ [cps]	484,469	243,419	506,528	242,415
encapsulation factor	2.55	1.55	2.45	1.49

The next table shows the measurements for the samples, which were diluted to a total lipid concentration of 3.0 mg/mL. This was done to work under the same conditions as the iloprost containing LI-1 and LI-2, which were also diluted to a total lipid concentration of 3.0 mg/mL. The encapsulation factor does not change when diluting the sample (2.52 for L-1 and 1.49 for L-2).

Table 3. 35: Fluorescence measurements with diluted L-1 (2.58 mg/mL POPC) and L-2 (2.07 mg/mL POPC) samples. For each sample the I_0 and I_∞ was measured.

3.0 mg/mL total lipid	L-1	L-2
I_0 [cps]	275,155	243,792
I_∞ [cps]	694,019	364,277
encapsulation factor	2.52	1.49

These samples were then nebulized with the eFlow® rapid and the encapsulation factor checked again after nebulization. As the following table shows the L-1 formulation surprisingly loses a lot of encapsulated fluorophore, whereas the L-2 formulation shows absolutely no change. The factor of L-1 decreases from 2.52 to 1.24, which means a loss of more than 50%. Also the remainder's factor decreases to 1.75. So obviously the nebulization process has a major influence on the encapsulation of L-1.

The factor for L-2 is completely unchanged, from 1.49 to 1.45 in the aerosol and 1.50 in the remainder. Once more these results suggest that L-2 is the more stable formulation for nebulization processes.

Table 3. 36: Fluorescence measurements with diluted L-1 (2.58 mg/mL POPC) and L-2 (2.07 mg/mL POPC) samples. For each sample the I_0 and I_∞ was measured.

eFlow® rapid	L-1 aerosol	L-1 remainder	L-2 aerosol	L-2 remainder
I_0 [cps]	564,576	406,276	247,576	241,156
I_∞ [cps]	701,497	711,896	359,352	361,556
encapsulation factor	1.24	1.75	1.45	1,50

4. Conclusion & Outlook

4.1 Liposomes for inhalation therapy

The use of liposomes as drug delivery systems for pulmonary applications is getting more and more into the focus of biomedical research. This is mainly due to various new drugs, such as peptides, proteins or nucleic acid derivatives, which are promising new therapeutic options for diseases that have been known for decades. The use of liposomes has a lot of advantages like the protection of the drug from degradation or other factors. Sensitive drugs need to be protected from several influences. Liposomal delivery systems ensure the therapeutic benefit and reduce the possibility of toxicity or side effects.

But another very important advantage of liposomal drug delivery is the possibility of creating sustained release. And this is the main objective by creating iloprost containing liposomes.

A prerequisite for the use of liposomes for pulmonary applications is that they are successfully transformed to an inhalable aerosol. There have already been a lot of studies on nebulized liposomes with many different encapsulated drugs. One of the first studies on nebulized liposomes was carried out by Waldrep et al. in 1994 [42]. They tested 18 different continuous-flow jet nebulizers with a liposomal beclomethasone dipropionate solution. This study mainly focused on the produced Mass Median Aerodynamic Diameter (MMAD) and the subsequent lung deposition. But they also analyzed drug output efficiency. For this reason they used an impactor and analyzed drug content on each stage. So they got a relation between drug contents and produced droplet size for each impactor stage.

These beclomethasone-DLPC liposomes were also delivered to the lungs of volunteers by Waldrep et al. in 1997 [43] and showed no adverse clinical or laboratory events.

These studies were followed by others investigating different liposome encapsulated drugs. One of these drugs was ciprofloxacin, which was loaded into liposomes and nebulized with 12 different jet nebulizers by Conley et al. in 1997 [44]. Interestingly they could show retention of the drug in the lungs and several fold enhanced efficacy. A further study carried out with liposome-encapsulated ciprofloxacin and 5 different

nebulizers found strongly differing amounts of liposomal disruption and strongly differing amounts of delivered ciprofloxacin among different nebulizers. [45] This study was also one of the first to compare air-jet with ultrasonic nebulizers. Interestingly in this study the ultrasonic nebulizer was not the least effective one. This study also gave an indication that nebulization characteristics and liposomal transport efficiency are nebulizer type specific or even nebulizer specific.

Several other studies were performed using different liposomal formulations encapsulating various drugs, e.g. ciprofloxacin and salbutamol sulfate [46], recombinant human copper-zinc superoxide dismutase (rh-Cu/Zn-SOD) [47], insulin [48] [49], cyclosporine A [50] [51] or VIP [52].

Lots of further nebulization trials have been performed with a multiplicity of different formulations. A pleasant overview was given by Gaspar et al. in 2008 [26].

4.2 Iloprost containing liposomes for human inhalers

The objective of this thesis was to investigate iloprost loaded liposomes and their suitability for aerosol applications. Iloprost containing liposomes for the treatment of PAH have already been produced by Kleemann et al. in 2007. They used DPPC/CH and DPPC/CH/DPPE-PEG liposomes for the encapsulation of iloprost, but they got only very poor EEs. Their highest iloprost EE was 4.4%, which is extremely low considering that the drug is very expensive.

Our formulations contain positive charges in the form of stearylamine. This is definitely one reason for the high EE of 60% to 90% in our formulations. The positive charge is responsible for retarding the iloprost within the membrane. Iloprost is an amphiphilic drug and thereby presumably intercalates within the lipid bilayer. The positive charges on the bilayers' surface retard the active drug.

Moreover our formulations do not contain cholesterol. The addition of cholesterol in the same formulations had negative effects on EE. As cholesterol also intercalates within the bilayer it apparently replaces the iloprost and leads to a lower EE. Exactly this effect was observed by Zaru et al. in 2007 [53]. They found out that lipid composition has a very high impact on EE. They used rifampicin as model drug, which is amphiphilic, has a large size and complex structure. Their EE was significantly higher with saturated phospholipids, but decreased when adding

cholesterol, which replaced rifampicin in the membrane. But they also stated that the addition of cholesterol had a positive effect on nebulization stability.

Furthermore our formulations contain polymer shields, either in the form of DPPE-PEG2000 or PVP. Such polymer shields are used to increase circulation time of liposomes in the human body if delivered intravenously. But this stability increase was also tested for pulmonary applications by Anabousi et al. in 2006 [54]. They nebulized plain and PEGylated liposomes and tested their stability post nebulization and after incubation in lung surfactant. They found that PEGylated liposomes are more stable in lung surfactant and retain over 80% of drug load over 48h. Concerning nebulization no major difference between plain and PEGylated liposomes could be found. So the addition of a polymer shield is advantageous for the retention in the lung, but not necessarily important for nebulization itself.

Elhissi et al. [55] investigated the stability of ultradeformable liposomes during nebulization. They also tested air-jet, ultrasonic and vibrating mesh nebulizer. The clear outcome was that those liposomes are extremely unstable during nebulization. They tended to aggregate and showed a drug loss up to 98%. Those components responsible for making the liposomes ultradeformable were responsible for the instability.

This leads to the conclusion that more rigid and smaller liposomes are better for the use of aerosolization. The positive influence of extrusion on liposomal stability was already investigated by Elhissi et al. in 2006 [56]. They could show that extrusion has a positive effect on nebulization performance. MLVs are not suitable for such purposes. But they also stated that extrusion through filters below 0.4 μm leads to reduced stability due to reduced lamellarity of the liposomes.

All these factors were considered when designing the appropriate formulations for iloprost. “The current goals of therapy are to relieve symptoms by reducing pulmonary vascular resistance, to increase cardiac output, and to improve oxygenation. [57]” This is done either by administration of prostanoids intravenously or by inhalation of iloprost solution (Ventavis). With this administration path severe adverse side effects could be reduced and there is no need for a central venous access. [57] But to further improve pulmonary delivery the developed liposomal

formulations were then examined for their stability during nebulization with different inhaler devices.

A major point, which was hardly considered in other papers, was the question of liposomal transport efficiency. This is a crucial point, as I investigated a discrepancy between total mass output and delivered liposomes of an inhaler. Total mass output only refers to the totally nebulized liquid, but contains no information about the liposomal content.

But this was exactly what was differing among nebulizers. All of them had a satisfying aerosolization rate, but only the vibrating mesh nebulizer (eFlow® rapid) was capable of transporting the same amount of liposomes to the aerosol as in the starting solution. The extreme opposite was the ultrasonic nebulizer (Optineb®-ir), which produced aerosol in satisfying amounts, but hardly transported any liposomes to the produced mist. The air-jet nebulizer's performance (MicroDrop® Pro) was in between.

So, it is not only important to consider total mass output, but also the liposomal content in the produced aerosol.

Moreover the size of liposomes post nebulization was analyzed with DLS. This is also very important to investigate changes on their shape. If any major changes occurred, this would indicate that the liposomes are not stable enough. No major changes occurred for our formulations, neither for average size nor for PDI. But LI-2 was even more stable than LI-1, as the changes for size and PDI were even smaller. Both formulations performed well, but LI-2 is the more stable one.

Another important point is the encapsulation efficiency (EE) pre and post nebulization. The EE pre nebulization was improved as already described above through changing components or influencing size.

The EE post nebulization had to be analyzed. The TLC and MS results were slightly different, but mainly drew the same picture. The EE was always better for LI-2 than for LI-1 for all nebulizers. The relative loss was always higher for LI-1. In terms of EE the vibrating mesh nebulizer was superior. Elhissi et al. [56] and Kleemann et al. [58] also found the vibrating mesh nebulizer less disruptive than the air jet.

The zeta potential of both formulations is positive, as they both contain the positive charges of stearylamine. But LI-2 contains PVP which is also positively charged and increases its zeta potential threefold. Zeta potentials bigger than 10 mV are needed to guarantee stability of the colloidal system.

The droplet size measurements showed that all three nebulizers are suitable for inhalation therapy delivering to the lower lungs, in which the air-jet nebulizer was the worst producing the biggest droplets. Liposomes had no effect on droplet size formation.

To sum up, the vibrating mesh nebulizer had the best performance concerning liposomal transport and encapsulation efficiency. It showed no significant changes of liposome size or PDI and was suitable concerning droplet size. So the vibrating mesh nebulizer is the device of choice.

4.3 Iloprost containing liposomes for mouse inhaler

The same formulations were tested for the M-neb mouse inhaler, which uses also vibrating mesh technology. The liposomal transport efficiency was very good and comparable with the human vibrating mesh device.

The produced droplets were very small and suitable for mouse application, but too small-sized for humans. The liposomes had no influence on droplet size either.

The EE was comparable to the human mesh device and better for LI-2. The M-neb has the same advantages and characteristics as the human vibrating mesh device and is suitable for animal experiments.

4.4 Outlook

Knowing about the nebulization performance of these different devices it is necessary to further optimize formulations and then start *ex vivo* or *in vivo* experiments to assess future human applications. The produced results are very promising and offer a lot of possibilities for further improvements.

At this point it has to be said that testing nebulizer devices and their impact on the biochemical and biophysical properties of aerosolized liposomes is just one aspect of

this application method. There are two *ex vivo* test systems in use to address the potential of liposomes to act as sustained release system for iloprost. The first one is a wire myograph to investigate vessel tone changes when applying liposomal emulsions. The second one is an *ex vivo* isolated perfused lung (IPL) model to study pulmonary arterial pressure (PAP) online when applying aerosolized drug solutions. The IPL model has been shown to be kinetically predictive of *in vivo* conditions despite some limitations. All these systems are essential to simulate the impact of this modified delivery system for iloprost with liposomes as close as possible on *in vivo* conditions. This is necessary to proceed in clinical trials in the future.

Iloprost loaded liposomes for a sustained release formulation may be used in the near future.

5. References

- [1] F. H. Netter, *The Ciba Collection of Medical Illustrations, Volume 5, A Compilation of Paintings on the Normal and Pathologic Anatomy and Physiology, Embryology, and Disease of the Heart*, Rochester, N.Y.: The Case-Hoyt Corp., 1978.
- [2] J. Fanghänel, F. Pera, F. Anderhuber and R. Nitsch, *Waldeyer Anatomie des Menschen*, 18. Auflage, Berlin: Walter de Gruyter GmbH & Co. KG, 2009.
- [3] M. Schünke, E. Schulte and U. Schumacher, *Prometheus, Hals and Innere Organe*, Stuttgart: Georg Thieme Verlag KG, 2005.
- [4] „Wikipedia,“ 9 January 2013. [Online]. Available: <http://en.wikipedia.org/wiki/Heart>.
- [5] „Wikipedia,“ 10 January 2013. [Online]. Available: http://en.wikipedia.org/wiki/Circulatory_system.
- [6] W. Siegenthaler and H. E. Blum, *Klinische Pathophysiologie*, 9. Auflage, Stuttgart: Georg Thieme Verlag, 2006.
- [7] W. Böcker, H. Denk, P. U. Heitz and H. Moch, *Pathologie*, 4. Auflage, München: Urban & Fischer Verlag/Elsevier GmbH, 2008.
- [8] M. Humbert and V. V. McLaughlin, „The 4th World Symposium on Pulmonary Hypertension,“ *Journal of the American College of Cardiology*, Vol. 54, No. 1, pp. 1-2, 2009.
- [9] S. Krug, A. Sablotzki, S. Hammerschmidt, H. Wirtz and H.-J. Seyfarth, „Inhaled iloprost for the control of pulmonary hypertension,“ *Vascular Health and Risk Management*, Vol. 5, pp. 465-474, 2009.
- [10] G. Simonneau, I. M. Robbins, M. Beghetti, R. N. Channik, M. Delcroix, C. P. Denton, C. G. Elliot, S. P. Gaine, M. T. Gladwin, Z.-C. Jing, M. J. Krowka, D. Langleben, N. Nakanishi and R. Souza, „Updated Clinical Classification of Pulmonary Hypertension,“ *Journal of the American College of Cardiology*, Vol. 54, No. 1, pp. 43-54, 2009.
- [11] G. Simonneau, N. Galiè, L. J. Rubin, D. Langleben, W. Seeger, G. Domenighetti, S. Gibbs, D. Lebrec, R. Speich, M. Beghetti, S. Rich and A. Fishman, „Clinical Classification of Pulmonary Hypertension,“ *Journal of the American College of Cardiology*, Vol. 43, No. 12, pp. 5-12, 2004.
- [12] S. G. Raja and S. M. Raja, „Treating pulmonary arterial hypertension: current treatments and future prospects,“ *Therapeutic Advances in Chronic Disease*, pp. 359-370, 2011.
- [13] L. J. Rubin and N. Galiè, „Pulmonary Arterial Hypertension: A Look to the Future,“ *Journal of the American College of Cardiology*, Vol. 43, No. 12, pp. 89-90, 2004.
- [14] D. B. Badesch, H. C. Champion, M. A. G. Sanchez, M. M. Hoeper, J. E. Loyd, A. Manes, M. McGoon, R. Naeije, H. Olschewski, R. J. Oudiz and A. Torbicki, „Diagnosis and Assessment of Pulmonary Arterial Hypertension,“ *Journal of the American College of Cardiology*, Vol. 54, No. 1, pp. 55-66, 2009.
- [15] S. G. Raja, M. D. Danton, K. J. MacArthur and J. C. Pollock, „Treatment of Pulmonary Arterial Hypertension With Sildenafil: From Pathophysiology to Clinical Evidence,“ *Journal of Cardiothoracic and Vascular Anesthesia*, Vol. 20, No. 5, pp. 722-735, 2006.

- [16] C. J. Ryerson, S. Nayar, J. R. Swiston and D. D. Sin, „Pharmacotherapy in pulmonary arterial hypertension: a systemic review and meta-analysis,“ *Respiratory Research*, 2010, 11:12.
- [17] H. Olschewski, G. Simonneau, N. Galiè, T. Higenbottam, R. Naeije, L. J. Rubin, S. Nikkho, R. Speich, M. M. Hoeper, J. Behr, J. Winkler, O. Sitbon, W. Popov, H. A. Ghofrani, A. Manes, D. G. Kiely, R. Ewert, A. Meyer, P. A. Corris and W. Seeger, „Inhaled Iloprost for severe Pulmonary Hypertension,“ *The New England Journal of Medicine*, Vol. 347, No. 5, pp. 322-329, 2002.
- [18] B. J. Whittle, A. Silverstein, D. Mottola and L. H. Clapp, „Binding and activity of the prostacyclin receptor (IP) agonists, treprostinil and iloprost, at human prostanoid receptors: Treprostinil is a potent DP1 and EP2 agonist,“ *Biochemical Pharmacology*, 2012.
- [19] C. Lehmann, „Tierexperimentelle Untersuchungen zur intestinalen Mikrozirkulation bei Endotoxinämie,“ 17 January 2013. [Online]. Available: <http://edoc.hu-berlin.de/habilitationen/lehmann-christian-2001-07-17/HTML/chapter2.html>.
- [20] S. J. Wilson and E. M. Smyth, „Internalization and Recycling of the Human Prostacyclin Receptor Is Modulated through Its Isoprenylation-dependent Interaction with the delta Subunit of cGMP Phosphodiesterase 6,“ *The Journal of Biological Chemistry*, Vol. 281, No. 17, pp. 11780-11786, 2006.
- [21] P. J. Leigh, W. A. Cramp and J. MacDermot, „Identification of the Prostacyclin Receptor by Radiation Inactivation,“ *The Journal of Biological Chemistry*, Vol. 259, No. 20, pp. 12431-12436, 1984.
- [22] L. Walch, C. Labat, J.-P. Gascard, V. d. Montpreville, C. Brink and X. Norel, „Prostanoid receptors involved in the relaxation of human pulmonary vessels,“ *British Journal of Pharmacology*, Vol. 126, pp. 859-866, 1999.
- [23] S.-A. Cryan, N. Sivadas and L. Garcia-Contreras, „In vivo animal models for drug delivery across the lung mucosal barrier,“ *Advanced Drug Delivery Reviews*, Vol. 59, pp. 1133-1151, 2007.
- [24] „Wikipedia,“ 18 January 2013. [Online]. Available: <http://en.wikipedia.org/wiki/Alveoli>.
- [25] „Wikipedia,“ 18 January 2013. [Online]. Available: http://en.wikipedia.org/wiki/Human_lung.
- [26] M. M. Gaspar, U. Bakowsky and C. Ehrhardt, „Inhaled Liposomes-Current Strategies and Future Challenges,“ *Journal of Biomedical Nanotechnology*, Vol.4, pp. 1-13, 2008.
- [27] D. Lasic, *Liposomes: from physics to applications*, Amsterdam: Elsevier Science Publishers B.V., 1993.
- [28] D. Vance and J. Vance, *Biochemistry of Lipids, Lipoproteins and Membranes*, 4th edition, Amsterdam: Elsevier BV., 2006.
- [29] M. Rosoff, *Vesicles*, New York: Marcel Dekker, Inc., 1996.
- [30] Y. Barenholz and D. D. Lasic, *Handbook of Nonmedical Applications of Liposomes: From Design to Microreactors*, Volume 3, Boca Raton, Florida: CRC Press, Inc., 1996.
- [31] M. S. G. Woodle, *Long Circulating Liposomes: Old Drugs, New Therapeutics*, Berlin Heidelberg: Springer-Verlag, 1998.
- [32] 21 January 2013. [Online]. Available: <http://www.scienceinyoureyes.com/index.php?id=75>.

- [33] D. D. Lasic and Y. Barenholz, Handbook of Nonmedical Applications of Liposomes: From Gene Delivery and Diagnostics to Ecology, Volume 4, Boca Raton, Florida: CRC Press, Inc., 1996.
- [34] „Wikipedia,“ 31 January 2013. [Online]. Available: <http://en.wikipedia.org/wiki/Nebulizer>.
- [35] L. Vecellio, „The mesh nebuliser: a recent technical innovation for aerosol delivery,“ *Breathe*, Vol. 2, No. 3, pp. 253-260, 2006.
- [36] L. Y. Yeo, J. R. Friend, M. P. McIntosh, E. N. Meeusen and D. A. Morton, „Ultrasonic nebulization platforms for pulmonary drug delivery,“ *Expert Opinion on Drug Delivery*, Vol. 7, No. 6, pp. 663-679, 2010.
- [37] „Avanti Polar Lipids, Inc.,“ 19 January 2013. [Online]. Available: http://avantilipids.com/index.php?option=com_content&view=article&id=1384&Itemid=372.
- [38] „invitrogen,“ 30 January 2013. [Online]. Available: <http://www.invitrogen.com/site/us/en/home/References/Molecular-Probes-The-Handbook/Technical-Notes-and-Product-Highlights/Assays-of-Volume-Change-Membrane-Fusion-and-Membrane-Permeability.html>.
- [39] M. Jones, „Wikipedia,“ 29 January 2013. [Online]. Available: http://en.wikipedia.org/wiki/Dynamic_light_scattering.
- [40] „The Hebrew University of Jerusalem, The Interdepartmental Equipment Facility,“ 23 January 2013. [Online]. Available: <http://departments.agri.huji.ac.il/zabam/zetasizer.html>.
- [41] U. T. Corporation, „Tyvaso Inhalation System, Instructions for Use,“ United Therapeutics Corporation, Research Triangle Park, North Carolina 27709, 2010.
- [42] J. C. Waldrep, K. Keyhani, M. Black and V. Knight, „Operating Characteristics of 18 Different Continous-Flow Jet Nebulizers With Beclomethasone Dipropionate Liposome Aerosol,“ *Chest*, Vol. 105, No. 1, pp. 106-110, 1994.
- [43] J. C. Waldrep, B. E. Gilbert, C. M. Knight, M. B. Black, P. W. Scherer, V. Knight and W. Eschenbacher, „Pulmonary Delivery of Beclomethasone Liposome Aerosol in Volunteers,“ *Chest*, Vol. 111, No. 2, pp. 316-323, 1997.
- [44] J. Conley, H. Yang, T. Wilson, K. Blasetti, V. Di Ninno, G. Schnell and J. P. Wong, „Aerosol Delivery of Liposome-Encapsulated Ciprofloxacin: Aerosol Characterization and Efficacy against Francisella tularensis Infection in Mice,“ *Antimicrobial agents and chemotherapy*, Vol. 41, No. 6, pp. 1288-1292, 1997.
- [45] W. H. Finlay and J. P. Wong, „Regional lung deposition of nebulized liposome-encapsulated ciprofloxacin,“ *International Journal of Pharmaceutics*, Vol. 167, pp. 121-127, 1998.
- [46] T. R. Desai, R. E. W. Hancock and W. H. Finlay, „A facile method of delivery of liposomes by nebulization,“ *Journal of Controlled Release*, Vol. 84, pp. 69-78, 2002.
- [47] A. Wagner, K. Vorauer-Uhl and H. Katinger, „Nebulization of Liposomal rh-Cu/Zn-SOD with a Novel Vibrating Membrane Nebulizer,“ *Journal of Liposome Research*, Vol. 16, pp. 113-125, 2006.
- [48] Y.-Y. Huang and C.-H. Wang, „Pulmonary delivery of insulin by liposomal carriers,“ *Journal of Controlled Release*, Vol. 113, pp. 9-14, 2006.

- [49] S. Chono, R. Fukuchi, T. Seki and K. Morimoto, „Aerosolized liposomes with dipalmitoyl phosphatidylcholine enhance pulmonary insulin delivery,“ *Journal of Controlled Release, Vol. 137*, pp. 104-109, 2009.
- [50] R. Egle, E. Bitterle, F. Gruber and M. Keller, „Physicochemical characteristics of a liposomal ciclosporin A formulation pre and post nebulisation in a customized eFlow electronic nebulizer,“ *PARI Pharma GmbH*, 2008.
- [51] J. Behr, G. Zimmermann, R. Baumgartner, H. Leuchte, C. Neurohr, P. Brand, C. Herpich, K. Sommerer, J. Seitz, G. Menges, S. Tillmanns and M. Keller, „Lung Deposition of a Liposomal Cyclosporine A Inhalation Solution in Patients after Lung Transplantation,“ *Journal of aerosol medicine and pulmonary drug delivery, Vol. 22, No. 2*, pp. 121-129, 2009.
- [52] F. Hajos, B. Stark, S. Hensler, R. Prassl and W. Mosgoeller, „Inhalable liposomal formulation for vasoactive intestinal peptide,“ *International Journal of Pharmaceutics, Vol. 357*, pp. 286-294, 2008.
- [53] M. Zaru, S. Mourtas, P. Klepetsanis, A. M. Fadda and S. G. Antimisariis, „Liposomes for drug delivery to the lungs by nebulization,“ *European Journal of Pharmaceutics and Biopharmaceutics, Vol. 67, No. 3*, pp. 655-666, 2007.
- [54] S. Anabousi, E. Kleemann, U. Bakowsky, T. Kissel, T. Schmehl, T. Gessler, W. Seeger, C. M. Lehr and C. Erhardt, „Effect of PEGylation on the stability of liposomes during nebulisation and in lung surfactant,“ *Journal of Nanoscience and Nanotechnology, Vol. 6, No. 9-10*, pp. 3010-3016, 2006.
- [55] A. Elhissi, J. Giebultowicz, A. A. Stec, P. Wroczynski, W. Ahmed, M. A. Alhnan, D. Phoenix and K. Taylor, „Nebulization of ultradeformable liposomes: The influence of aerosolization mechanism and formulation excipients,“ *International Journal of Pharmaceutics, Vol. 436*, pp. 519-526, 2012.
- [56] A. Elhissi, M. Faizi, W. F. Naji, H. S. Gill and K. Taylor, „Physical stability and aerosol properties of liposomes delivered using an air-jet nebulizer and a novel micropump device with large mesh apertures,“ *International Journal of Pharmaceutics, Vol. 334*, pp. 62-70, 2007.
- [57] R. E. Van Dyke and K. Nikander, „Delivery of Iloprost Inhalation Solution With the HaloLite, Prodose and I-neb Adaptive Aerosol Delivery Systems: An In Vitro Study,“ *Respiratory Care, Vol. 52, No. 2*, pp. 184-190, 2007.
- [58] E. Kleemann, T. Schmehl, T. Gessler, U. Bakowsky, T. Kissel and W. Seeger, „Iloprost-Containing Liposomes for Aerosol Application in Pulmonary Arterial Hyertension: Formulation Aspects and Stability,“ *Pharmaceutical Research, Vol. 24, No. 2*, pp. 277-287, 2006.
- [59] „Wikipedia,“ 20 January 2013. [Online]. Available: <http://en.wikipedia.org/wiki/Liposomes>.

6. Appendix

6.1 List of Figures

Figure 1. 1: Drawing of the exposure of the human heart.....	1
Figure 1. 2: Structure diagram of the human heart from an anterior view.	2
Figure 1. 3: Circulation of blood through the human heart.	3
Figure 1. 4: Pathogenesis and pathobiology of pulmonary arterial hypertension.....	7
Figure 1. 5: Chemical structure of prostacyclin (left) and iloprost (right).....	10
Figure 1. 6: Graphical representation of the human lung.....	11
Figure 1. 7: Graphical representation of a pulmonary alveolus.....	12
Figure 1. 8: Simple cross-section scheme of a liposome.....	13
Figure 1. 9: Graphical representation of a “stealth liposome”	15
Figure 1. 10: Schematic representation of liposome classification according to their surface properties.	17
Figure 1. 11: Schematic illustration of the fate of an inhaled drug.....	18
Figure 1. 12: Drawing of the first pressurized inhaler invented by Sales-Giròns in 1858.	19
Figure 1. 13: Schematic illustration of working principles of a typical (A) air-jet nebulizer and (B) ultrasonic nebulizer.	21
Figure 1. 14: Schematic illustration of the working principle of a vibrating mesh nebulizer.....	23
Figure 2. 1: Tested nebulizer devices	24
Figure 2. 2: M-neb mouse inhaler (NEBU-TEC) for IPL system.....	25
Figure 2. 3: Liposome preparation procedure as carried out for the experiments.	26
Figure 2. 4: Applied fluorophore-quencher system consisting of the fluorescent dye ANTS and the quencher DPX.....	31
Figure 2. 5: Scheme of the working principle of Dynamic Light Scattering DLS.....	32
Figure 2. 6: Calibration curve for the determination of phosphorus made with a KH_2PO_4 standard...	34
Figure 2. 7: Picture of a cuvette suitable for zeta potential measurement.	36
Figure 3. 1: First prototype of aerosol condensation equipment arranged with the Optineb [®] -ir.....	37
Figure 3. 2: Description of the main user items of the Optineb [®] -ir.....	38
Figure 3. 3: Filling the water reservoir with 45 mL of distilled water and inserting the medicine cup. 38	
Figure 3. 4: Boost signaling for the patient’s inhalation pattern.	39
Figure 3. 5: Experimental set-up for the condensation experiments with the MicroDrop [®] Pro nebulizer.....	40
Figure 3. 6: Experimental set-up for the condensation experiments with the eFlow [®] rapid nebulizer.	42
Figure 3. 7: Photos of the compressor (left) and the lung simulator (right).	44
Figure 3. 8: Final assembly of the condensation equipment for the Optineb [®] -ir.....	44
Figure 3. 9: Final experimental set-up of the condensation equipment for the MicroDrop [®] Pro.....	45

Figure 3. 10: Final experimental set-up of the condensation equipment for the eFlow® rapid.....	46
Figure 3. 11: L-1 before nebulization DLS result curve and table show size distribution vs. intensity.	48
Figure 3. 12: L-1 aerosol after nebulization DLS result curve and table show size distribution vs. intensity.....	49
Figure 3. 13: L-1 remainder after nebulization DLS result curve and table show size distribution vs. intensity.....	49
Figure 3. 14: Liposomal concentration in samples without iloprost when nebulized with MicroDrop® Pro (n=1).....	51
Figure 3. 15: Liposomal concentration in samples without iloprost before and after nebulization with Optineb®-ir (n=1).....	53
Figure 3. 16: Liposomal concentration in samples without iloprost before and after nebulization with eFlow® rapid (n=1).....	54
Figure 3. 17: Liposomal concentration [mg/mL] in samples with iloprost before and after nebulization with MicroDrop® Pro (mean ± S.D., n=3).	56
Figure 3. 18: Liposomal concentration [%] in samples with iloprost before and after nebulization with MicroDrop® Pro (mean ± S.D., n=3).	56
Figure 3. 19: Liposomal particle size in samples with iloprost before and after nebulization with MicroDrop® Pro (mean ± S.D., n=3).	57
Figure 3. 20: Liposomal particle PDI in samples with iloprost before and after nebulization with MicroDrop® Pro (mean ± S.D., n=3).	57
Figure 3. 21: Liposomal concentration [mg/mL] in samples with iloprost before and after nebulization with MicroDrop® Pro (n=1).....	58
Figure 3. 22: Liposomal concentration [mg/mL] in samples with iloprost before and after nebulization with Optineb®-ir (mean ± S.D., n=3).....	59
Figure 3. 23: Liposomal concentration [%] in samples with iloprost before and after nebulization with Optineb®-ir (mean ± S.D., n=3).....	60
Figure 3. 24: Liposomal particle size in samples with iloprost before and after nebulization with Optineb®-ir (mean ± S.D., n=3).....	60
Figure 3. 25: Liposomal particle PDI in samples with iloprost before and after nebulization with Optineb®-ir (mean ± S.D., n=3).....	61
Figure 3. 26: Liposomal concentration [mg/mL] in samples with iloprost before and after nebulization with Optineb®-ir (n=1).....	62
Figure 3. 27: Liposomal concentration [mg/mL] in samples with iloprost before and after nebulization with eFlow® rapid (mean ± S.D., n=3).	62
Figure 3. 28: Liposomal concentration [%] in samples with iloprost before and after nebulization with eFlow® rapid (mean ± S.D., n=3).	63
Figure 3. 29: Liposomal particle size in samples with iloprost before and after nebulization with eFlow® rapid (mean ± S.D., n=3).	64
Figure 3. 30: Liposomal particle PDI in samples with iloprost before and after nebulization with eFlow® rapid (mean ± S.D., n=3).	64
Figure 3. 31: Liposomal concentration [mg/mL] in samples with iloprost before and after nebulization with eFlow® rapid (n=1).	65
Figure 3. 32: Iloprost encapsulation efficiency before nebulization with MicroDrop® Pro,	66

Figure 3. 33: LI-1 iloprost encapsulation efficiency after nebulization with MicroDrop® <i>Pro</i> ,	66
Figure 3. 34: LI-2 iloprost encapsulation efficiency after nebulization with MicroDrop® <i>Pro</i> ,	66
Figure 3. 35: Iloprost encapsulation efficiency before nebulization with Optineb®-ir,	67
Figure 3. 36: LI-1 iloprost encapsulation efficiency after nebulization with Optineb®-ir,	67
Figure 3. 37: LI-2 iloprost encapsulation efficiency after nebulization with Optineb®-ir,	68
Figure 3. 38: Iloprost encapsulation efficiency before nebulization with eFlow® rapid,	68
Figure 3. 39: LI-1 iloprost encapsulation efficiency after nebulization with eFlow® rapid,	68
Figure 3. 40: LI-2 iloprost encapsulation efficiency after nebulization with eFlow® rapid,	69
Figure 3. 41: Droplet size distribution of the MicroDrop® <i>Pro</i> measured with laser light scattering. .	74
Figure 3. 42: Droplet size distribution of the Optineb®-ir measured with laser light scattering.	75
Figure 3. 43: Droplet size distribution of the eFlow® rapid measured with laser light scattering.	75
Figure 3. 44: Compared droplet size distribution among all three tested nebulizers.	76
Figure 3. 45: Liposomal concentration [mg/mL] in samples with iloprost before and after nebulization with M-neb (n=1).....	77
Figure 3. 46: Liposomal concentration [%] in samples with iloprost before and after nebulization with M-neb (n=1).....	77
Figure 3. 47: Droplet size distribution of the M-neb nebulizer measured with laser light scattering. .	79
Figure 3. 48: Droplet size distribution of the M-neb nebulizer measured with laser light scattering. .	79
Figure 3. 49: Droplet size distribution of the M-neb nebulizer measured with laser light scattering. .	79

6.2 List of Tables

Table 1. 1: Updated Clinical Classification of Pulmonary Hypertension (Dana Point, 2008)	5
Table 3. 1: Liposomal composition for L-1 and L-2.....	47
Table 3. 2: Volumes of the samples before and after nebulization with MicroDrop® Pro for L-1 and L-2.....	47
Table 3. 3: Size and PDI results from the liposomes L-1 and L-2 before and after nebulization with MicroDrop® Pro.....	47
Table 3. 4: Liposomal concentration in samples without iloprost when nebulized with MicroDrop® Pro (n=1).....	50
Table 3. 5: Volumes of the samples before and after nebulization with Optineb®-ir for L-1 and L-2. .	51
Table 3. 6: Size and PDI results from the liposomes L-1 and L-2 before and after nebulization with Optineb®-ir.	52
Table 3. 7: Liposomal concentration in samples without iloprost before and after nebulization with Optineb®-ir (n=1).....	53
Table 3. 8: Volumes of the samples before and after nebulization with eFlow® rapid for L-1 and L-2.	53
Table 3. 9: Size and PDI results from the liposomes L-1 and L-2 before and after nebulization with eFlow® rapid.....	54
Table 3. 10: Liposomal concentration in samples without iloprost before and after nebulization with eFlow® rapid (n=1).....	55
Table 3. 11: Liposomal concentration [mg/mL] in samples with iloprost before and after nebulization with MicroDrop® Pro (mean ± S.D., n=3).	55
Table 3. 12: Liposomal concentration [%] in samples with iloprost before and after nebulization with MicroDrop® Pro (mean ± S.D., n=3).	56
Table 3. 13: Liposomal particle size in samples with iloprost before and after nebulization with MicroDrop® Pro (mean ± S.D., n=3).	57
Table 3. 14: Liposomal particle PDI in samples with iloprost before and after nebulization with MicroDrop® Pro (mean ± S.D., n=3).	57
Table 3. 15: Liposomal concentration [mg/mL] in samples with iloprost before and after nebulization with MicroDrop® Pro (n=1).....	58
Table 3. 16: Liposomal concentration [mg/mL] in samples with iloprost before and after nebulization with Optineb®-ir (mean ± S.D., n=3).....	59
Table 3. 17: Liposomal concentration [%] in samples with iloprost before and after nebulization with Optineb®-ir (mean ± S.D., n=3).....	59
Table 3. 18: Liposomal particle size in samples with iloprost before and after nebulization with Optineb®-ir (mean ± S.D., n=3).....	60
Table 3. 19: Liposomal particle PDI in samples with iloprost before and after nebulization with Optineb®-ir (mean ± S.D., n=3).....	61
Table 3. 20: Liposomal concentration [mg/mL] in samples with iloprost before and after nebulization with Optineb®-ir (n=1).....	61

Table 3. 21: Liposomal concentration [mg/mL] in samples with iloprost before and after nebulization with eFlow® rapid (mean ± S.D., n=3).	62
Table 3. 22: Liposomal concentration [%] in samples with iloprost before and after nebulization with eFlow® rapid (mean ± S.D., n=3).	63
Table 3. 23: Liposomal particle size in samples with iloprost before and after nebulization with eFlow® rapid	64
Table 3. 24: Liposomal particle PDI in samples with iloprost before and after nebulization with eFlow® rapid (mean ± S.D., n=3).	64
Table 3. 25: Liposomal concentration [mg/mL] in samples with iloprost before and after nebulization with eFlow® rapid (n=1).	65
Table 3. 26: Zeta potential of the investigated liposomes.	73
Table 3. 27: Droplet size distribution of the MicroDrop® Pro defined by d(0.1), d(0.5) and d(0.9). ...	74
Table 3. 28: Droplet size distribution of the MicroDrop® Pro defined by d(0.1), d(0.5) and d(0.9). ...	75
Table 3. 29: Droplet size distribution of the MicroDrop® Pro defined by d(0.1), d(0.5) and d(0.9). ...	76
Table 3. 30: Liposomal concentration [mg/mL] in samples with iloprost before and after nebulization with M-neb (n=1).....	76
Table 3. 31: Liposomal concentration [%] in samples with iloprost before and after nebulization with M-neb (n=1).....	77
Table 3. 32: Liposomal size and PDI in samples with iloprost before and after nebulization with M-neb (n=1).	78
Table 3. 33: Droplet size distribution of the M-neb nebulizer defined by d(0.1), d(0.5) and d(0.9).....	78
Table 3. 34: Fluorescence measurements with undiluted L-1 (3.41 mg/mL POPC) and L-2 (2.79 mg/mL POPC) samples.....	81
Table 3. 35: Fluorescence measurements with diluted L-1 (2.58 mg/mL POPC) and L-2 (2.07 mg/mL POPC) samples.....	82
Table 3. 36: Fluorescence measurements with diluted L-1 (2.58 mg/mL POPC) and L-2 (2.07 mg/mL POPC) samples.....	82

6.3 Nebulized and collected sample volumes

Table 6. 1: Volumes of the samples before and after nebulization with MicroDrop® Pro for LI-1 and LI-2

Volumes [μL]	start	aerosol	remainder	loss
3.0 mg/mL samples				
LI-1 (No.1)	3000	440	800	1760
LI-1 (No.2)	3000	200	1100	1700
LI-1 (No.3)	3000	290	700	2010
LI-2 (No.1)	3000	380	1000	1620
LI-2 (No.2)	3000	200	850	1950
LI-2 (No.3)	3000	480	950	1570
0.6 mg/mL samples				
LI-1	3000	550	800	1650
LI-2	3000	630	950	1420

Table 6. 2: Volumes of the samples before and after nebulization with Optineb®-ir for LI-1 and LI-2

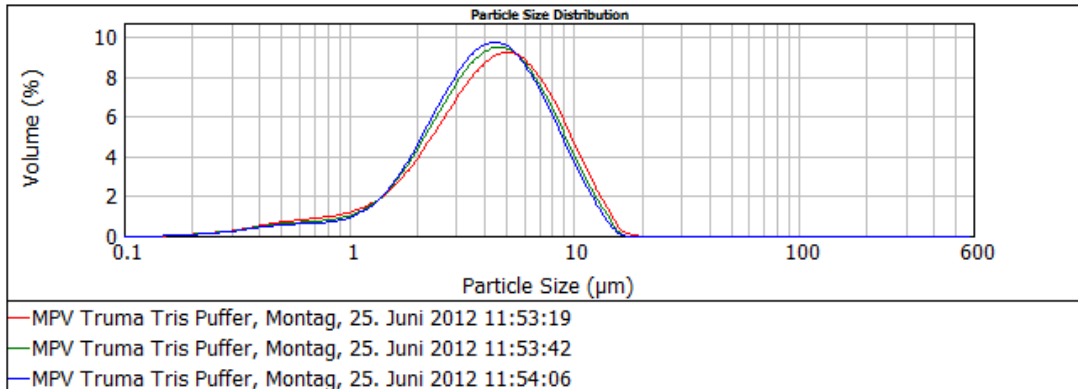
Volumes [μL]	start	aerosol	remainder	loss
3.0 mg/mL samples				
LI-1 (No.1)	2500	550	750	1200
LI-1 (No.2)	3000	480	1020	1500
LI-1 (No.3)	3000	520	1300	1180
LI-2 (No.1)	2500	410	970	1120
LI-2 (No.2)	3000	480	1250	1270
LI-2 (No.3)	3000	460	1400	1140
0.6 mg/mL samples				
LI-1	3000	520	1150	1330
LI-2	3000	540	1060	1400

Table 6. 3: Volumes of the samples before and after nebulization with eFlow® rapid for LI-1 and LI-2

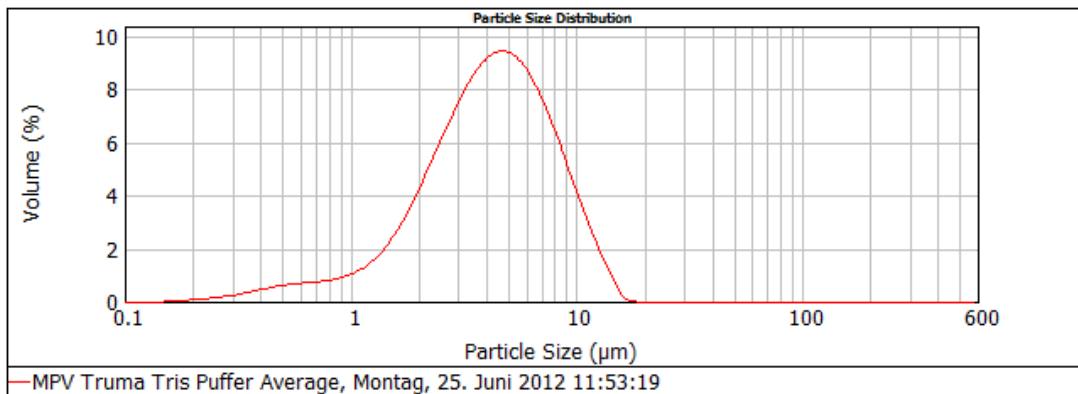
Volumes [µL]	start	aerosol	remainder	loss
3.0 mg/mL samples				
LI-1 (No.1)	3000	1350	950	700
LI-1 (No.2)	3000	1500	1000	500
LI-1 (No.3)	3000	1750	850	400
LI-2 (No.1)	3000	1380	980	640
LI-2 (No.2)	3000	1850	700	450
LI-2 (No.3)	3000	1620	1050	330
0.6 mg/mL samples				
LI-1	3000	1500	950	550
LI-2	3000	1600	1000	400

6.4 Droplet size measurements

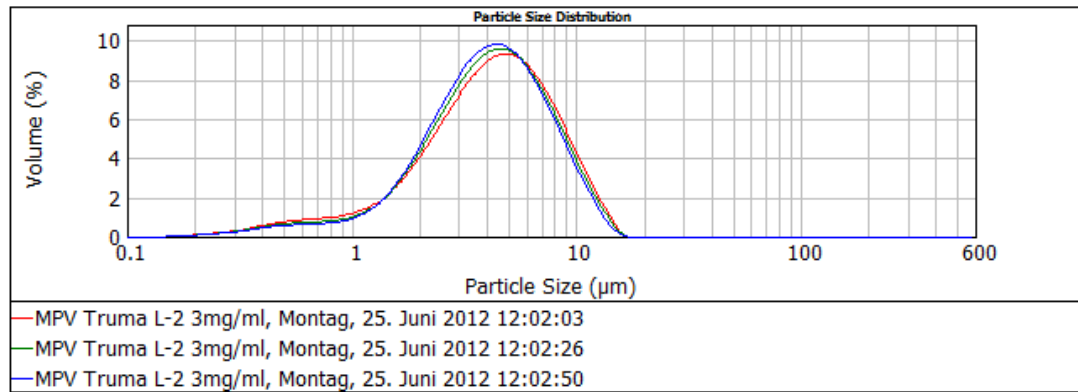
MicroDrop® Pro – Tris Buffer 10mM pH7.0



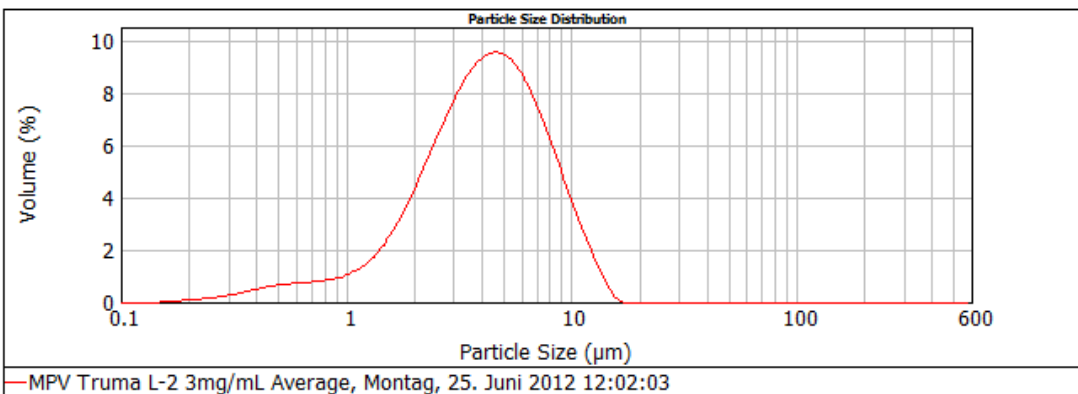
d(0.1): 1.562 μm d(0.5): 4.225 μm d(0.9): 8.889 μm



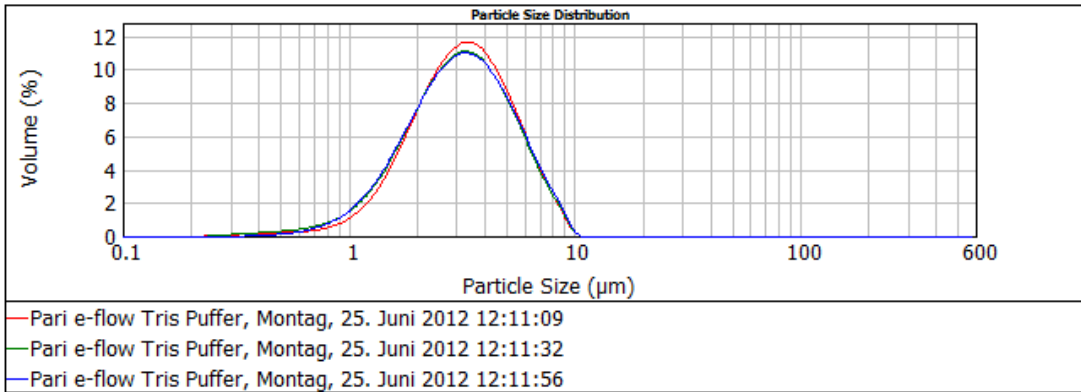
MicroDrop® Pro – L-2 3mg/mL



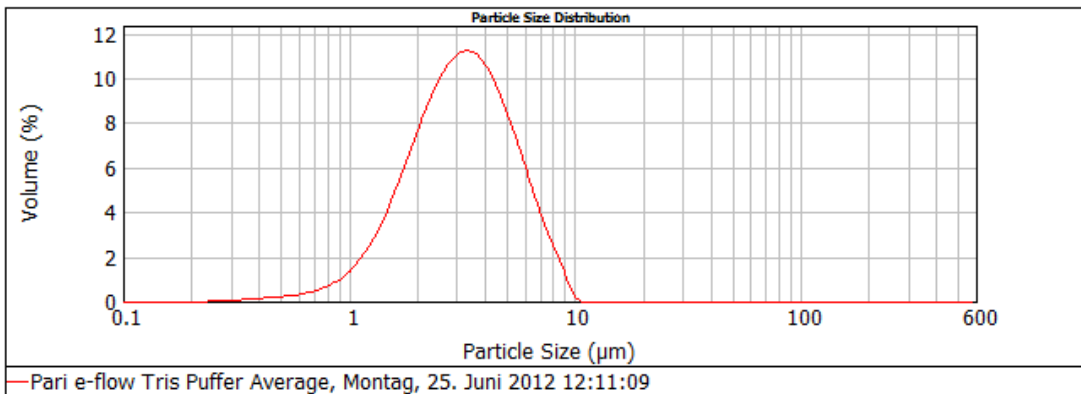
d(0.1): 1.533 μm d(0.5): 4.149 μm d(0.9): 8.657 μm



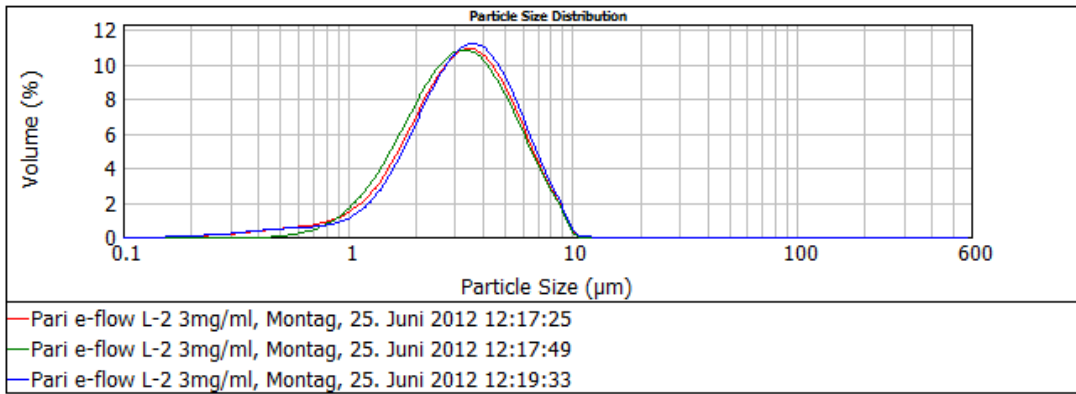
eFlow® rapid – Tris Buffer 10mM pH7.0



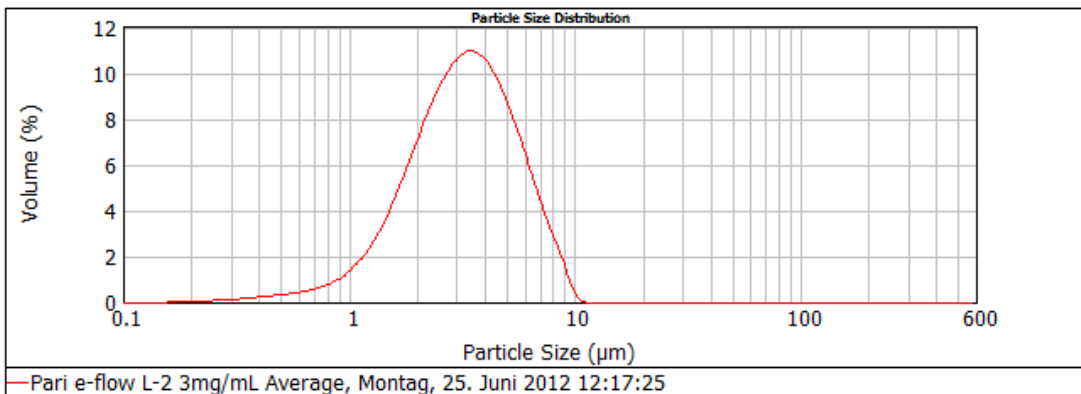
d(0.1): 1.516 um d(0.5): 3.168 um d(0.9): 6.014 um



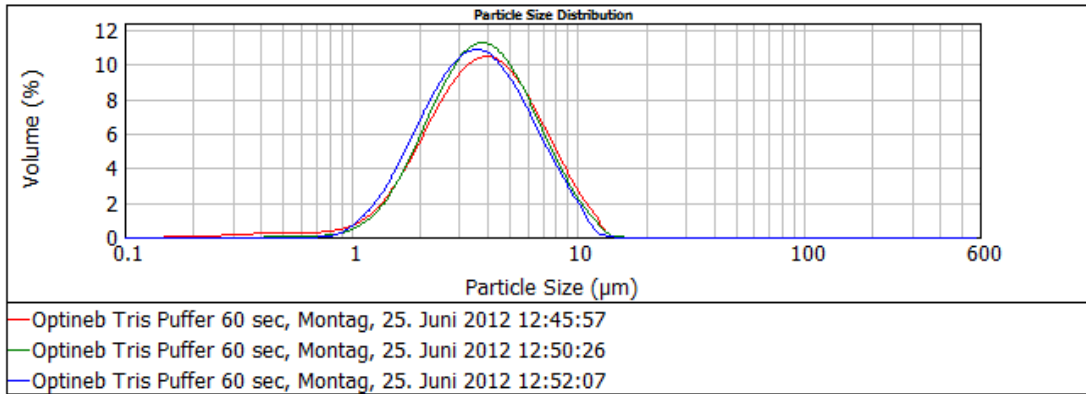
eFlow® rapid – L-2 3mg/mL



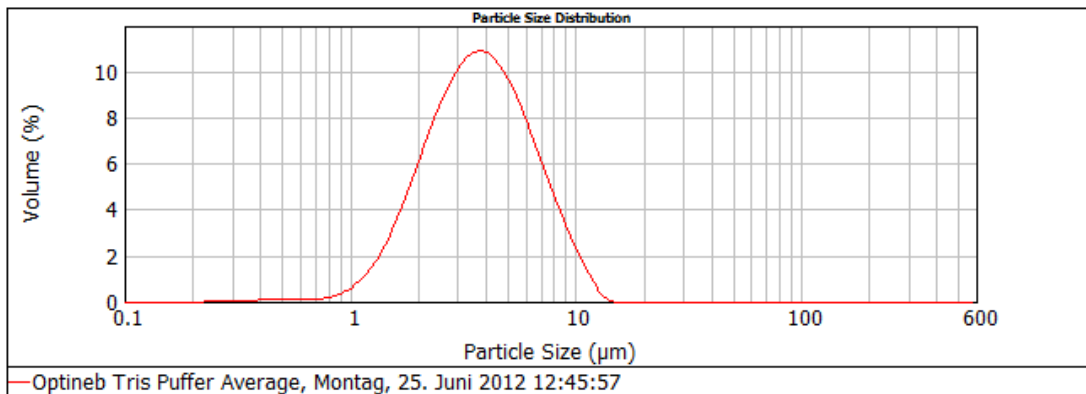
d(0.1): 1.480 um d(0.5): 3.243 um d(0.9): 6.204 um



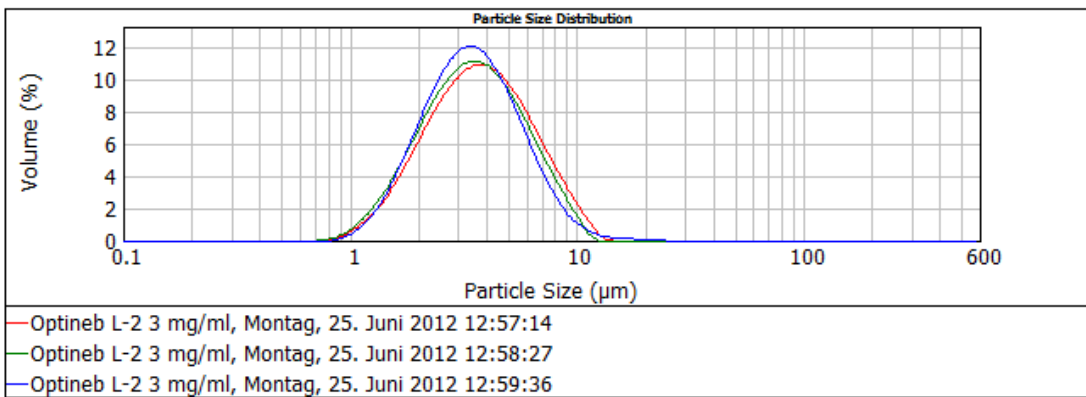
Optineb®-ir – Tris Buffer 10mM pH7.0



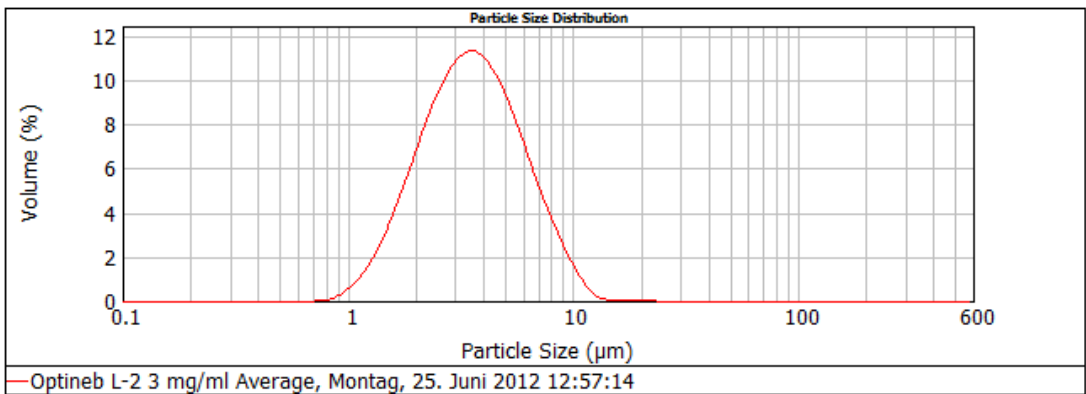
d(0.1): 1.829 um d(0.5): 3.730 um d(0.9): 7.395 um



Optineb®-ir – L-2 3mg/mL



d(0.1): 1.807 um d(0.5): 3.535 um d(0.9): 6.874 um



6.5 MS results

Table 6. 4: eFlow® rapid MS calculations

Sample name	µM	µg/mL	total volume [µL]	sample volume [µL]	after separation [µL]	dilution factor	µg/mL corr.	abs. amount [µg]
eFlow LI1 Mist A / Lipos	17,33	6,25	1500	200	250	1,25	7,81	11,71
eFlow LI1 Mist A / EtOH	42,93	15,48			200	1,00	15,48	23,22
eFlow LI1 Remainder A / Lipos	16,70	6,02	1000	200	250	1,25	7,52	7,52
eFlow LI1 Remainder A / EtOH	42,36	15,27			200	1,00	15,27	15,27
eFlow LI2 Mist A / Lipos	25,48	9,19	1850	200	250	1,25	11,48	21,24
eFlow LI2 Mist A / EtOH	18,39	6,63			200	1,00	6,63	12,26
eFlow LI2 Remainder A / Lipos	25,58	9,22	700	200	250	1,25	11,53	8,07
eFlow LI2 Remainder A / EtOH	18,84	6,79			200	1,00	6,79	4,75

Table 6. 5: Optineb®-ir MS calculations

Sample name	µM	µg/mL	total volume [µL]	sample volume [µL]	after separation [µL]	dilution factor	µg/mL corr.	abs. amount [µg]
OptiNeb-ir LI1 Mist A / Lipos	4,65	1,68	480	200	250	1,25	2,10	1,01
OptiNeb-ir LI1 Mist A / EtOH	12,40	4,47			200	1,00	4,47	2,15
OptiNeb-ir LI1 Remainder A / Lipos	2,27	0,82	1020	50	250	5,00	4,10	4,18
OptiNeb-ir LI1 Remainder A / EtOH	11,03	3,98			200	4,00	15,92	16,24
OptiNeb-ir LI2 Mist A / Lipos	5,16	1,86	480	200	250	1,25	2,33	1,12
OptiNeb-ir LI2 Mist A / EtOH	4,63	1,67			200	1,00	1,67	0,80
OptiNeb-ir LI2 Remainder A / Lipos	3,56	1,28	1250	50	250	5,00	6,40	8,00
OptiNeb-ir LI2 Remainder A / EtOH	5,90	2,13			200	4,00	8,52	10,65

Table 6. 6: MicroDrop® Pro MS calculations

Sample name	µM	µg/mL	total volume [µL]	sample volume [µL]	after separation [µL]	dilution factor	µg/mL corr.	abs. amount [µg]
MPV Truma LI1 Mist B / Lipos	12,68	4,57	290	200	250	1,25	5,71	1,66
MPV Truma LI1 Mist B/ EtOH	19,68	7,10			200	1,00	7,10	2,06
MPV Truma LI1 Remainder B/ Lipos	8,69	3,13	700	100	250	2,50	7,83	5,48
MPV Truma LI1 Remainder B/ EtOH	20,69	7,46			200	2,00	14,91	10,44
MPV Truma LI2 Mist B / Lipos	19,16	6,91	480	200	250	1,25	8,63	4,14
MPV Truma LI2 Mist B/ EtOH	10,79	3,89			200	1,00	3,89	1,87
MPV Truma LI2 Remainder B/ Lipos	10,88	3,92	950	100	250	2,50	9,80	9,31
MPV Truma LI2 Remainder B/ EtOH	9,66	3,48			200	2,00	6,97	6,62

Table 6. 7: M-neb calculations

Sample name	µM	µg/mL	total volume [µL]	sample volume [µL]	after separation [µL]	dilution factor	µg/mL corr.	abs. amount [µg]
Lipos (LI-1 Aerosol)	6,08	2,19	170	100	220	2,20	4,82	0,82
EtOH (LI-1 Aerosol)	15,27	5,50			200	2,00	11,01	1,87
Lipos (LI-1 Remainder)	6,04	2,18	1280	100	240	2,40	5,22	6,69
EtOH (LI-1 Remainder)	15,29	5,51			200	2,00	11,03	14,11
Lipos (LI-2 Aerosol)	9,23	3,33	540	100	190	1,90	6,32	3,41
EtOH (LI-2 Aerosol)	6,87	2,48			200	2,00	4,96	2,68
Lipos (LI-2 Remainder)	8,47	3,05	1960	100	200	2,00	6,11	11,97
EtOH (LI-2 Remainder)	6,99	2,52			200	2,00	5,04	9,88